Measuring the Electrophysiological Effects of Direct Electrical Brain Stimulation during Awake Surgery of Low Grade Glioma

Marion Vincent

Collège Doctoral du Languedoc-Roussillon

THÈSE

Pour obtenir le grade de

Docteur

Délivré par l'**Université de Montpellier**

Préparée au sein de l'école doctorale **I2S**
Et de l'unité de recherche **CAMIN**

Spécialité: **Systèmes Automatiques et Microélectroniques**

Présentée par **Marion Vincent**

Mesure des Effets Electrophysiologiques de la Stimulation Electrique Directe du Cerveau lors des Chirurgies Eveillées des Gliomes de Bas Grade.

Soutenue le 7 Novembre 2017 devant le jury composé de

M. David	Directeur de Recherche	INSERM U1216	Rapporteur
Mme Marque	Professeur	Université de Technologie Compiègne	Rapporteur
M. Mandonnet	Professeur, Praticien Hospitalier	Université de Paris 7 Diderot	Examinateur
M. Bonnetblanc	Maitre de conférence, HDR	Université de Bourgogne	Directeur
M. Guiraud	Directeur de Recherche	INRIA Equipe CAMIN	Co-directeur
M. Duffau	Professeur, Praticien Hospitalier	Université de Montpellier	Co-encadrant

Université de Montpellier

cnrs

camin

Résumé de la thèse

Les gliomes infiltrants de bas grade OMS type II (GIBG) sont des tumeurs cérébrales dont le développement continu est lent. Ils envahissent progressivement les voies de la substance blanche. Il est désormais établi que les GIBGs changent de nature biologique et évoluent vers des gliomes de haut grade, avec une médiane de survie estimée à 10 ans [Duf05]. Alors que l'excision préventive de GIBGs a longtemps été discutée, cette option est désormais considérée comme la plus efficace. Ainsi, la chirurgie éveillée consiste à retirer le tissu tumoral pour tenter de limiter son développement et retarder sa dégénérescence tout en préservant les fonctions (cognitives par exemple) : chez un patient éveillé, le neurochirurgien pratique une cartographie anatomo-fonctionnelle du cerveau en stimulant électriquement les zones proches de la tumeur, pour différencier celles qui sont fonctionnelles de celles qui ne le sont plus. Pendant la chirurgie le patient est impliqué et réalise des tâches comportementales d'intérêt (évaluations peropératoires). En induisant des perturbations transitoires chez le patient, la stimulation électrique directe (SED) permet de détecter en temps-réel des aires corticales et sous-corticales "essentielles pour la fonction" et ainsi de préserver la connectivité fonctionnelle. Opérer un patient conscient permet de retirer un maximum de tissu tumoral, tout en minimisant le risque de séquelles. Les effets inhibiteurs de la stimulation sont mis en évidence par les évaluations neuropsychologiques réalisées par le patient. Cependant les effets electrophysiologiques sont moins connus.

Afin de maximiser la résection et valider la connectivité anatomo-fonctionelle, il est nécessaire de connaître en temps réel et *in vivo* l'état électrophysiologique des réseaux fonctionnels activés. En effet, ceci permettra de comprendre la connectivité spatiale (et temporelle) ainsi que la dynamique des réseaux. On attend de telles informations qu'elle donnent une meilleure connaissance des mécanismes neurophysiologiques sous-jacents à la SED mis en jeu au niveau des réseaux à courte et longue distance.

En physiologie, un potentiel évoqué est défini par la modification de l'activité électrique du système nerveux en réponse à un stimulus externe. Enregistrer ces PEs donne des informations sur le fonctionnement des réseaux stimulés. Afin d'évaluer l'organisation des ces réseaux, des mesures de connectivités peuvent être utilisées.

Les potentiels évoqués fournissent une opportunité unique de suivre in vivo et de manière directe la connectivité entre aires corticales et sous-corticales. Dans le cadre de la chirurgie éveillée des GIBG, il est d'un certain intérêt de mesurer des PE:

Sur la surface corticale, lorsque la SED est appliquée aux environs du point d'enregistrement. Cela mettrait en évidence les effets locaux de la SED.

- En sous-cortical et en cortical, lorsque la SED est appliquée sur les voies de la substance blanche révélées par la résection tumorale, ou sur sa sortie corticale supposée. Ces mesures amèneraient de nouvelles conanissances sur les différentes étapes de la propagation de la SED dans les réseaux neuronaux et sur la connectivité sous-corticale entre les régions corticales fonctionnelles.

- A distance du site de stimulation, telle que dans d'autres zones corticales distantes ou même une activité externe du cerveau. Dans ce cas, la réponse enregistrée ne serait pas un potentiel direct, mais plutôt une réponse intégrée, impliquant une plus grande population de neurones.

À ce jour, seules deux techniques d'enregistrement électrophysiologique permettent d'enregistrer des PE locaux et distants: l'électrocorticographie (ECoG, mesure directe invasive des zones corticales) et l'électroencéphalographie (EEG, mesure non invasive sur le crâne). En théorie, l'étude des caractéristiques des PE enregistrés peut également donner des informations sur la propagation du signal physiologique induit. En particulier, en corrélant les formes, les latences et les amplitudes des PE au type d'éléments neuronaux (par exemple fibre axonale, soma) et leur vitesse de conduction (par exemple myélinisée vs non myélinisés), on pourra supposer quels types de fibres sont activés.

Enregistrements ECoG peropératoires et potentiels évoqués

Les enregistrements présentés ci-dessous ont été réalisés sur six patients, après résection de la tumeur et une fois le patient rendormi (anesthésie générale) afin de ne pas perturber

le bon déroulement de la chirurgie. Le protocole expérimental mis en place pour réaliser les enregistrements ECoG peropératoires est détaillé ci-après.

Une ou deux bandes (strip) de quatre électrodes (ECoG) sont disposées sur la surface exposée du cortex. Les enregistrements sont réalisés en mode différentiel (contacts 1 à 3) et mode référencé (contact 4). Le mode différentiel consiste à effectuer la différence des potentiels mesurés par deux électrodes actives adjacentes. Ainsi, seule l'activité électrique locale (sous les électrodes) est enregistrée, ce qui augmente la résolution spatiale et la qualité de la mesure. La mesure en mode référencée est quant à elle réalisée entre une électrode active, placée sur le cortex, et une électrode de référence (point électriquement "neutre"), localisée sur le mastoïde ipsi-latéral à la zone tumorale. Les signaux sont d'abord amplifiés (gain de 1000) et filtrés ([0.5 Hz ; 3 kHz]). La fréquence d'acquisition est fixée à 10 kHz. Un filtre réjecteur de 50 Hz est aussi activé afin de s'affranchir au maximum du bruit électrique environnant très présent au bloc opératoire.

L'effet des différents paramètres de stimulation, tels que la fréquence et l'intensité ont aussi été étudiés. La modulation fréquentielle (de 1 Hz à 30 Hz) doit permettre de voir si les PEs observés correspondent à des réponses "intégrées" par le cerveau ou des réponses synchrones d'un petit pool de neurones uniquement. En effet, on peut s'attendre à ce qu'une réponse intégrée varie en fonction de la fréquence car cette dernière porte de l'information. A l'inverse, une réponse purement électrophysiologique directe d'un petit pool de neurones ne doit pas dépendre de la fréquence de stimulation. La modulation en amplitude a pour but de mettre en évidence le seuil de déclenchement des PEs.

Pré-requis méthodologiques

Les signaux ECoG enregistrés sont composés des activités électriques basale et évoquée du cerveau perturbées par le bruit électrique ambiant et l'artefact de stimulation. Des pré-requis méthodologiques sont nécessaires afin de différencier les signaux physiologiques des perturbations induites par la chaine de mesure.

Dans ce but, l'artéfact de stimulation a été caractérisé car non seulement ce pulse, mais aussi son filtrage peut conduire à de mauvaises interprétations. Les caractéristiques techniques de la chaine d'acquisition étant connues, le filtrage de l'artéfact a donc été

simulé. Cette modélisation a montré que des oscillations dues au filtre réjecteur de 50 Hz (filtre notch) pouvaient apparaître. De plus, ces oscillations présentent le même décours temporel que les potentiels évoqués (période d'oscillation et latences d'une vingtaine de millisecondes). Cependant, afin de pemettre une visualisation des potentiels évoqués en temps-réel, l'utilisation de ce filtre est nécessaire dans l'environnement bruité qu'est le bloc opératoire. De plus, avec l'utilisation du filtre notch, le moyennage direct des stimuli n'est plus adapté, la réponse de l'artéfact s'annulant uniquement en cas de stimulation avec polarité alternée .

Une première manipulation peut aider à la distinction du signal physiologique de la réponse de l'artefact: la validité de tout potentiel évoqué peut être vérifiée en inversant la polarité du courant de stimulation, i.e. en inversant les pôles de la sonde de stimulation. La polarité des potentiels physiologiques est conservée, quel que soit le sens des pôles, alors que celle de l'artefact est inversée. Dans la plupart des cas référencés dans la littérature, le courant de stimulation biphasique est alterné dans le seul but d'effacer les artefacts de stimulation lors du moyennage des signaux. Cependant moyenner, dans ce cas, empêche la détermination du bruit électrique induit par le système d'acquisition.

Ainsi, une attention particulière doit être portée aux perturbations potentiellement induites par le système, et plus particulièrement par le filtrage. Dans notre cas d'oscillations résultantes du filtrage de l'artefact de stimulation, il est dans un premier temps nécessaire d'étudier les stimulations non pas dans leur ensemble (moyenne), mais stimulus par stimulus. Ceci permet d'identifier et retirer précisément ces perturbations non-physiologiques [VGD$^+$17].

Algorithme de correction de la réponse de l'artéfact

Retirer la réponse de l'artefact de stimulation (oscillations) consiste à soustraire le patron de sa réponse dont on ne connait pas l'amplitude. Un algorithme permettant un retrait optimal de cette réponse a donc été développé. Ce dernier est basé sur la détection précise de la localisation de l'oscillation dans le signal suivie d'un retrait adaptatif de celle-ci. Dans l'optique d'une implémentation pour un traitement en temps réel, un calcul explicite est effectué (plutôt que des routines d'optimisation) à partir des extrema de l'oscillation. Le signal ECoG enregistré est composé de l'oscillation, du signal physiologique et de "bruit".

Pour limiter les effets de ces bruits dans la reconstruction du signal physiologique, une approximation linéaire au premier ordre en a été faite. Les composantes d'ordre supérieur ont été négligées.

L'algorithme a été appliqué avec succès sur des enregistrements ECoG peropératoires, permettant ainsi une meilleure visualisation des potentiels évoqués sur les signaux non moyennés.

Potentiels évoqués induits par la SED

Méthode d'analyse Sur tous les enregistrements ECoG réalisés, tous les canaux pour lesquels la tension mesurée excédait les ± 5 V ont été rejetés, au regard des spécifications techniques de l'amplificateur (fiabilité de la mesure entre ± 5 V). Ceci a conduit à ne conserver que 351 stimulations sur 568, tout patient et canaux confondus (SED corticale : 230/376 (61%); SED sous-corticale : 121/192 (63%)).

Pour chaque stimulation, les potentiels moyens ont été calculés en moyennant les stimuli synchronisés sur le début de l'artefact de stimulation. Même s'ils sont visibles sur les signaux moyennés, les potentiels ne sont pas toujours présents après chaque artéfact. Ainsi, un seuil de significativité a été défini, afin d'accepter ou rejeter les signaux. Si un minimum de 50 % des stimuli n'induit pas de PE, alors le signal est rejeté, ceci même si le PE est visible sur la moyenne. Malgré un certain nombre de stimulations, des potentiels évoqués n'ont été mesurés que sur 35 d'entre elles. Deux caractéristiques, latence et amplitudes, ont été étudiées sur les potentiels mesurés. Celles-ci sont calculées relativement à la position de l'artéfact de stimulation, à la fois sur le signal moyenné, mais aussi indépendamment sur chaque stimulus.

Trois groupes de potentiels ont été mesurés : réponses corticales directes (DCR), potentiel évoqué axono-cortical (ACEP) et cortico-axono-cortical (CACEP). Les potentiels corticaux ont été séparés en deux groupes suivant la distance entre le site de stimulation et leur site d'enregistrement. Les potentiels ont été considérés comme DCR pour des distances inférieures à 2 cm et CACEP pour des distances plus grandes.

Caractéristiques des potentiels évoqués Quels que soient les paramètres de stimulation (intensité, fréquence) utilisés, la SED appliquée sur la surface corticale au voisinage

(< 2 cm) des sites d'enregistrement induit des DCR. Celles-ci apparaissent avec une latence de 26 ms après le stimulus. Les DCRs mesurées chez les patients inclus dans l'étude sont semblables à celles décrites dans les travaux de Goldring et al. [GJH$^+$61]. Cependant, une augmentation de l'intensité de stimulation n'a ici jamais induit le second pic, ni les spikes.

Pour les ACEPs, deux profils d'ondes ont pu être observés. Le premier présente un unique pic $N1$ avec une latence d'environ 20 ms. Il s'agit très probablement des ACEPs mesurés précédement par Yamao et al. [YMK$^+$14] et Mandonnet et al. [MDP$^+$16]. Le second profil est composé du même pic $N1$ suivi après 20 ms d'un deuxième pic de même polarité.

La SED corticale évoque des potentiels à des distances de plus de 2 cm. Ces CACEPs consistent en un pic avec une latence de 26 ms correspondant au pic $N1$ défini par Matsumoto et al. [MNL$^+$04, MNL$^+$07]. Le second pic $N2$ mentionné dans ces études n'a jamais été mesuré dans notre cas.

Ainsi le pic $N1$ apparaît comme une composante commune aux trois types de potentiels mesurés (DCR, ACEP, CACEP). De plus, ce pic $N1$ apparaît avec la même latence quel que soit le site de stimulation. Cette particularité laisse penser que la latence du pic $N1$ est limitée et déterminée au niveau de la sortie corticale.

Par conséquent, nous ne sommes pas en mesure de déterminer si la propagation de la stimulation induisant les DCRs se fait via les fibres U courtes, car elle peut être purement cortico-corticale. Dans le cas des ACEP, la vitesse de conduction de l'axone stimulé n'a aucune influence sur la réponse négative puisque sa forme et ses latences sont similaires aux DCRs et aux CACEPs. Enfin, pour les CACEPs, si les potentiels d'action se propagent sur l'épaisseur corticale, des latences plus longues et une forme plus large seraient attendues. Dans nos enregistrements peropératoires ceux-ci ressemblent à des ACEP, ce qui suggère qu'ils se propagent à travers les voies de la substance blanche sous-corticale.

Goldring et al. [GHG94] ont défini ce pic $N1$ comme le "potentiel négatif principal". La forme de cette première onde négative (grand PE avec une longue latence) suggère qu'aucun axone myélinisé n'a été impliqué dans cette réponse. Il est attribué à la réponse corticale des potentiels excitateurs post-synaptiques des dendrites apicales [LC62, SGO64].

Li et Chou [LC62] ont montré que pour des stimulations basses des trains de spikes suivaient ce premier pic $N1$.

Perspectives

La mesure électrophysiologique au bloc opératoire reste difficile : chaque patient est unique ; les signaux sont faibles et acquis dans un environnement électroniquement bruité. Aujourd'hui, la fiabilité et la reproductibilité du protocole de mesure mis en place ont été validées. L'analyse des enregistrements recueillis sur six patients a donné des résultats prometteurs quant à la mise en évidence des effets de la stimulation électrique directe.
Il est donc maintenant nécessaire de pousser plus loin l'analyse des potentiels évoqués, afin d'étudier les effets immédiats et persistants de la SED sur la connectivité entre différents sites. Ainsi, la prochaine étape devrait porter sur la relation entre les potentiels évoqués et les perturbations fonctionnelles induites chez le patient éveillé. Ceci peut être notamment fait en appliquant la SED et en enregistrant des PE sur des sites corticaux fonctionnels et non-fonctionnels précis et déterminés par la cartographie à 60 Hz sur un patient éveillé. A terme, l'état électrophysiologique (niveau d'excitabilité par exemple) d'une aire donnée pourrait être determiné en temps réel et in vivo par l'analyse des potentiels évoqués.

Mieux comprendre les mécanismes sous-jacents à la SED, notamment au travers de la mesure des réponses électrophysiologiques, doit permettre de proposer des protocoles peropératoires plus objectivés. Cela doit rendre l'approche plus robuste encore aux variations liées au patient et à la chirurgie, et ainsi et diminuer plus encore les séquelles potentielles. Tout cela afin d'améliorer la planification chirurgicale et la qualité de vie des patients.

Contents

Nomenclature

ACEP Axono-cortical evoked potential

AP Action potential

CACEP Cortico-axono-cortical evoked potential

CCEP Cortico-cortical evoked potential

CSF Cerebrospinal fluid

DCR Direct cortical response

DES Direct electrical stimulation

DM Differential mode

DTI Diffusion tensor imaging

ECoG Electrocorticography

EEG Electroencephalography

EMG Electromyography

ENG Electroneurography

EP Evoked potential

EPSP Excitatory post-synaptic potential

ES Electrical stimulation

fMRI Functional magnetic resonance imaging

GA General anaesthesia

iEEG Intra-operative electroencephalography

IPSP Inhibitory post-synaptic potential

LA Local anaesthesia

LGG Low grade glioma

MEG Magnetoencephalography

MRI Magnetic resonance imaging

NoR Node of Ranvier

RM Referenced mode

RMP Resting membrane potential

SCEP Subcortico-cortical evoked potential

SEEG Stereoelectroencephalography

SLF Superior longitudinal fasciculus

SPES Single-pulse electrical stimulation

List of Figures

List of Tables

Introduction

Being able to change or inhibit the activity of a region or population of neurons in the brain is an essential approach in fundamental neuroscience, because it helps the researcher to determine the functional role of neurons. This approach is also important at a more applied level, such as when assessing the functional status of tissues around a particular lesion during neurosurgery. It is well known that electrical stimulation (ES) affects neural activity by modifying the voltage gradient across the neuronal membrane. When a current crosses cells, it can change their membrane potential and trigger neuronal responses. However, this general principle can be applied via several different in vivo approaches.

In vivo brain ES was developed more than a century ago. Indeed, Fritsch and Hitzig [FH09] first developed ES of the brain (in the dog) during the 19th century (1870). By stimulating the motor cortex and eliciting movements, they showed that the brain was divided into different functional areas. Direct application of ES to the exposed surface of the brain is usually referred to as direct electrical stimulation (DES). After this pioneering work, DES was used to characterise the organisation of the brain motor centres in the macaque [Fer74] and in great apes [SG01]. Leyton and Sherrington [LS17] reported the orderly mapping of different areas of the body along the precentral gyrus but noted a significant degree of overlap between the different representations (see also [Lem08]). During the same period, Krause [Kra09] and Cushing [Cus09] were among the first to perform DES on the human brain and thus elicit motor responses. Subsequent experiments with DES of the motor cortex in humans [PB37, Pen47] prompted the concept of a simplified somatotopic representation of the body on the cortical surface (the so-called homunculus). Very early on, some researchers attempted to relate the effects of DES to the functional and physiological properties of the cortex. Hence, Vogt and Vogt [VV19] used DES to link different brain functions to the underlying cortical architectonics. Foerster and Altenburger [FA35] were the first to use electrocorticography (ECoG) to record electrophysiological responses to DES in various parts of the brain distant from the motor

areas. Purpura et al. [PPF+57] used DES of the human cortex to study the contribution of dendritic potentials to the modulation of electrical activity at the surface of the brain.

DES (as used by Ferrier (1874) and Penfield (1947)) is still an important technique for the functional investigation of the human brain. In the last decades, DES was successfully used to guide resection during wide-awake neurosurgery of slow-growing, infiltrating brain tumours [Duf05, DBD07].

The "Awake brain surgery" combined with direct electrical stimulation (DES) mapping consists in removing some slow-growing brain tumour tissue (low-grade glioma , LGG) to delay its development while preserving the functions: in an awake patient, the surgeon performs an anatomo-functional mapping of the brain by electrically stimulating brain areas near the tumour to discriminate functional versus non-functional areas. During the surgery, the patient undertakes behavioural tasks of interest. The DES procedure associated to the intra-operative functional assessments is a critical aspect. However, our current understanding of the electrophysiological effects of DES remains limited. For instance, few is known about the spreading of DES currents within the brain, particularly through subcortical networks.

In light of these observations, this work aimed at better understanding the electrophysiological effects of DES during awake surgeries, and in the end, improving the protocol of electrical stimulation and the functional mapping. We performed electrophysiological intra-operative recordings on several cortical sites.

The structure of the thesis is as follows.

Chapter 1 gives a brief description of the diffuse low-grade glioma pathology and introduces the awake brain mapping surgery procedure. The biophysical principles of neural activity and ES of neural tissue are then detailed. A review of the evoked potentials measurement is finally described.

Chapter 2 deals with the design of an acquisition chain for intra-operative electrophysiological recordings of brain activity. The chapter also validates the developed set-up with cortical EPs recordings on one patient undergoing awake surgery of LGG. The criterion for the acquisition chain selection, the experimental setup and the protocols are explained.

In Chapter 3 a method of stimulation artefact removal is proposed, to disentangle the physiological signals from the purely electrical ones (only linked to the stimulus artefact).

Chapter 4 reports the intra-operative ECoG recordings performed on six patients. Evoked potentials obtained from the post-processing of these recordings, i.e. once the stimulation artefact algorithm applied, are then presented.

Chapter 5 summarizes the results and conclusions of this thesis and proposes perspectives for future investigations.

Chapter 1

Direct electrical stimulation and brain mapping.

Contents

1.1 Surgery of diffuse low-grade glioma

1.1.1 Low-grade gliomas (LGG)

Low-grade gliomas (LGG, WHO II) are slow-growing and infiltrative tumours. They follow three ways of evolution [Duf05]: (1) a continuous growth (about + 4 mm of diameter/ year); (2) a gradual invasion of white matter pathways ipsilateral to the tumour initially, then contralateral to the tumour via the corpus callosum and (3) an anaplastic transformation into high-grade gliomas. LGG systematically evolve into high-grade gliomas with a median of transformation around 7-8 years and a median of survival estimated at 10 years [WK03]. This transformation associated with the optimization of surgical techniques is the main reason for choosing the surgery. While the preventive excision of low-grade tumours has long seemed questionable, this option is now considered the most effective. The idea is to remove the tumour and the infiltrated tissue in an attempt to limit the tumour development and to delay its degeneration [DSL00]. During the period that precedes the degeneration of the tumour, and despite some minor cognitive abnormalities [TK04], the patients exhibit most of the time a normal neurological evaluation and have normal social and professional lives [WK03]. In fact, over 80% of LGG are revealed by epileptic seizures, effectively treated by antiepileptic drugs [DeA01].

The intraoperative use of DES during general or local anaesthesia has been widely recommended for the removal of slow-growing, infiltrating tumours located in eloquent areas [BR97, Duf05].

1.1.2 Awake surgery and direct electrical stimulation (DES)

During awake surgery, patients perform a number of neuropsychological tests while DES is applied to the cortical surface or to subcortical white matter pathways, in order to detect and thus preserve connectivity (especially for critical white matter pathways) (Fig. 1.1). By generating transient disturbances, DES enables the real-time detection of cortical areas and subcortical networks that are functionally essential during complex cognitive and motor tasks.

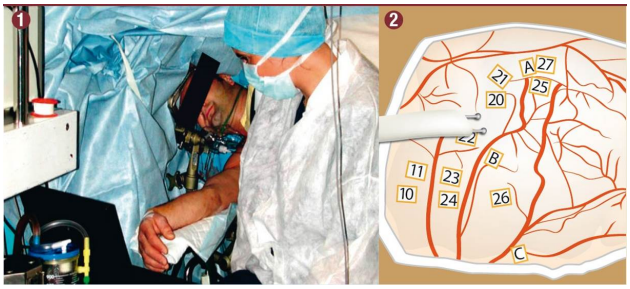

Figure 1.1: Awake surgery of LGG and functional brain mapping. 1. Awake surgery consists in removing an infiltrative tumour in an awake patient simultaneously performing neuropsychological functional tests. 2. The neurosurgeon uses DES to test areas close to the tumour and thus draws up a functional mapping of the brain. DES is applied both cortically and subcortically to detect and preserve connectivity in real-time. From the "Lettre de l'ARC n°11, decembre 2009 ".

1.1.2.1 Stimulation modalities

Electrical stimulation waveforms are defined by the following characteristics: the frequency F (number of pulses in one second, in Hz), the pulse-width P_w (sec.), the intensity I (mA) and the total duration of stimulation d (sec.). Patterns of stimulation can be either monophasic or biphasic with alternating polarity. In biphasic stimulation, the two pulses are separated by the inter-pulse duration ($[0 - P_w]$ ms), adjustable according to the stimulator properties.

Direct electrical stimulation (DES) consists in a constant-current biphasic square wave pulse delivered through a bipolar probe at frequencies of 50 – 60 Hz. Intensity is set from 1 to 6 mA (local anaesthesia), and 4 to 18 mA (general anaesthesia), with single-pulse duration between 0.3 and 1 ms. The intensity is increased by steps of 0.5 mA until stimulation elicits a response but without inducing seizures. DES is performed on the whole exposed area, every 5 mm^2 (as the electrode tips are spaced 5 mm apart), at least three non-consecutive times for each site. Intensities can be increased by steps of 1 – 2 mA for subcortical stimulations [Duf04].

The duration of the effective stimulation must be defined considering the mapped function: 1 s to induce positive motor and sensitive response and up to 4 s to inhibit the cognitive ones. In the context of *in vivo* functional brain mapping, the understanding of the effects of DES cannot be considered apart from intra-operative evaluations. The precision of these latter is critical for understanding the effects of DES and determining

the DES parameters that can maximise an effect or a perturbation of the investigated function.

1.1.2.2 Functional assessment

Defining a stimulated area as eloquent involves an adequate individual selection of functional tests, according to the lesion location, the pre-operative imagery and the functional assessment. Sensory-motor tests are quite simple: the patient must either stay passive or perform a periodic movement. In this case, the impact of DES is determined by evaluating the motion disturbances (involuntary movement, pins and needles feeling, etc.). Note that motor mapping can sometimes be performed under general anaesthesia. However, cognitive tasks such as calculation, language (e.g. picture naming), and visuo-spatial representation (line bisection) requires an important focus from the patient [MWD10]. Evaluation accuracy is brought by a neuropsychologist or a speech therapist who performs the assessment of the functional disturbance. Each cortical site is tested at least three non-consecutive times [OOLB89] to ensure reliability. If a functional disturbance is consistently induced the surgeon must then avoid the resection of the stimulated area.

As the functional mapping is performed all along the surgery (i.e. with both cortical and subcortical DES) it allows an effective monitoring of anatomo-functional gray and white matter pathways throughout the resection [DCS$^+$02, KLL$^+$04]. This technique enables functional mapping of the area near or within the tumour, so that as much non-functional, infiltrated tissue as possible can be removed while minimizing sequelae: the tumour resection is performed with regard to functional boundaries.

1.1.3 Clinical benefits of using DES in awake surgery

The value of DES for *in vivo* brain mapping is emphasised by the clinical observations recorded in the aftermath of wide-awake surgery. Indeed, the success of this surgical strategy depends largely on the excised tumour volume: no anaplastic transformations have been observed over a median follow-up time of 5–6 years, and postoperative MRI showed that all of the tumour has been removed [Duf05]. Given that these tumours are often widespread, large-scale resections (often around 90 cc) are frequently required [YMGD11]. Nevertheless, over 95% of all patients recover well; indeed, 3 months after surgery, none presented marked impairments on standard neurological scales [Duf05]. This point is illustrated in Figure 1.2. The good clinical outcomes observed for patients with

slow-growing tumours contrast with the "conventional" outcomes observed in the context of strokes, where most patients have permanent disabling impairments [BDD06, DBD07].

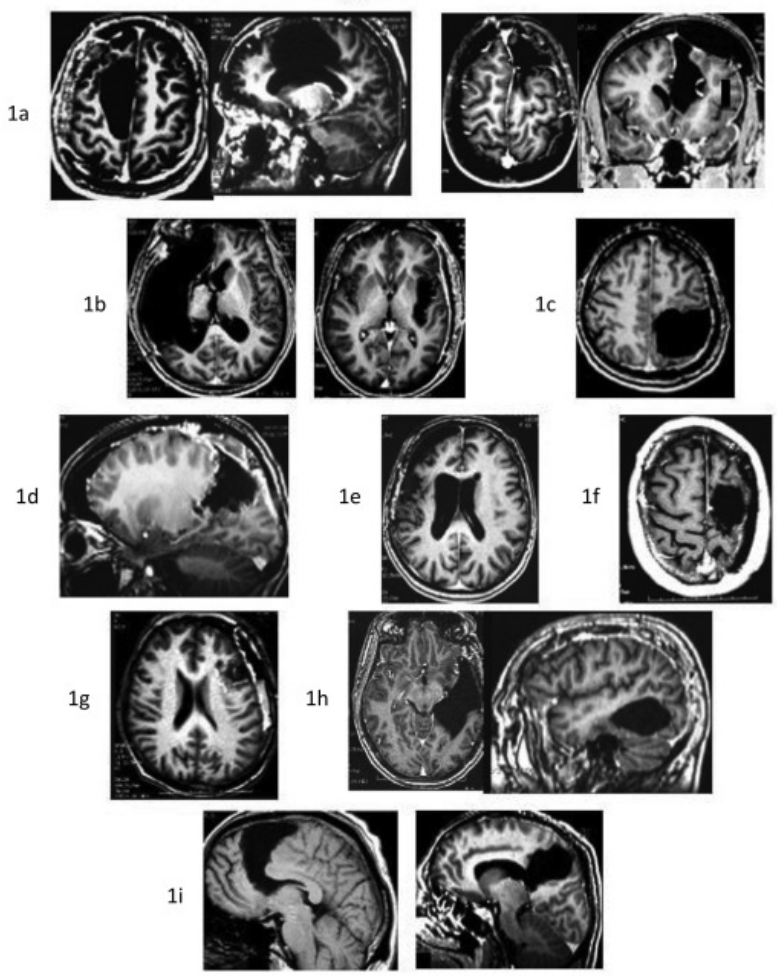

Figure 1.2: Examples of surgical resection of the tumor, without functional consequence (Karnofsky Score maintained between 90 and 100), as confirmed by neurological and neuropsychological repeated evaluations, and despite the removal of structures, which are classically considered as "critical": fronto-mesial regions, i.e. supplementary motor area ± cingulum (right or left) (Fig. 1a); insular lobe ± frontobasales and temporal structures (right or left) ± right striatum (Fig. 1b); primary sensorimotor area (Fig. 1c), parietal lobe (Fig. 1d); primary motor area of the face (nondominant side) (Fig. 1e) or hand (Fig. 1f) Broca's area (Fig. 1g); dominant temporal lobe left (Fig. 1h) and the corpus callosum (Fig. 1i). Adapted from [VRH+16].

1.2 Understanding the effects of DES on brain networks

Undoubtedly, intraoperative DES fuctional mapping during awake surgery of LGG has significantly improved the resection outcome, by identifying both cortical and subcortical structures essential for the function [DWHRZ+12]. Furthermore, DES has given us a better understanding of the brain's functional organisation [DSL00].

1.2.1 The brain connectome

In the long-standing localizationist organisation of the central nervous system, one given brain area corresponds to one and only one function (e.g. Wernicke's area, involved in the comprehension or understanding of written and spoken language). Nevertheless, insights from DES functional mapping have demonstrated that this vision was in no instance reflecting the real cerebral working.

On the contrary, brain functions are supported by vast parallel horizontally and vertically distributed circuits. This circuits are organised as (i) cortical epicentres likely synchronous connected via (ii) cortico-cortical association of white matter tracts (horizontal connections) and (iii) subcortical modulatory structures linked to the cortex (vertical connections). Thus, connectivity can be anatomically identified (Fig. 1.3):

- *Cortico-cortical connectivity* which anatomically links different cortical areas together. It mainly consists of U-fibers and associative pathways (local short connections of both sides of a sulcus, and longer intra- and inter-hemispherical connections respectively),
- *Cortico-subcortical connectivity* which consists in the projection pathway (from cortical areas to central grey nuclei or spinal cord).

Thanks to this anatomical connectivity, a function is not underpinned by a specific cortical area but by several distant areas working together via axonal connectivity. Moreover, the same hub can participate in several functions, depending on its temporary connections to other cortical areas. In other words, complex brain processes are possible only thanks to the dynamic interactions existing between subnetworks according to the task required.

By gathering cortical and axonal sites on which DES induces the same disturbances, different complex networks have been redefined: sensorymotor, visuospatial, language and socio-cognitive systems among others (see [Duf15] for a review).

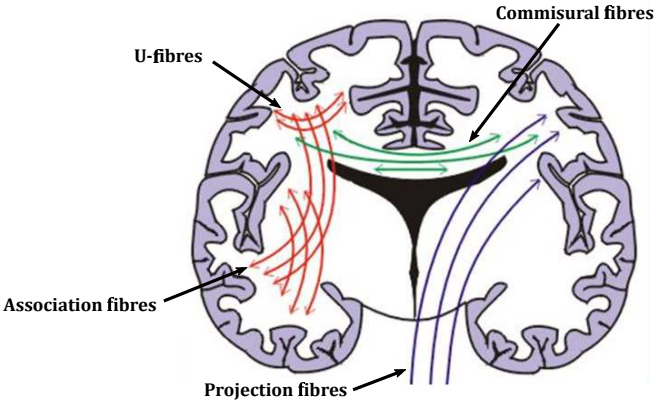

Figure 1.3: White matter connectivity: associative and projection pathways

1.2.2 Necessity of an individual brain mapping

Functional imagery on healthy subjects has shown an important inter-individual anatomo-functional variability. Indeed, although the neural structures are common to all, their organization remains proper to each. This specificity is even more marked for LGG patients. Indeed, the disturbances induced by inta-operative DES mapping have enabled to conclude that not only the networks interact together but can also compensate each other to a certain extent: that is the plasticity phenomenon. For example, DES performed in LGG surgery showed that cerebral functions can be redistributed to remote networks when brain copes with slow growing lesions [THMG$^+$14, DBD07].

Neuroplasticity is limited by the cortico-subcortical connectivity. Indeed, affecting the underlying pathways of a functional network prevents the synchronisation of the cortical epicentres. Identical functional disturbances will be induced by a subcortical lesion, independently from its anatomical localisation on the subcortical pathway. However, a cortical lesion may be counterbalanced by a redistribution of the cortical output, as long as subcortical connectivity is preserved [Duf05].

Interestingly, this phenomenon of reorganization seems to be favoured by slow-growing lesions. The astonishing ability of post-operative functional recovery could be thus explained by the slow-growing property of LGG. On the contrary, fast and acute lesions, such as cerebrovascular accidents, induce permanent functional deficits or a longer recovery [DBD07]. Finally, the brain shows a functional post-surgical re-organisation. In case of relapse, the functional mapping established on a second LGG resection will be slightly different from the first one.

Because of these variations, it is thus mandatory to perform functional mapping with DES for each patient. Knowledge of anatomical landmarks is essential, but insufficient for an optimal resection.

1.2.3 Reliability of the functional and behavioral effects of DES

Undoubtedly, DES improves the outcomes of surgery [Duf05, SB08a, SCL+08] in terms of maximum tumour removal and preservation of the patient's quality of life [DGM+08, SB08b] (for a recent meta-analysis, see [DWHRZ+12]). Furthermore, DES has given us a better understanding of the brain's functional organisation [DSL00]. However, do we really know how DES works in the brain?

Despite DES's effective use in tumour resection, many aspects have not been completely clarified. When DES was first used during surgery for epilepsy, it was assumed that transient disturbances were generated by applying DES to a functional (cortical) "epicenter" [OOLB89, MWD10]. This principle alone is, however, insufficient for the effective performance of wide-awake surgery. Brain mapping (cortical mapping, in this case) is mainly guided by the behavioural effects obtained with DES.

However, wide-awake brain surgery does require a very detailed knowledge of cortical and subcortical neuro-anatomy in order to both (i) determine *a priori* functional cortical epicentres and (ii) search for subcortical pathways and fascicles linking the functional cortical points together before corroborating them by DES. This latter approach searches the correlation between cortical and subcortical effects of DES based on precise hypotheses about neuro-anatomical networks. It is assumed that DES "desynchronises" functional points that are structurally linked together.

In other words, to ensure consistent, reliable effects of DES and thus effectively guide the surgery, DES cannot be applied without strong *a priori* hypotheses and detailed knowledge of how networks are organised. The neuro-anatomical hypotheses are then confirmed using DES.

1.2.4 DES clinical concerns

As described before, the main goal of awake surgery using DES is to maximize the tumour resection with respect to the functional boundaries to preserve the quality of life. DES mapping relies on the surgeon's detailed knowledge of both cortical and subcortical neuroanatomy in order to (i) determine the functional cortical epicentres *a priori* and (ii) search for the subcortical pathways binding these cortical outputs together before confirmation by DES mapping.

To date, it is possible to perform LGG resection with a very good accuracy ($\sim 100\%$) when using the standard DES technique(see section 1.1.2.1) in other words, false negatives are rarely induced by DES, which offers a good functional preservation. This is why DES is currently considered as the gold standard for brain mapping in awake surgery of LGG.

However, the lack of specificity, to a low extent, is the main disadvantage of DES mapping [MWD10]. Indeed, false positives can be induced by DES (i.e. the stimulated area is functional) whereas the resection was possible. Firstly, the stimulation could have reached an other network, essential to the function, due to the electrical conduction along axons. Secondly, the stimulated area could be functionnaly compensated by other epicentres in a close region, thanks to the plasticity mechanisms. In both cases, the resection would not have induced permanent deficits. Moreover, the intraoperative assessment of a function is generally subjective (especially for cognitive tasks) and might significantly depend on the patient's level of commitment (consciousness and cooperativeness). Finally, the parameters of ES can also have an impact on the mapping as they are important for the activation/inhibition of the neuronal elements - and thus of the network (see section 1.4.1 for details).

1.3 Probing the functional networks connectivity

1.3.1 Rationale of this work

To maximise the resection and validate the anatomical and functional connectivity, knowing in real-time and *in vivo* the electrophysiological state of the activated functional network could be useful to understand how cortical and axonal DES work.

It is believed that each functional area assessed by ES is an input gate to a large-scale cortico-cortical and cortico-subcortical network rather than an isolated discrete functional site. Recording the remote effects of subcortical (axonal) ES would probe the networks recruitment and organisation.

In other words, **measuring** and **understanding** the **electrophysiological effects of DES** is necessary to **probe *in vivo* and in real-time the spatial (and temporal) connectivity and dynamics of both short- and long-range networks**.

Such information is expected to give a better knowledge of the neurophysiological mechanisms underlying DES involved at the scale of both short and long-range networks. Over time, this would enable developing operative protocol less subjective and more robust to the patient and the surgery variations, and thus, decrease the potential sequelae.

1.3.2 Cortical vs. subcortical DES effects: a first hypothesis

DES applied to white matter pathways and axons has major behavioural effects. For instance, Thiebaut de Schotten et al. [dSUD$^+$05] demonstrated that stimulation of the right inferior parietal lobule or the caudal superior temporal gyrus (but not the rostral superior temporal gyrus) determined rightward deviations in a line bisection task. However, the strongest shifts occurred with subcortical stimulation. Fibre tracking identified the stimulated site as a portion of the superior longitudinal fasciculus. This result suggests that the subcortical effects of DES are primarily related to alteration of the communication between different areas of the brain. In this case, DES might perturb a network of interconnected brain areas (rather than a single brain area) when it is applied at the cortical surface. This was confirmed by applying DES to the investigation of the connectome underlying language [Duf14, DMGM14].

This concept is even more evident when considering inter-hemispheric coordination (bimanual coordination, for instance). Rech et al. [RHMGD14] observed that during bimanual coordination, all patients completely stopped moving both hands during unilateral subcortical stimulation. These findings (i) suggest that a bilateral corticosubcortical network connecting the premotor cortices, basal ganglia and the spinal cord is involved in the control of bimanual coordination, and (ii) demonstrate that subcortical stimulation of white matter pathways disconnects distant and remote cortical areas that are usually considered to act synergistically during bimanual coordination. Interestingly, the effects observed by Rech et al. were also specific to movement coordination.

It is often considered that DES of white matter can inhibit the corresponding cortico-cortical functional network (for a review, see [Duf15]). It would thus be possible to apply DES subcortically with a certain degree of specificity. Effects may selectively and directly affect nervous communication along white matter pathways and indirectly affect cortical areas that are connected through transiently and virtually disconnected pathways. Information exchange and communication within the network may thus be altered. This interpretation is explained in Figure 1.4.

Figures 1.4a-A) and 1.4b-A) represents a schematic view of the hypothesised cortical vs. subcortical stimulation effects on functional networks. For a given specific function involving an A to B network, applying cortically DES in A "desynchronizes" A from B and impairs the function specifically. Same impairments are induced when DES is applied to the cortical site B. Both functional and behavioural effects of cortical DES are independent of the orientation of the electrode tips (an isotropic effect). Increasing the intensity yields to more complex behavioural effects. Subcortical stimulation affects the networks in a different manner. Indeed, for a given specific function involving an A to B network, application of DES to the subcortical site C (i.e. on the white matter associative pathway linking A and B) "desynchronizes" A and B and impairs the function specifically. In contrast to cortical DES, a change in the orientation of the electrode tips has different, more complex behavioural effects if associative white matter pathways are affected (an anisotropic effect). Increasing the intensity also yields to more complex behavioural effects. The same rationale can be applied when the boundaries of the cavity are near different projection pathways.

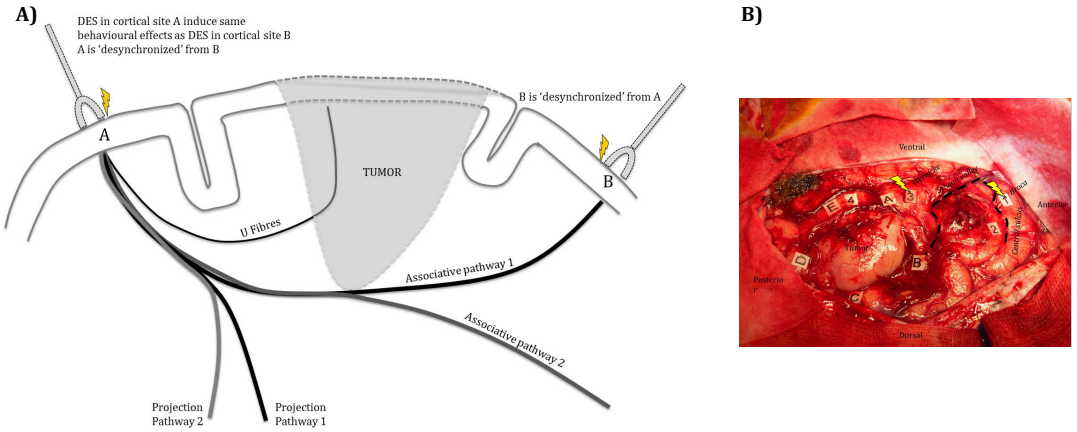

(a) Cortical mapping.

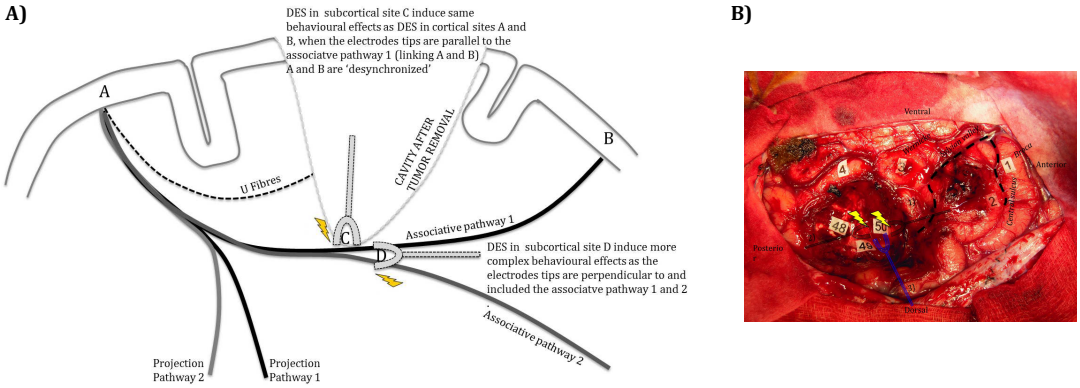

(b) Subcortical mapping.

Figure 1.4: Cortical vs. subcortical stimulation. Schematic behavioural effects and uses of DES during awake brain surgery (left panels) and the corresponding intra-operative views (right panels).

These hypothesis are based on the intraoperative functional mapping. Figures 1.4a-B) and 1.4b-B) represents an intraoperative view of mapping in a patient with a diffuse low-grade glioma in the parietal area. DES is set to ∼2 mA and delivered at a frequency of 60 Hz. Independently of the orientation of the electrode tips, DES (yellow lightning symbols) applied cortically to area 1 (the ventral premotor cortex) or area 3 (Wernicke's area) induced postural (joint) disorders. It is known that these two sites are linked by the lateral part of the superior longitudinal fascicles [DMGM14]. This link is then confirmed by subcortical mapping with DES applied to a white matter pathway, also inducing postural (joint) disorders. If the current intensity is increased over ∼2 mA, more complex behavioural effects can be observed (isotropic spreading). The letters correspond to the tumour's margins: 4 is a site for which anomia was revealed by DES, and 2 is a

somatosensorial site for the face (in the retrocentral gyrus). DES applied to area 50 (the lateral portion of the superior longitudinal fascicle) induced postural (joint) disorders, confirming the role of this pathway in linking areas 1 and 3. Electrode tips are parallel to the fascicle. When applied to areas 48 and 49 (the deeper portion of the superior longitudinal fascicle, i.e. the arcuate fascicle), DES induced phonemic paraphasia. The electrode tips are parallel to the fascicle. When electrode tips are perpendicular (blue electrodes) to the fascicles 48/49 and 50, DES induces a more complex effect, including postural (joint) disorders and phonological paraphasia. Note that this complex effect is induced without increasing the current intensity. Thus, at the subcortical level, the effects of the DES depend on the orientation of electrodes tips with respect to the fascicles (i.e. anisotropic spreading) [MP11].

1.3.3 Interest of electrophysiological recordings for brain mapping

In physiology, an evoked potential is defined as the modification of the electrical activity of the nervous system, in response to an external stimulus. Recording the EPs give information on the working process of the stimulated pathway. To evaluate the network organisation of the human connectome, measures of connectivity can be used.

The connections between functional epicentres involved in a specific neural network can be defined by structural, functional and effective connectivity. These three approaches do not assess connectivity at the same level. Structural connectivity stands for the anatomical connections between pools of neurons or brain areas at the level of white matter tracts. This mapping can be performed thanks to non-invasive neuroimaging (magnetic resonance imaging (MRI) and diffusion tensor imaging (DTI)).

However, evoked potentials mapping provides a unique opportunity to track, *in vivo* and directly, the connectivity between both cortical and subcortical areas: i.e. how information between two connected sites A and B flows from A to B and the other way round.

Thus, DES combined with intra-operative electrophysiological recordings can be used to probe *in vivo* and in real-time the spatiotemporal connectivity and dynamics of both short- and long-range networks. In this vein and in the context of awake brain surgery, it is of a certain interest to measure EP:

- *Cortically*, when cortical DES is applied close to the recording point. This would highlight the local effects of DES. If the stimulated site is supposed functional, it would also assess the delineation of the cortical area corresponding to the function.

- *Subcortically and cortically* when DES is applied on the white matter pathways revealed by tumour resection, or on its assumed cortical output. These measurements would shed new light on the different stages of the propagation of DES within neural networks and on the axonal connectivity between functional cortical regions.

- *At remote distances* from the DES site, such as at other distant cortical areas or even external brain activity. In this cases, the recorded response would not be the direct EPs but rather an integrated response, involving a wider population of neurons.

To date, only two electrophysiological recording techniques enable the recording of local and remote EPs: electrocorticography (ECoG, invasive direct measure of cortical areas) and electroencephalography (EEG, non-invasive measurement from the skull). These recording techniques of brain activity are detailed further down the document. In theory, investigating the recorded EPs features can also give information on the induced physiological signal propagation. In particular, by correlating shapes, latencies and amplitudes of the EPs to the neuronal elements type (e.g. axonal fibre, soma) and their conduction velocity (e.g. myelinated vs. unmyelinated), it is possible to assume which types of fibre are activated.

1.4 Evoked potentials induced by direct electrical stimulation

Potentials evoked by DES consists in the electrophysiological response of a bunch of neuronal elements. Their diversity and complex structuration make understanding the effects of brain ES challenging. Indeed, it is unclear in many cases what neuronal elements are activated by the stimulation [Ran75]. Knowledge from biophysic, especially given by ES of the peripheral nervous system, can give leads on the understanding of activated neural structures.

1.4.1 Physiology of neuronal activity

1.4.1.1 The action potential

Most of the neurons in the nervous system have the same main structures: a cell body (soma), an axon, potentially wrapped by a myelin sheath, and dendrites. Once a natural action potential (AP) has been initiated in the soma, it flows without attenuation along the membrane of the axon to the next neural element, at the synapse junction point.

The vast majority of synapses in the mammalian nervous system are classical axo-dendritic synapses (axon synapses upon a dendrite). The junction between two neurons occurs at the synaptic cleft. The arrival of an AP at the level of the pre-synaptic element induces the release of a neurotransmitter at this junction. Depending on the nature of this molecule, the second neuron can be either hyperpolarized or depolarized. The resulting induced post-synaptic AP will be excitatory (EPSP) or inhibitory (IPSP) respectively. As the soma is reached by several synapses, the post-synaptic excitation is determined by the summation of all EPSPs and IPSPs.

If EPSPs are more important, synaptic currents produce brief changes in the distribution of charge along the somatic membrane, which elicits another AP up to the axon. Voltage-gated sodium (Na^+) and potassium (K^+) ionic channels are sensitive to fluctuations of the axon membrane potential. The APs are carried along the axon by the sequential opening and closing of these gated channels. The resting membrane potential (RMP) typically varies between -60 mV and -100 mV.

In response to the synaptic current, Na^+ ions enter the cell so that the inside becomes less negative [HH52]. The axon's membrane potential increases as a function of the number of open channels (depolarisation). An axonal AP is triggered when the potential reaches the activation threshold of the cell, and the membrane voltage rises by up to around 30 mV. Once this maximum voltage is reached, the axon's membrane potential drops back to the RMP as the Na^+ channels close and the K^+ channels open (repolarisation). However,the significant release of K^+ ions hyper-polarises the cell, leading to a membrane potential below the RMP. Lastly, a few K^+ ions diffuse out of the cell through potassium leakage channels, bringing the cell back to its RMP. Another axonal AP cannot be generated until the membrane potential has returned to the activation threshold; this period is referred to as the absolute refractory period. However, once this period has ended, the initiation

of a second AP is inhibited but not impossible (during the relative refractory period). These mechanisms are illustrated in Figure 1.5.

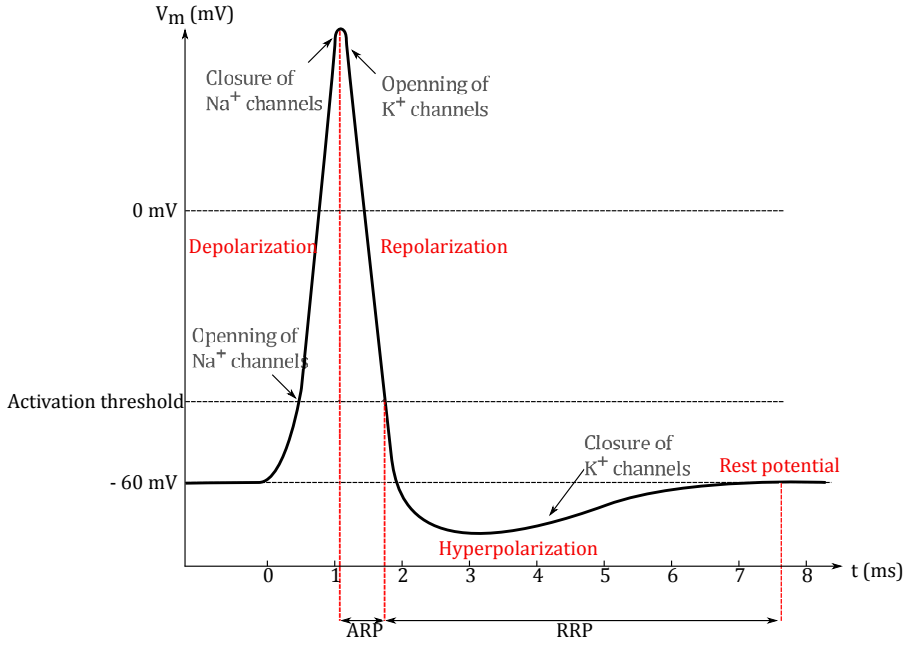

Figure 1.5: A natural AP: transmembrane axon potential (V_m) and ion channels [VRH+16].

The conduction velocity of an AP along an axon is influenced by both the diameter of the axon and its resistance to current leakage. Because the axon membrane is not a perfect insulator, some current leaks out of the axon. Some axons have an insulating myelin sheath that prevents current leakage. Conduction velocities range from 0.5 to 10 ms^{-1} in unmyelinated axons but can be as high as 150 ms^{-1} in myelinated axons [PAF01]).

1.4.1.2 Brain electrical activity

When measuring brain electrical activity, the potential recorded at a given location (with respect to a reference potential) consists in the superimposition of all electrical activities of neuronal cells within a volume of brain tissue. The extracellular potential is thus a combination of all potentials variations from dendrites, soma, axons, etc. The characteristics of the recorded signals (brain activity) depend on the properties of these electrical sources. The amount and specificity of the recorded information depend on the distance between the recording point and the electrical point. The further away from the source, the less specific the signal is. Indeed, the electrical potential amplitude decreases with

the inverse of the recording-emitting distance and more neuronal elements contributions are recorded when this distance increases.

1.4.2 Electrical stimulation of nervous system

1.4.2.1 Electrical stimulation technical principles

Electrical stimulation (charge-injection) is always performed between two points: the working electrode and the counter electrode. The delivered current depends on the difference between the two electrodes own potentials. The charge-injection in the tissue can be controlled using two different methods: the voltage-controlled stimulation and current-controlled stimulation. For brain ES, the latter one is commonly used. Indeed, as explained hereinafter, the stimulation intensity is the crucial parameter for activating neurons. In case of voltage-controlled ES, the delivered intensity cannot be directly monitored, as it depends on the stimulated environment (of unknown resistivity, Ohm law).

Stimulation profiles Current can be delivered in two ways. A monophasic stimulation (monophasic pulse) consists in a current that is passed from the working electrode to the counter electrode for a given period a time (pulse duration or pulse width P_w). This pulse can be followed by second pulse with a reversed direction: this two-phase stimulation is then called biphasic.

The amount of charge injected by one pulse is given by the product of its current intensity by its pulse width. In the biphasic case, the stimulation is balanced when the charges delivered by each pulses are equals. Balancing the amount of charges aims at avoiding electrode and tissue damages (see [MBJ05] for details on possible damages in ES).

In monophasic stimulation, the pulse shape is designed to elicit activation of the stimulated element (the active phase). In biphasic stimulation, one of the pulses is the active phase, while the other pulse balance the charges (reversal phase). Usually, the active phase consists in a cathodic pulse (negative), where the working electrode is driven negative with respect to its pre-pulse potential and to the counter electrode. The passive phase stands for an anodic (positive) pulse, where the working electrode is driven positive. In some cases, pulses can be separated by a specific interval, the inter-pulse, and the anodic

pulse can induce activation (not discussed here, [MBJ05]).

Stimulations are characterised by some key parameters (Fig. 1.6): the frequency F, the pulse width P_w, the current intensity I, the inter-pulse duration d_{ip} and the stimulus train duration (duration of the stimulation phase).

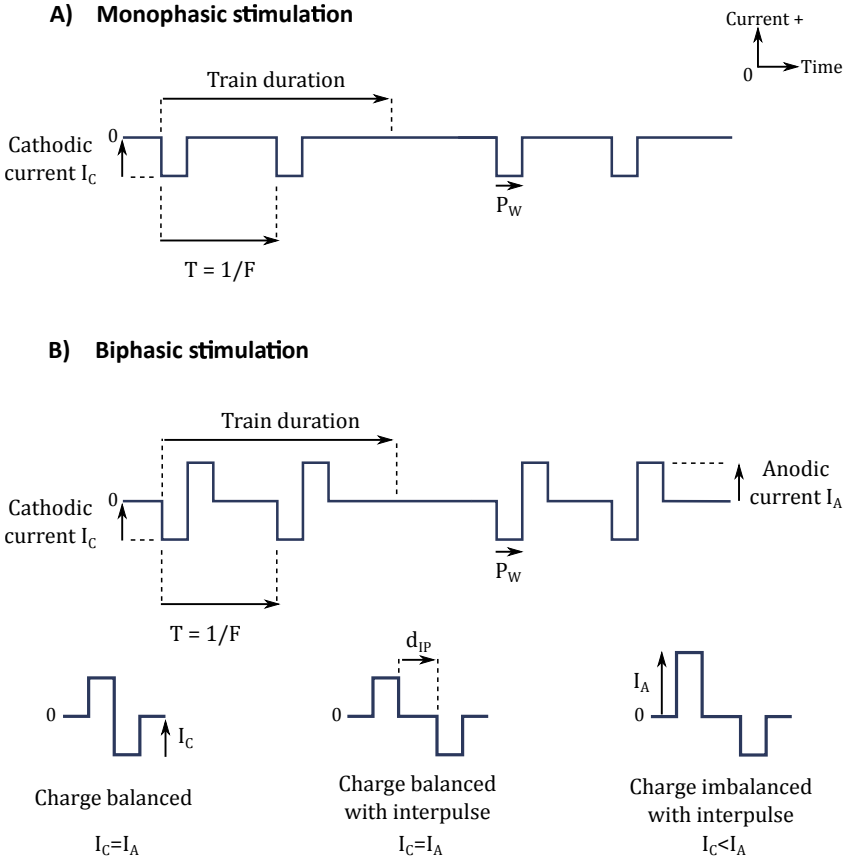

Figure 1.6: Stimulation types and parameters

Multipolar stimulation Different electrode configurations can be used to perform ES. Even if two electrodes are always necessary to deliver a current, the following N-polar configurations are defined, according to the number N of active (delivering the active pulse) electrodes (poles) involved in the stimulation (see Figure 1.7):

- *Unipolar or monopolar stimulation*: the working electrode is set on the targeted tissue to stimulate while the counter electrode, named the reference electrode, is placed at a distant site,

- *Bipolar stimulation*: both working and counter electrodes are a few-centimetres apart and located on the neuronal element. In biphasic stimulation, anodic and cathodic electrodes are reversed between the first and second phase (pulse) of stimulation,
- *N-polar configuration:* the bipolar configuration can be extended to N electrodes, with several anodic and cathodic electrodes (at least one of each, e.g. one cathode, two anodes).

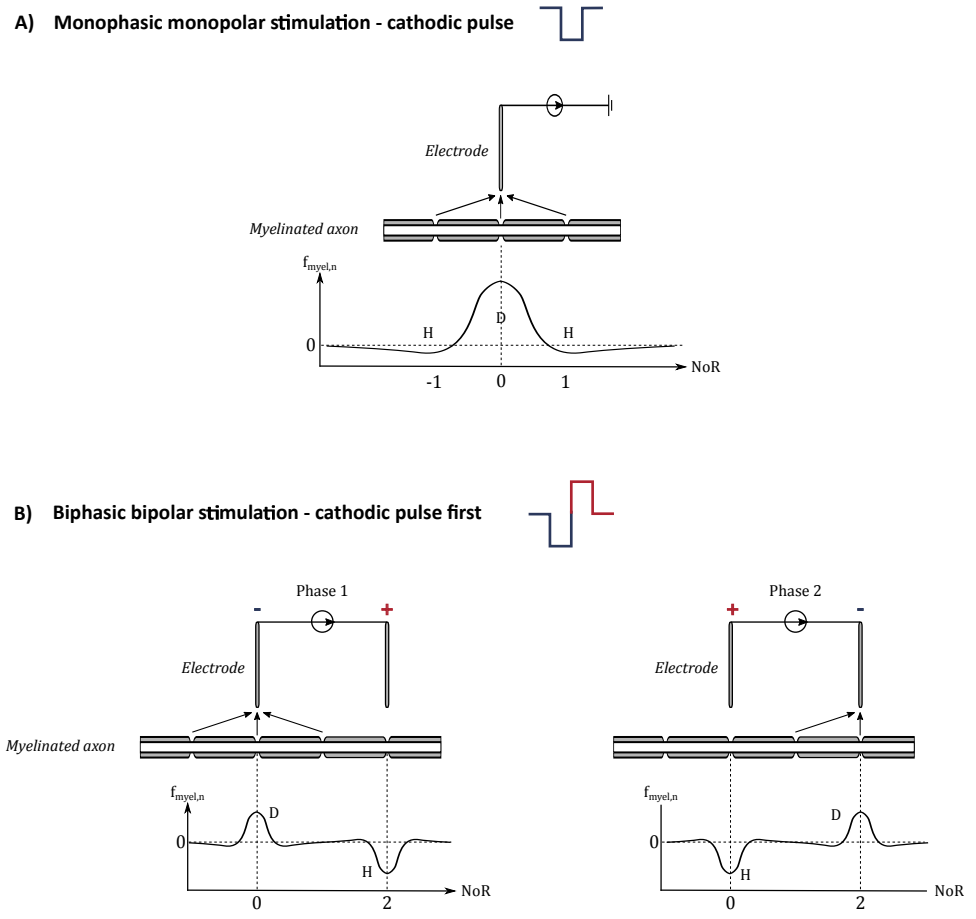

Figure 1.7: Stimulation configuration and the resulting activating function $f_{myel,n}$ at the n node of Ranver (NoR). D: depolarisation – H: hyperpolarisation.

1.4.2.2 Activation of neuronal elements by electrical stimulation

The effects of electrical stimulation of neuronal elements have been well characterized for ES of neuronal fibers (axon), especially when myelinated. Even if the brain is a

complex system of diverse neuronal elements, the knowledge from axonal ES principles can give insights on direct brain stimulation effects: how could an electrical current stimulus activate a neuronal element? In the following part, the general working principle of ES configurations and the impact of ES parameters are succinctly described. For a detailed biophysic see Vincent et al. [VRH+16].

The activating function To understand and predict the activation of a nerve fibre (depolarisation or hyperpolarisation by an electrical pulse), Warman et al. [WGD92] and Rattay [Rat99] have defined the concept of *activating function*. The activating function f_n has been described for myelinated axons and represents spatially the axon's membrane state of polarisation (Fig. 1.7): depolarisation when $f_n > 0$ (cathodic pulse), hyperpolarisation when $f_n < 0$ (anodic pulse).

The anodal surround and bipolar stimulation As explained above, cathodic monopolar stimulation leads to membrane depolarisation under the electrode tip and hyperpolarisation on either side. During monopolar stimulation, APs are generated on each side of the stimulation point and propagate away in opposite directions. However, an AP generated at a depolarised site on the stimulated fibre can only cross the hyperpolarised area if the latter is not too large. This effect (known as the "anodal surround") prevents the generation of APs in a zone close to the electrode [Dur99]. Bipolar stimulation is used to force the current to propagate in a single direction. The fibre is then subjected to both cathodic and anodic stimulations. One electrode tip (the cathode) delivers a negative current and the other tip (the anode) delivers a positive one. By increasing the width of hyperpolarisation, i.e. the current amplitude, the AP generated by the cathode (and which goes towards the anode) can be blocked [Ran75].

Moreover, in the case of bipolar stimulation, the activating function decreases more rapidly in function of the distance from the stimulation point. Thus, bipolar stimulation is more focal than monopolar stimulation.

Determination of ES parameters for optimized and safe stimulation When designing a stimulation protocol, both pulse intensity and duration must be chosen carefully.

First of all, to be effective, the electrical stimulus has to be long enough and intense enough to induce a change in the membrane potential that exceeds the natural excitation

threshold. In fact, the activation of neural elements in the central nervous system follows the principle of an "all-or-none" response. The relation between the pulse duration P_w and the minimal intensity I_{th} necessary to initiate an AP is given by the strength-duration curve (Fig. 1.8).

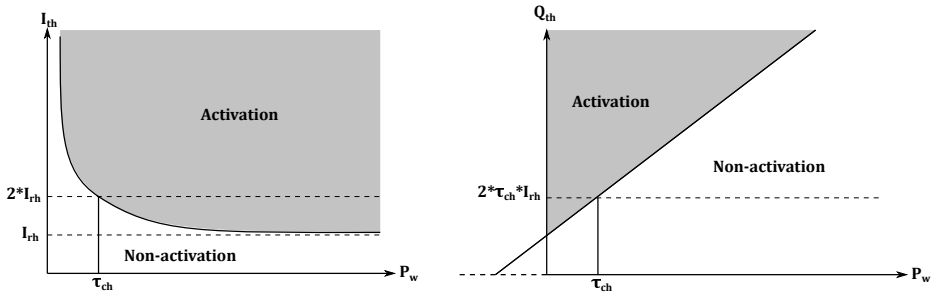

Figure 1.8: Strength-duration curve and electrical charge necessary to induce an AP.

The smallest current able to activate the fibre is called the rheobase current I_{rh}. Moreover, the quantity of charge Q_{th} injected by the stimulation must be as low as possible, so as not to damage the stimulated fibre and the electrode material [MBJ05]. In theory, the value of Q_{th} is lowest when the pulse duration P_w is infinitely short, i.e. when the stimulation current I_{th} is minimal. Optimal stimulation should thus minimize both the intensity and the quantity of current. The pulse duration at this point is called the chronaxie τ_{ch} (Fig. 1.8). The current amplitude at $P_w = \tau_{ch}$ is twice the rheobasic intensity [Wei90, Lap07].

Chronaxies of the different main neuronal elements (Table 1.1) have been determined experimentally.

Table 1.1: Chronaxie for different elements of a neuron [Ran75].

Neural element	Chronaxies range (ms)
Cell bodies	1 – 10
Unmyelinated axons	0.4 – 6
Myelinated axons	
Small	0.2 – 0.7
Large	0.05 – 0.15

Even though the chronaxie is often considered to be a critical parameter in stimulation protocols [BHLK12, MWD10], standard chronaxie values have been determined in specific environmental conditions. Given that the environmental factors are independent of the type of neural tissue stimulated, they can significantly limit the utility of chronaxie when determining optimal ES parameters. Thus, the above-mentioned theory should be applied very cautiously and cannot be used solely to determine the ES settings (especially for *in vivo* ES of the brain).

1.4.3 From extracellular stimulation of an axon to brain direct electrical stimulation

1.4.3.1 DES parameters: an empirical setting

Even if DES parameters are supposed to be in accordance to the above-mentioned biophysical principles, they appear to have been empirically chosen since Penfield's work. Table 1.2 provides an overview of the stimulation parameters used in a number of DES studies. It is generally acknowledged (for safety reasons) that the charge density should not exceed 40 $\mu C.cm^2$ per phase [AM87, UG86]. However, the majority of the charge densities used in brain stimulation protocols exceeds this value. Indeed, ES parameters are commonly set to 0.2 – 1 ms (for pulse duration) and 1 – 15 mA (for intensity). Thus, on average, the amount of charge per pulse delivered by DES ranges from 0.4 to 37.5 nC.

According to Ranck et al. [Ran75], parameters (current amplitude and pulse duration) set for DES in epilepsy mainly target axons. However, DES used in most awake-surgical procedures is at the very lower limit of cell bodies activation (Fig. 1.9). Importantly, even if the chronaxie is often mentioned as essential in the setting of DES parameters, no single strength-duration curve can fit all the studies.

These results have to be considered with caution, since the safety limit was determined in animal studies. Gordon et al. [GLR+90] published several explanations for the difference between the supposed safety limit and the charge density actually used in DES: external probe vs. implanted stimulation (ECoG electrode), stimulation train duration and total stimulation schedule. As DES is only performed sporadically, i.e. only through the surgery, it seems that higher charge densities can be delivered to the human cortex without inducing structural damages.

Independently from these chronaxie concerns, it should be noted that it was initially recommended to increase DES current intensity by 2 mA when applied subcortically [BR97]. This amplitude modulation is neither logical nor necessary, as white matter tracts (myelinated axons) excitability is higher than the cortical structures one. However, increasing the intensity is clinically relevant as it lowers the risk of epileptic seizure for subcortical DES. Taken as a whole, this strongly suggests that DES parameters are mostly set empirically, as no biophysical rationale explains its parameters.

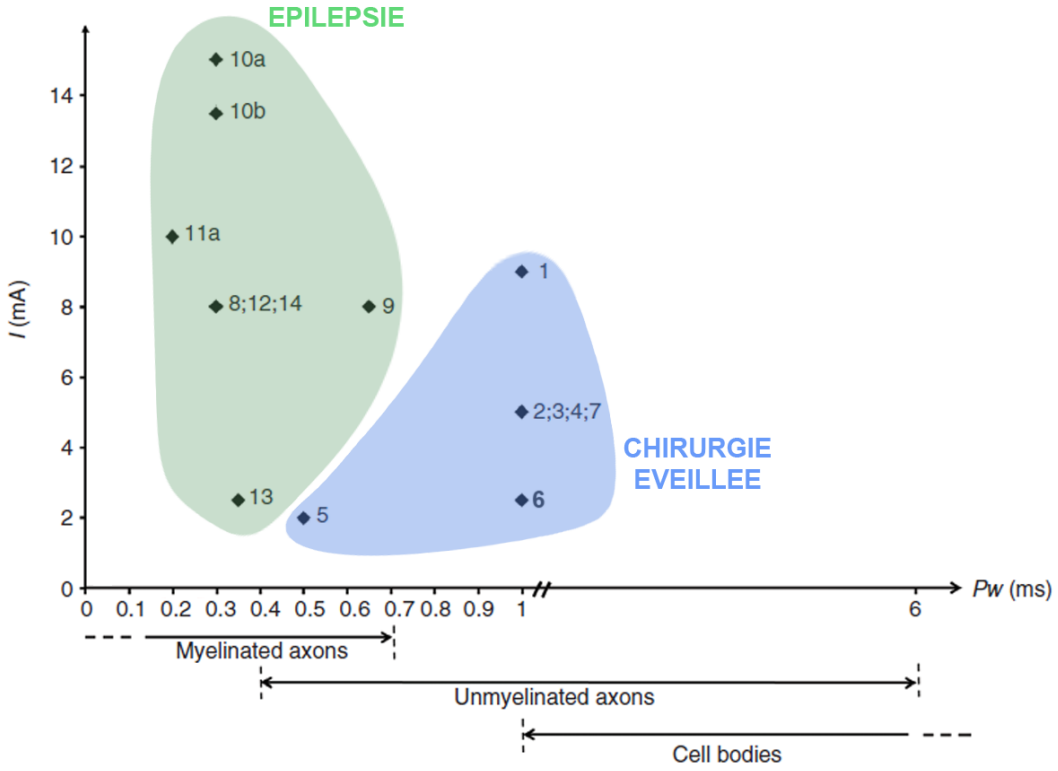

Figure 1.9: Strenght-duration curves for the studies listed in Table 1.2. Adapted from [VRH+16]

1.4.3.2 From biophysic theory to its application for brain ES.

Understanding the stimulation's configuration and parameters is essential to perform ES of neural tissues. Actually, depending on their setting (orientation of the probe, amount of charge delivered, etc.), different neuronal element will be activated. It is thus difficult to know to what extent the recorded brain activity is induced by the stimulation current diffusion or by the propagation of the natural neural activity through the networks.

Table 1.2: Main characteristics of various DES protocols. Adapted from [VRH+16]

References		Goal	Frequency (Hz)	Intensity (mA)	Pulse duration (ms)	Charge (µC) min	Charge (µC) max	Stimuli	Stimulation
Awake surgery - External eletrode tip									
(1)	Berger et al., 1993	Brain mapping during awake surgery	60	2 - 16	1	2	16	biphasic	bipolar
(2)	Duffau et al., 2008		60	2 - 8	1	2	8	biphasic	bipolar
(3)	Thiebaut de Schotten et al., 2005		60	2 - 8	1	2	8	biphasic	bipolar
(4)	Desmurget et al., 2009		60	2 - 8	1	2	8	biphasic	bipolar
(5)	Bello et al., 2014		60	≥ 2	0.5	1		biphasic	bipolar
(6)	Rech et al., 2013		60	1 - 4	1	1	4	biphasic	bipolar
(7)	Tate et al., 2014		60	2 - 8	1	2	8	biphasic	bipolar
Epilepsy – Implanted grids									
(8)	Crone et al., 1998	Mapping sensorimotor cortex	50	1 - 15	0.3	0.3	4.5	monophasix	bipolar
(9)	Hammer et al., 2002	Focal clonus elicited by ES of motor cortex	1 - 50	1 - 15	0.3 - 1	0.3	15	monophasic + (biphasic)	monopolar
(10a)	Matsumoto et al., 2004, 2007	Brain mapping	50	*leq* 15	0.3	4.5		biphasic	bipolar
(10b)		CCEP	1	12 - 15	0.3	3.6	4.5	single pulse	bipolar
(11a)	Keller et al., 2014	CCEP	0.5	10	0.2	2		single pulse	bipolar
(11b)		Brain mapping	20 -50	3 - 15	x	x		x	bipolar
(12)	Yamao et al., 2015	Neural correlates between laughter and mirth	50	1 - 15	0.3	0.3	4.5	single pulse	bipolar
(13)	Vansteensel et al., 2013	Mapping motor cortex	50	1 - 4	0.2 - 0.5	0.2	2	monophasic	bipolar
(14)	Sinai et al., 2005	Mapping naming	50	1 - 15	0.3	0.3	4.5	biphasic	bipolar

Biophysical principles are well known for the ES of unitary neuronal fibres or of small groups of neurons. However, in the case of brain cortical and subcortical stimulation, theses principles cannot be applied directly. Indeed, numerous unknowns remain on the brain architectony relatively to the ES. For example, little is known on the brain neuronal organisation, fibres orientation, neurons characteristics and the stimulation probe orientation relatively to the fibres.

Knowing the stimulation configuration (parameters, probe orientation, etc.) still gives insights, although limited, on how and which neuronal elements are activated. Understanding the effects of ES parameters on brain stimulation could lead to new paradigms of stimulation, which may be more optimal. Nevertheless, these aspects have been poorly investigated.

1.4.4 State of the art on evoked potentials induced by direct cortical and subcortical electrical stimulation

Electrical stimulation can induce both local – underneath the stimulation point, or distant effects, by activating a certain amount of neuronal networks. This activation leads to potential changes that can be recorded to understand the functional networks organisation. In the literature reviewed below, EPs were generally acquired with the following parameters: sampling frequency ranging from 2 to 5 kHz, bandpass filter of 0.08 to 1,500 Hz.

1.4.4.1 Direct cortical responses

Adrian et al. [Adr36] defined the "direct cortical response" (DCR) as the immediate electrical potential change induced in the surrounding of a focal cortical stimulation – 2 mm or less from the stimulation site. This cortical stimulation evokes a 15-30 ms surface negative deflection analogous to the excitatory postsynaptic potentials (EPSPs) of apical dendrites measured in cats [PPF$^+$57].

Goldring et al. [GJH$^+$61] characterized the standard DCR pattern on patient who underwent various neuro-surgical procedures. Stimulation was delivered through electrodes arranged in a tripolar fashion, surrounding one "monopolar" recording electrode. All electrodes were 1 mm diameter platinum discs [GHG94]. Depending on the stimulation conditions, recording sites and pathologies, DCR shapes differ. However, a "primary

negative potential" – a negative deflection – occurs 20 ms after stimulation, as defined by Adrian et al. [Adr36]. A "second negative potential" appears with strong stimuli, representing EPSPs with a higher activation threshold. In cases of weak stimulus, a lower and longer positive phase called "after-positivity' follows this primary peak. The second negative potential amplitude increases with the stimulation frequency whereas the primary negative potential is lowered.

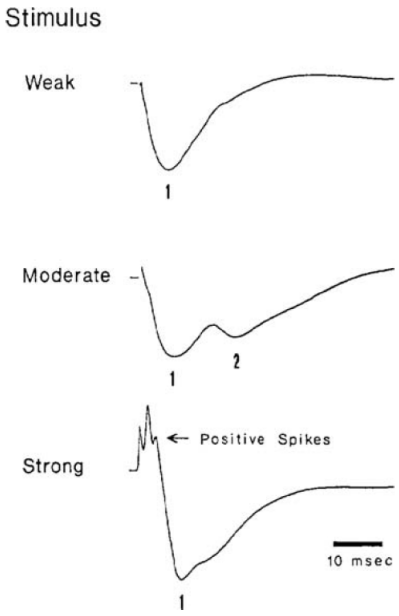

Figure 1.10: Representation of DCR components, showing the primary (1) and second (2) negative potentials. The second negative potential (2) is not present in the response to a strong stimulus to illustrate that its existence depends on the anaesthetic agents used. From [GHG94]

Regarding the recorded and stimulated area, the DCR profile varies according to the local architectonic organisation. Indeed, positive short spikes (1 ms) precede the first negative deflection on DCR elicited in the primary sensorimotor area by strong stimulations. Theses peaks probably stand for an all-or-none discharge of cortical neurons soma. However, DCRs obtained from the motor hand area do not present the second negative potential. The inter-stimulating electrodes distance also affects the DCR features. Goldring et al. [GHG94] demonstrated that a minimal inter-electrode distance is necessary to trigger both positives spikes and second negative potential on the DCR, even at high intensities. Indeed, a minimal distance of 8 mm at an intensity of about 20 mA is necessary to elicit these two features reliably. These properties were evidenced by

performing both stimulation and recording on the premotor, motor and somatosensory areas of the hand and face.

Finally, it is important to note that using anaesthetics induces modification of brain responses. For instance, barbiturate anaesthesia erases the second negative potential but not the primary negative potential [GJH+61].

1.4.4.2 Cortico-cortical evoked potentials

A similar method to the aforementioned one has also been used to study the functional connectivity of two distant areas. Matsumoto et al. [MNL+04] aimed at highlighting the cortico-(axono)-cortical connections between one stimulated and one recorded regions through subdural electrodes (ECoG grids) in patients with medically intractable epilepsy undergoing surgical evaluation of seizure epicentre resection. In this vein, they defined as cortico-cortical evoked potential (CCEP), the cortical potential resulting from an electrical stimulus applied to a distant region on the cortex. CCEPs (Fig. 1.11) typically consist in two negative deflections, an early peak N1 followed by a later peak N2 appearing 10 – 30 ms and 80 – 250 ms after the stimulus onset respectively. The N2 peak is more spread over time than the N1.

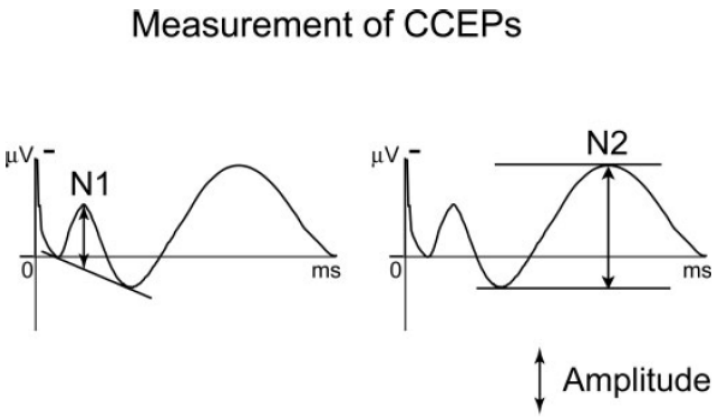

Figure 1.11: CCEP typical nomenclature. Adapted from [MNL+04]

Keller et al. [KHM+14] and more recently Kunieda et al. [KYKM15] reviewed the contribution of CCEP to brain mapping.

The intracranial monitoring of CCEP with chronically implanted electodes can be performed in two ways. First, the *grid and strip* approach involves the setting up of two-dimensional strips or grids of ECoG electrodes (usually 3 mm diameter, 1 cm inter-electrode distance, see section 2.2.1 for details) enabling the recording of brain activity directly from the cortical surface. The second approach, the stereoelectroencephalography consists in placing multi-contact electrode leads deeper in the brain [Lüd08]. Only the *grid and strip* approach is further detailed, as it can be used in the context of LGG awake surgery.

Mapping in epilepsy CCEPs have been used intra-operatively to probe epileptogenicity and to map functional networks. This approach is performed by combining classic (cortical and subcortical 50 Hz DES) and 1Hz ES (single-pulse electrical stimulation, SPES).

A standard functional mapping is first performed (50 Hz, 1 – 5 ms) as part of the presurgical evaluation. This mapping aims at identifying the eloquent structures that must be preserved during the resection of the epileptic epicentre. A CCEP mapping is then completed. Usually, constant-current monophasic square pulses (0.1–1 s pulse width) of alternating polarity are generally delivered in a bipolar fashion (between two adjacent electrodes) at low frequency (1 Hz) and high intensity (10–15 mA). ECoG is simultaneously recorded on all the other electrodes, referenced to a scalp electrode located on the contralateral mastoid of the grid implantation. This provides a minimal distance of 1 cm between the stimulated and recorded cortical area. Single-pulse stimulation is delivered to a certain functional site, 10 to 100 times, and the CCEP results of the averaging of the induced responses.

Apart from these intra-operative mapping, CCEPs have been used in the context of epilepsy with chronically implanted electrodes (ECoG or SEEG). It enabled mapping eloquent networks: for language system [EMP$^+$13, KLS$^+$12, MNL$^+$04], motor network [CED$^+$11, EMP$^+$13, SCC$^+$12, KMM$^+$12, MNL$^+$07, MNI$^+$12]), and directionality in visual networks [MJA13]. Connectivity is determined according to metrics such as the CCEP peak amplitude or latency (time-locked to the stimulus onset).

CCEP recording in brain tumor surgery Even though CCEP recording is more and more used to study connectivity in patient with medically intractable epilepsy, it surprisingly is hardly ever performed during brain tumor surgery.

Yamao et al. [YMK+14] attempted to preserve the language pathways in patients undergoing awake surgery for brain tumours located close to the perisylvian language areas in the language-dominant left hemisphere. ECoG electrodes were placed according to a noninvasive presurgical fMRI and tractography findings. Intraoperative CCEP mapping (SPES as described in [MNL+04]) was performed under both GA and LA. The evolution of CCEP was followed during all the surgery. They showed that the N1 amplitude increased while the patient was waking up, but did not decrease after tumor resection (in 4/6 patients).

Monitoring CCEP during awake craniotomy has also been performed by Saito et al. [SMM+15] to predict the language outcome after surgery and determine the optimal resection of the neoplasm. Strip of ECoG electrodes were positioned above the frontal language and temporal language areas, which were identified previously using intraoperative DES or preliminary mapping with implanted chronic ECoG. SPES was delivered in a bipolar fashion for CCEP monitoring. The obtained CCEP responses were correlated with the postoperative language function.

Similarly, CCEP mapping was used by Tamura et al. [TOK+16]. Patients with intraaxial tumor in their dominant hemisphere underwent conscious resection of their lesion with passive mapping. SPES was applied on language areas on the temporal lesion. Both recording and stimulation were performed thanks to ECoG grids. ES applied to the temporal language area evoked CCEPs on the frontal lobe.

1.4.4.3 Subcortico-cortical evoked potentials

In the same vein as for CCEPs, mappings of subcortico-cortical – or axono-cortical – evoked potentiels (SCEP and ACEP respectively) have been very recently performed (two cases only) in the context of brain tumor surgery.

Yamao et al. [YMK+14] have reported that stimulation over the arcuate fasciculus induced SCEP in the frontal and perisylvian language areas. SCEP mapping was per-

formed on 6 patients with brain tumors located close to the perisylvian language areas in the language-dominant left hemisphere. ECoG strips (3 mm diameter, 1cm inter-electrode distance) were used to perform both stimulation and recording. Bipolar stimulation (a pair of two adjacent electrodes) was delivered as close as possible to the arcuate fasciculus tract (as determined by the neuro-navigation, and confirmed with classical 50 Hz stimulation combined with reading and picture naming tasks), after tumor resection. Low-frequency ES (square-wave pulses of alternating polarity, pulse width of 0.3 ms, 1 Hz $10-15$ mA) was then applied to this same subcortical site, in order to track its cortical terminations at the language cortices by recording the evoked SCEPs from the ECoG on the frontal and temporoparietal cortices.

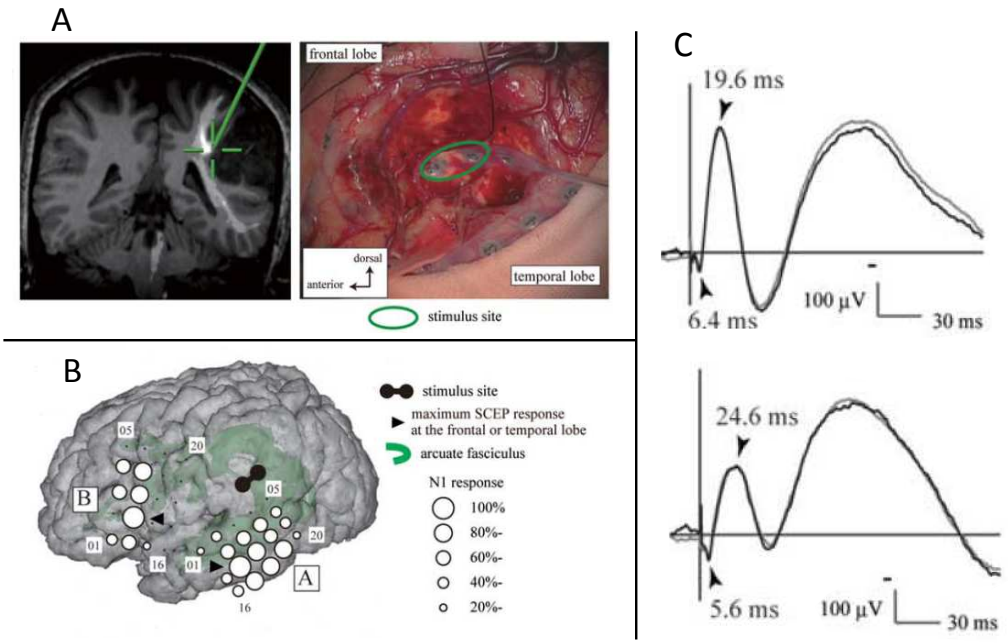

Figure 1.12: SCEP. A: Site of white matter stimulation. Electrode pair (highlighted by a green circle) was stimulated at the floor of the removal cavity (right). The stimulus site (cross hairs) was attached to the arcuate fasciculus (AF, long segment) in the neuro-navigation (left). High-frequency (50 Hz) stimulation at this site induced the arrest of naming. B: SCEP distribution in the frontal and temporal areas. Circle maps were made separately for SCEP responses in the frontal and temporal areas, based on the SCEP amplitude percentage distribution. C: The largest responses features. Adapted from [YMK+14].

Enatsu et al. [EKO+16] used SCEP to identify motor (pyramidal tract) and language (arcuate fasciculus) networks. After resection of the tumor, one ECoG strip was placed on the floor of the removal cavity and SPES (1 Hz, 10 mA) of alternating polarity was delivered in a bipolar manner through two adjacent electrodes. SCEP were recorded thanks to an ECoG grid placed on the central cortical areas. Subcortical stimulation induced SCEP depending on the fiber-stimulus distance: ES applied within 15 mm of the fiber trigger SCEPs but not when ES was distant from 20 mm.

More recently, Mandonnet et al. [MDP+16] reported consistent observations. In both cases, 1 Hz ES was bipolar, but with different stimulation settings. First, whereas ECoG strip were used in Yamao's study, ES was delivered thanks to a bipolar probe (1 mm diameter electrodes with a pitch of 6 mm) in this latter study. Then, ES consisted in biphasic square wave of 0.5 ms pulses width and an intensity of 2 mA only. Two trips of ECoG were placed over "Broca's" area and the fronto-parietal operculum, for SCEP recordings, while ES was delivered to the axonal eloquent site identified by 60 Hz DES. Despite this ES variations, a similar N1 peak was observed. However, latencies were found shorter than in Yamao et al. (11–14.8 ms vs. 20 ms respectively). Conversely, in no case a second deflection, the N2 peak, was measured.

1.4.4.4 Limitations of evoked potentials mapping

Even if evoked potentials mapping can be used to assess connectivity between several areas, it is essential to keep in mind that the connectivity does not correspond to entirely *normal* brain networks as data can only be obtained from patients with neural pathologies (epilespy and tumor). Moreover, due to the limited exposed brain surface, identified connections do probably not reflect the entire stimulated network.

The mechanisms of evoked potentials are not fully understood. Indeed, it is difficult to estimate to what extent the evoked response results from the activation of axons induced by ES.

Importantly, the ES modalities are not consistent, from electrode types (SEEG, ECoG grids) to stimulation parameters (amplitude ranging from 1 to 15 mA, pulse duration from 0.1 to 0.5 ms, biphasic vs. monophasic stimulation, see Table 1.2). EPs have almost always been measured when high amount of charges are injected to the brain. This

is not consistent with the amount of charge required to elicit functional disturbances.

None of the above-mentioned recording set up has enabled to view raw EPs, in real-time. Indeed, analysis have been only performed on averaged data among many ES trials (20 to 100), which prevents an intra-operative use of EPs for functional mapping.

Finally, depending on the cognitive state of the patient and the recorded cortical areas, evoked potentials characteristics might be modified. For example, it has been shown that anaesthesia, antiepileptic medication can impair latencies and EPs shapes [GJH+61]. Thus, even if consistent results across patients seem to validate the connectivity between neural areas, it is difficult to define generic characteristics of EPs induced by DES.

1.5 Objectives

Evoked potential mapping, as presented above, has been proven to be a valuable tool to evaluate the connectivity in both cortical and subcortical networks of the human brain.

In the context of epilepsy, the two language and motor networks have been now widely studied by the few research groups working on EP monitoring. Recently, they started to investigate the relationship between the recorded EPs and the functional disturbances in awake patients. This relationship between electrophysiology (EP) and behaviour (function) is crucial in LGG surgery, as it can help defining which cortical areas must be preserved and kept connected to the underlying functional network. It is an important constraint in LGG surgery.

To date, connectivity has been assessed empirically by applying cortically single pulses of electrical current while recording its evoked response. The negative potential N1 seems, in the literature, to be a common property to all cortical responses to both cortical (locally, DCR and at distant sites CCEP), and subcortical (ACEP or SCEP) ES. The term CCEP should be further replaced by CACEP (cortico-axono-cortical EP) as they involve axonal conduction (unlike DCR). The use of ACEP is a promising technique to assess the effective connectivity under GA. Only two studies have this day reported consistent information on the connectivity of eloquent areas involved in the language function. The reliability of this technique needs to be assessed in further studies.

Nevertheless, in all the above-mentioned studies, the reported EPs recording and analysis can be questioned as they depend on the performed processing of the data. First of all, the physiological veracity of the measured EPs has never been questioned nor mentioned. The evidenced properties of EPs (latencies, shape) are similar among studies, and consistent with the electrophysiological properties of neurons. Even so, it is crucial to ensure the validity of the measurement, i.e. to ensure the physiological aspect of the recorded signal.

As DES is applied closely to the recording sites, the acquired signal is composed not only by the physiological brain activity, but also by the stimulus artefact. **Thus, to disentangle what is physiological from what is purely *artificial*, it is necessary to characterise the acquisition chain used to perform EP recordings**. Indeed, filters and acquisition parameters set up, can lead to some signal distortion, in the range of the physiological signal. This processing will enable having a robust and reliable measure.

Secondly, only averaged EPs have been presented in the reviewed literature, which prevent a real-time analysis of the electrophysiological responses. Recording EPs *in vivo*, during the surgery aims at studying the functional networks connectivity that can give information to optimise the surgery. **A new recording set-up, allowing real-time identification of the EPs, needs to be developed.**

Thirdly, although awake surgery of brain tumours offers a unique opportunity to map white matter tracts *in vivo* in humans, neural connectivity (apart from the two ACEP studies mentioned above) has never been studied in this context. DES in LGG awake surgery is performed with a different stimulation configuration (bipolar probe, biphasic stimulation, injected charge) from the one commonly used in epilepsy.

Investigating the recorded EPs features in LGG awake surgery will give informations on the induced physiological signal propagation in a partially resected brain. By correlating shapes, latencies and amplitudes of the EPs to the neuronal elements type and their conduction velocity, it would be possible to assume which types of fibres are activated.

In order to understand the electrophysiological effects of DES (spreading and neuronal activation), the EPs recording method will be used. This will allow:

- measuring the on-line connectivity of stimulated brain networks by recording cortico-axono-cortical evoked potentials (CACEP) and axono-cortico-potentials (ACEPs),
- linking these EPs to the functional state, and thus, highlighting the networks functional boundaries,
- establishing in real-time and *in vivo* the electrophysiological state of a particular local area (by measuring DCR) as for instance the level of excitability.

To do so, a set-up allowing the real-time view of raw EPs is designed. A specific stimulation protocol and the characterisation of the acquisition chain will allow the validation the EPs measurement.

Note that the general term "cortical EP" will be further used, when it is not possible to confirm if DCR or CACEP have been measured. Also, the term ACEP will be used instead of SCEP for all the following document.

Chapter 2

Intra-operative electrophysiological recordings for DES evoked potentials mapping

Contents

2.1 Recording brain activity

2.1.1 Electrophysiological monitoring of brain activity

Electrical brain activity consists in the summation of the electric current contributions from all active neurons within a volume of brain at a given extracellular location. The differences between the generated potential at different sites creates electrical fields. The latter can be monitored by extracellularly placed electrodes and can be used to study brain activity. Electrical potentials can be measured (in μV range) at different distances from their sources (Fig. 2.1a) and refer to local-field potentials when electrodes are implanted into the cortex, electrocorticography (ECoG) when the activity is recorded directly on the cortical surface and electroencephalography (EEG) when recorded from the scalp. Figure 2.1b presents standard electrophysiological signals [1].

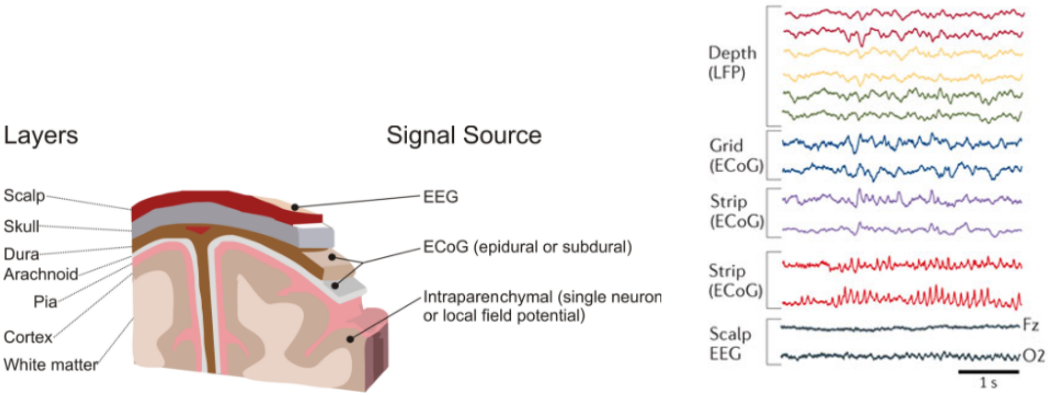

(a) Recording techniques according to the brain "layers". (b) Typical brain signals. From [BAK12]

Figure 2.1: Brain activity recordings.

[1] Simultaneous recordings from three depth electrodes (two selected sites each) in the left amygdala and hippocampus (measuring the local field potential (LFP)); a 3x8 subdural grid electrode array placed over the lateral left temporal cortex (measuring the electrocorticogram (ECoG); two four-contact strips placed under the inferior temporal surface (measuring the ECoG); an eight-contact strip placed over the left orbitofrontal surface (measuring the ECoG); and scalp electroencephalography (EEG) over both hemispheres (selected sites are the Fz and O2) in a patient with drug-resistant epilepsy. The signal amplitudes are larger and the higher-frequency patterns have greater resolution at the intracerebral (LFP) and ECoG sites compared to scalp EEG.

Several neuroimaging modalities, invasive or not, provide information on brain activity. Choosing the one to use depends on the neural characteristics to study as they provide specific spatial and temporal resolutions (Fig. 2.2).

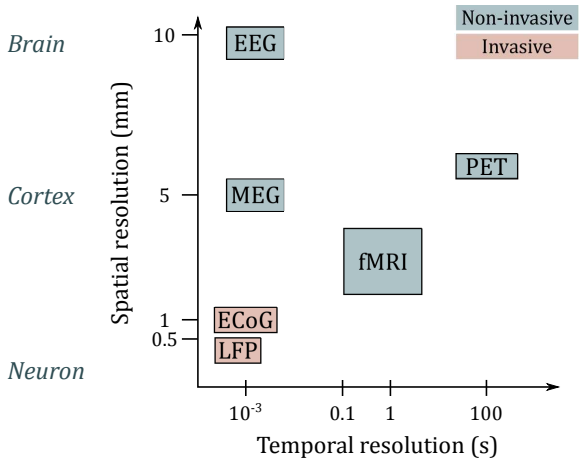

Figure 2.2: Temporal and spatial resolutions of functional neuroimaging techniques measuring electrophysiological (EEG, ECoG, micro-electrodes for LFP analysis) activities compared to other common techniques based on metabolic (fMRI, PET) and magnetic (MEG) informations. Adapted from [NAGG12, LBT09].

Scalp electroencephalography (EEG) Since its introduction by Hans Berger in the 1920's, scalp electroencephalography (EEG) has remained the major non-invasive way to measure brain activity. Changes in the type and number of activated neurons lead to variations of the frequencies and amplitudes of the brain waves. These cerebral "rhythm" are divided up into five groups defined by a frequency and amplitude criterion [RHN+15]. First, the alpha waves (8 – 13 Hz, 20 –200 µV) are associated to a calm waking state (eyes closed, mental rest). Slower waves, delta (0.5 – 4 Hz, 20 –200 µV) and theta (4 – 8 Hz, 10 µV), characteristic of sleep, may express signs of pathological lesions. Beta rhythm, with a frequency higher than 13 Hz and in the 5 – 10 µV amplitude range, appears in awakening conditions. Finally, high-frequency gamma rhythms (> 30 Hz, with low amplitude) are involved in higher processing tasks as well as cognitive functioning. Each electrode records the mean activity of a few-centimetre layer of neurons underneath. In most of the cases, electrodes are set according to the international 10–20 system, a standard in the electrode placement on the scalp. Each electrode is tagged after a specific association of letter and number (Fig. 2.3b). Letters indicate the anatomical position (A: ear lobe, C: central, F: frontal, P: parietal, Fp: frontal polar, O: occipital, T: temporal

and Z the central axis). Odds and even numbers stand for the left and right side of the brain, respectively.

EEG gives real-time information with a temporal resolution of about milliseconds, but with a low spatial resolution ($\geq$ 8 mm). Indeed the current measured below each electrode crossed several resistive layers (nervous tissues, the cerebro spinal fluid and the skull) that ease the transmission. Consequently, EEG is a weighted sum of underlying neuronal electrical sources, which leads to a poor spatial resolution.

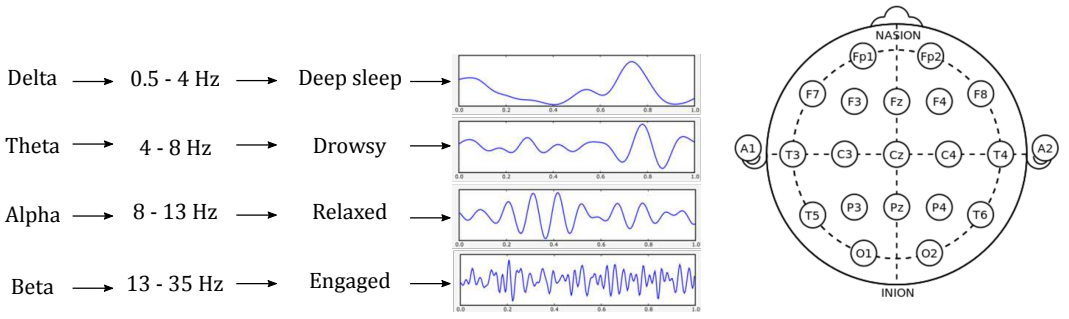

(a) EEG main frequency bands. (b) International 10-20 system.

Figure 2.3: EEG characteristics.

ElectroCorticography (ECoG) Unlike EEG, ECoG requires the opening of a small window of the cranium to place a grid of electrode directly on the cortical surface. The spatial and temporal resolutions of the recordings are thus improved (about millimetre, and millisecond respectively) as ECoG bypasses the signal distorting materials and the distance between electrodes is reduced. Moreover, ECoG is less subject to electrophysiological and movements artefacts (blinks, eye movements). ECoG does not have standards of electrode nomenclature as the positioning is surgical and patient dependent. Although common brain rhythms are defined for frequencies under 30–40 Hz, ECoG allows the acquisition of frequencies up to a hundred hertz as the signal is less eased. Finally, ECoG provides signals of higher amplitude (50 – 100 μV) than EEG (5 – 20 μV).

2.1.2 Acquisition mode

Both EEG and ECoG signals represent a difference of potential between a measuring (active) electrode and a reference electrode that can be set up in different modes.

Referenced mode (RM) The measuring electrodes are located above a brain area of "interest", on the scalp (EEG following the 10-20 standard) or on the cortex (ECoG). All measuring electrodes are referenced to the same electrode. The voltage difference should correspond to the signal value recorded under the "active" electrode only. To do so, the reference electrode must to be as neutral as possible, as null reference does not exist in practice. The choice of the reference electrode is thus critical as it determines the quality and the validity of the measure. For EEG, the reference electrode is usually placed in a "neutral point", i.e. a point where the potential is assumed to be constant, like the mastoid.

Differential mode (DM) In a differential mode, the measured signal consists in the difference of signals recorded under two nearby active electrodes. Consequently, the acquisition becomes independent from the reference electrode as its potential is removed in the DM. Signals correspond to the local activity underneath the electrodes, which increases the spatial resolution of the recorded signals. It is more specifically the case in ECoG as two electrodes of the same grid are used. This method also improves the signals quality as it removes all signal common to the two electrodes, such as the ambient electrical noise. Indeed, the DM limits the foreign contributions of brain activity in the recorded signal, as they disrupt the recordings electrodes in the same way. In the case of EEG, the DM mode is usually computed off-line, re-referenced from RM recordings.

2.2 Data acquisition

2.2.1 Material constraints

Nimbus i-Care stimulator: The Nimbus i-Care (Innopsys, France) is an neuro-physiological intra-operative monitoring and stimulating device allowing the stimulation of both Central and Peripheral Nervous System. It is chronically used to perform direct electrical stimulations for functional mapping in the awake surgery of low-grade glioma. The delivered biphasic current of stimulation can be modulated in frequency (1 – 800 Hz), pulse width (60-1600 µs), and intensity (0 – 16 mA). Finally, the specific bipolar probe dedicated to cortical stimulation consists in two straight 0.5 mm diameter electrode tips with a pitch of 5 mm, forming a "Y".

Figure 2.4: Nimbus i-Care ®

Biosignal amplifier: The g.BSamp (Gtec, Austria) is a 16-channel biosignal amplifier designed for physiological data acquisition (Fig. 2.2.1). Both referenced and differential recordings are feasible at it provides a specific 'negative' input for each channels. The red and black safety sockets represent the plus and minus input respectively. Every 2-bipolar amplification channels use the next nearest socket on the right as the corresponding ground. The module can also be divided into two 8-channel blocks, with separate grounds. All ground sockets of the same color are internally connected. The amplifier offers four selectable parameters, the bandwidth of frequencies and the sensitivity (i.e. the amplification gain) of the measure. A first order high-pass filter and a second order Bessel low-pass filter allow the user to select frequencies higher than [0.5 ; 2] Hz and lower than [1 ; 5] kHz respectively. An additional 50 Hz rejection filter (Notch filter), can be activated to remove as much as possible the surrounding electrical noise (from 220 V power supply). The input signal can be acquired with a sensitivity of 0.5 mV or 5 mV (real input voltage corresponds to 5 V in the output signal). This system is CE marked, and meets the medical European standards.

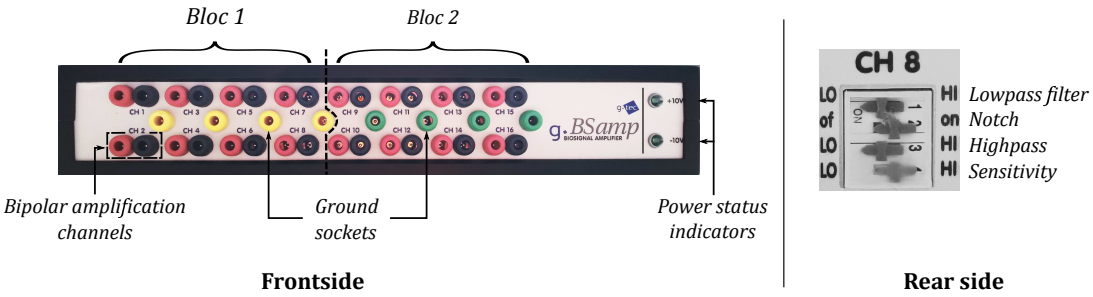

Figure 2.5: Biosignal amplifier, g.BSamp.

Acquisition system: The acquisition system (PowerLab, ADInstrument) is an acquisition unit devoted to the recording of electrophysiological signals such as EEG, EMG or ENG with a sampling frequency up to 200 kHz per channel. The acquisition is managed via a specific software, LabChart, which allows a real-time viewing of the acquired data. LabChart provides a large set of features enabling both on-line and off-line data-processing (digital filters, frequency analysis...).

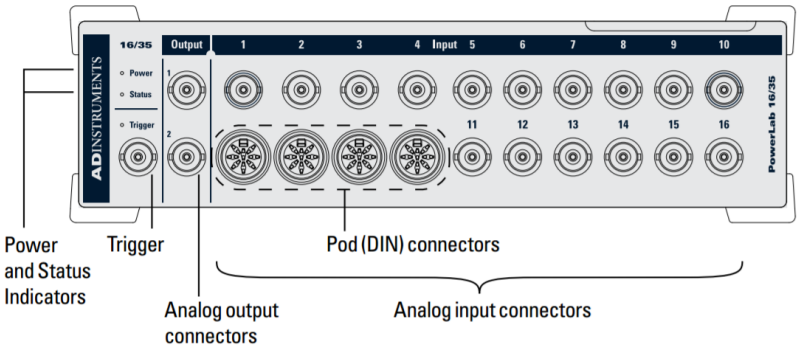

Figure 2.6: Front panel of the PowerLab 16-35, ADInstrument

ECoG recordings: Cortical strips of electrodes (Fig. 2.7, Dixi Medical, France) specially designed for functional neurophysiological exploration of the cortex are used for ECoG aquisition. They consist in 4 mm exposed surface stainless steel contacts, 10 mm spaced, with an unshielded 1.8 mm connexion cable directly compatible with the amplifier described above thanks to touch-proof connectors.

Figure 2.7: Cortical electrode strip for intraoperative recording of brain activity - Dixi Medical

2.2.2 Surgical theatre environment

Numerous apparatus are present in the theatre, to ensure a smooth running of the surgery. The most commonly used in awake brain surgery are listed below:

- A warming system maintaining normothermia,
- Multi-parameters monitors, to supervise vital constants, such as oxygen saturation, pulse and blood pressure,
- A medical ultrasound, used to determine the tumour localisation after craniotomy,
- Several syringe drivers, used for administering injectable drugs,
- A workstation for anaesthesia,
- A surgical ultrasonic instrument (scalpel) allowing a dissection with respect to blood vessels.
- Scialytic surgical lights,
- Video recording system to film the entire surgery,
- A laptop displaying the patient medical file (pre-operative fMRI).

2.2.3 Data acquisition

Intra-operative ECoG recordings remain challenging as it is operating-theatre dependant. First, the ECoG position cannot be exactly reproducible, as it is up to the brain exposed area - and so to the tumour localization. Furthermore, this recordings require to forecast as best as possible all the environmental conditions. By using an home-made set-up, all the technical parameters regarding filtering, sampling frequency and connections defined in the lab might be modified in real-time during the surgery. Indeed, the surgical environment is loaded up with electrical noise (due to the amount of medical electrical devices) that is caught by the ECoG unshielded wires. Finally, performing real ECoG measurements in the lab is obviously impossible (ECoG strip were tested with EMG acquisition). The experimental set-up designed hereinafter (Fig. 2.8) results from several intra-operative trials.

Two ECoG 4-contacts strips are placed on the exposed cortex, in accordance with the resected area. Signals are recorded using differential (contacts 1 to 3) and referenced mode (contact 4) configurations. For the classical referenced configuration the signal is

measured between each channel of interest (anode) and a reference electrode (cathode). A cupule-electrode located on the ipsilateral mastoid to the surgery serves as reference. For the bipolar mode, both anode and cathode are two adjacent electrodes of one strip.

The differential mode proposed here differs from the one commonly used for ECoG. Here, by performing differential measurements step by step, the spatial resolution of the recordings in the three dimensions (in surface and in depth) is increased. The acquisition is also less sensitive to noise. Indeed, when a potential is measured between two distant points, the variations around these two points are well distinct and thus are visible on the measured potential. On the contrary, their effects decrease as the two points get closer, leaving only the local variations on the measured potential.

All channels share the same ground: a patch-electrode located on the left acromion. ECoG signals are sampled at 10 kHz and band-pass filtered from 0.5 Hz to 1 kHz. To avoid the saturation of the front–end amplifier, signals are recorded with a gain of 1,000. The 50 Hz-Notch filter integrated in the amplifier is always active to protect from the environmental electrical noise surrounding. Unused amplifier channels are bypassed.

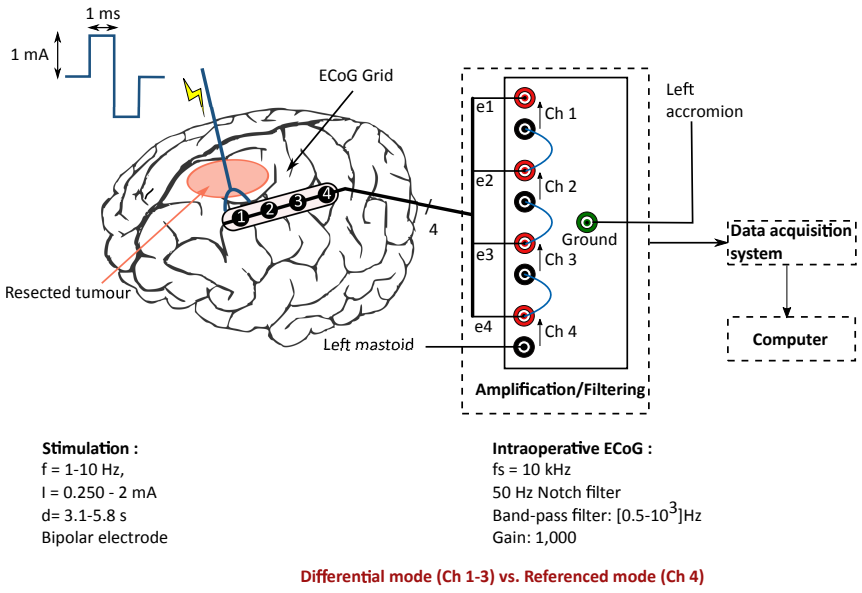

Figure 2.8: General set-up for one ECoG strip. The same recording configuration is kept for a second ECoG grid when recorded.

2.2.4 Overview on the experimental protocol

The clinical protocol used in all following reported studies was approved by the Ethic Committee of the University Hospital Centre of Montpellier (protocol: UF 965, n° 2014-A00056-43). The patients gave their signed written informed consent to participate in the study.

General surgery: The protocol was performed under general anaesthesia for all the cases presented in section 4.1.1. Subjects were placed in right lateral decubitus. General anesthesia was then induced by intravenous infusion of DIPRIVAN ® (propofol) and Reminfentanyl, short-acting medication and opioid analgesic drug respectively, that have a rapid onset and rapid recovery time. A 3-pins skull clamp stabilized the head during all the surgery. After craniotomy, the patient is awaken while the dura-matter is opened. Both cortical and subcortical mappings were then perfomed as described in section 1.1.2.1.

Electrodes setting up: The proposed protocol does not interfere with the classical surgical intervention as it is run after the DES standard procedure and surgery. It only requires positioning both reference and ground electrode before the surgical drape and craniotomy, i.e. before the DES procedure. The two 4-contacts ECoG strips are set after the tumour resection is complete, under general anaesthesia.

Finding the "hot-spots": Being able to identify both cortical and subcortical areas where DES induces electrophysiological brain responses (EP or DCR), is a critical point. Using 60 Hz DES implies latencies of 16 ms which is inadequate to enable measuring brain responses. Indeed, latencies of $\sim 16 - 20$ ms going up to 100 ms were noticed for the last components. Previous studies probing CCEP or ACEPs [MNL$^+$07, MDP$^+$16, YMK$^+$14] were performed at a very low frequency (1 Hz). Although single-pulse stimuli and 1 Hz DES can produce CCEPs or ACEPs, lowering the stimulation frequency to only 5 – 10 Hz would be a sufficient time-window between two stimuli. As averaging on a certain number of stimuli is necessary to detect the brain response, upper DES frequencies allow shorter stimulation durations as stimuli are delivered more rapidly. Moreover, it would facilitates real-time averaging to detect these CCEPs and ACEPs for further on-line analysis of brain connectivity during the surgery.

Thus, in the proposed experimental set-up, ECoG electrodes are placed on specific functional areas evidenced by DES cortical mapping. Low-frequency stimulation (1 – 10

Hz) is then applied near the functional site in order to trigger brain responses. Intensities are adapted on-line (0.5 to 2 mA, starting at the DES mapping intensity), to avoid saturation of the amplifier. When a stimulated site is apparently inducing a response, a second identical stimulation is performed with a 180 ° rotation of the stimulation probe (i.e. inversion of the cathodic and anodic electrode tips). In this way, physiological signals variations can be differentiated from anything linked by the stimulation. Indeed, all non-physiological signal will be inverted as the stimulus does, whereas physiological ones are independent.

Modulation of stimulation parameters: The effect of the different stimulation parameters, such as the frequency and the intensity, are also studied. Cortical and subcortical sites identified as generating EPs are stimulated at different frequencies and amplitudes after the tumour resection, under general anaesthesia. The frequency modulation (1 to 15 Hz) must help determined if the measured EPs correspond to integrated responses of the brain or only to synchronous responses of a small pool of neurons. Indeed, one could expect that an integrated response varies in function of the frequency because this latter carries the information. This can only be probed on an awake patient performing functional tests. Conversely, the electrophysiological response of a group of neurons must be independent from the stimulation frequency. The amplitude modulation aims at identifying the neurons activation threshold and the all-or-none principle of neuronal firing.

2.3 Preliminary validation of the acquisition set-up with 10 Hz DES.

In the following case, a comparison is made between 10 Hz and 60 Hz DES effects on ECoG recordings in differential mode. This experiment aimed at validating the designed set-up by investigating whether it is possible to detect both cortical EPs or ACEPs at 10 Hz with a higher spatial resolution, and if possible, to determine their properties.

2.3.1 Methods

The patient was a right-handed 31-years old patient presenting a left pre-central gyrus (rolandic area of the left hemisphere) LGG detected after an inaugural seizure with no functional impairments.

2.3.1.1 Direct electrical stimulation and anatomical sites of stimulation

Usual cortical and white matter mappings were completed on awake patients (constant-current biphasic square wave pulse of 1 ms duration each, 60 Hz, 2 mA). Initial (sub)-cortical mapping at 60 Hz(tags) and electrodes strips of ECoG are shown in Figure 2.9-A and Figure 2.10-A). Cortical stimulations in 1 and 2 lead to complete anarthria that identifies the premotor ventral cortex in the lateral part of the precentral gyrus. The subcortical mapping highlighted the different language pathways. Laterally, in 48, stimulations of the superior longitudinal fasciculus generate also a complete anarthria. Articulatory troubles but also facial movements representative of the pyramidal tracts are induced more mesially, in 47. At the bottom of the cavity, and more anteriorly than previously, in 49, the stimulations lead to semantic paraphasia suggesting the presence of the inferior fronto-occipital fasciculus.

2.3.1.2 Experimental protocol

After the resection was completed, and under general anaesthesia (to avoid patient's fatigue and to not disturb the surgical procedure) , stimulations were then performed in five of the specific functional sites determined during the awake part of the surgery. Both 60 Hz and 10 Hz DES were applied under general anaesthesia for durations ranging from 3.1 to 5.8 s. Cortical DES occurred in two sites: twice in the pars opercularis of the left inferior frontal gyrus – i.e. "Broca's area" (near electrode 6, right strip) and once in the posterior part of the superior temporal gyrus – i.e. "Wernicke's area" (near electrode 2, left strip). Three DES were then delivered subcortically, with the electrodes oriented along the different language pathways: the inferior fronto occipital fasciculus (49), the superior longitudinal fasciculus (48) and the pyramidal tract (47).

2.3.2 Evoked potentials induced by DES

In this present case, channels 4 and 8 (electrodes 4 and 8) were recorded in a referenced mode whereas the differential mode was used for all other channels (see section 2.2.3 for the detailed set-up).

Cortical EPs were observed only for channels 6 (electrodes 6-7) and 7 (electrodes 7-8) of the right strip, for the first and second stimulation of pars opercularis of the left inferior frontal gyrus respectively. Note that between these two stimulations, the right ECoG

strip was further displaced upper and on the right. Thus, the electrode 7 ended up nearly at the previous location of electrode 6 (Fig. 2.9-A and Fig. 2.10-A). This explains why cortical EPs were measured on channel 6 then on channel 7 for the two DES at a same location. Cortical EPs were not detected on all the other electrodes of both strips, nor for the second site of cortical DES. For subcortical DES of white matter pathways, no pattern of ACEPs was detected for both ECoG strips.

A subset of the raw signal and the averaged potential for each channel (6 and 7) are shown in Figure 2.9-B,C and Figure 2.10-B,C respectively. Mean cortical EPs were obtained by averaging 37 potentials for channel 6 and 31 for channel 7. In both cases, the averaged potential contains a first negative deflection after the DES artefact (with a latency of 23.7 $\pm$ 1.19 ms and 25.92 $\pm$ 5.16 ms respectively) followed by a positive increase (with a latency of 59.4 $\pm$ 7.1 ms and 45.4 $\pm$ 6 ms respectively). Latencies are given according to the starting point of the stimulation artefact.

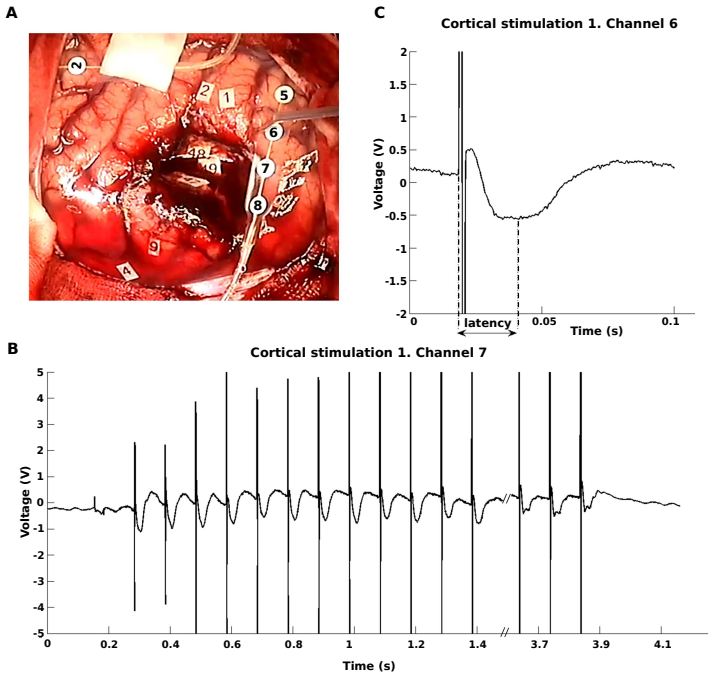

Figure 2.9: Intra-operative cortical EP induced by 10 Hz DES. A) DES is applied cortically near electrode 6 during 3.7 s. B) Zoom on the ECoG signal corresponding to the stimulation (with the 10^4 gain). Cortical EPs can be observed after each stimulation artefact. The last cortical EPs are distorted due to the amplifier. C) Mean EP over 37 stimuli, with a latency of 23.7 $\pm$ 1.19 ms

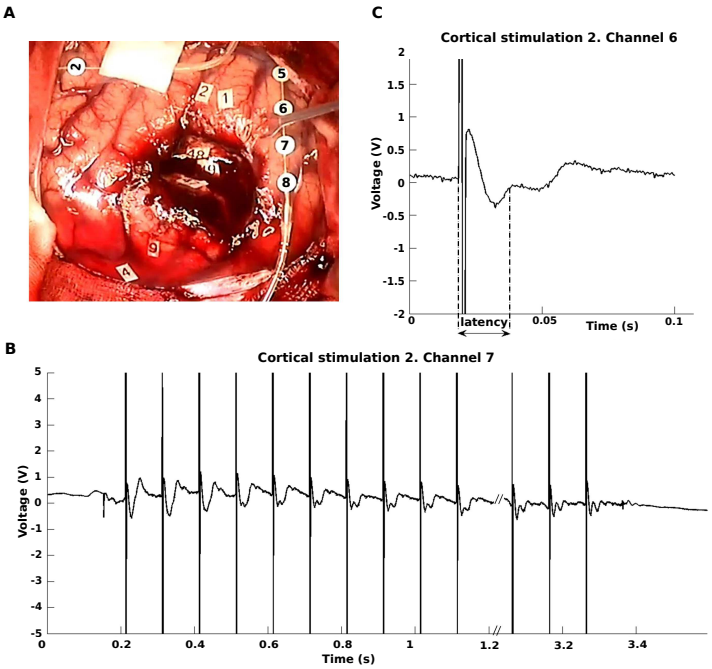

Figure 2.10: Second intra-operative cortical EP induced by 10 Hz DES. A) DES is applied cortically near electrode 7 during 3.1 s. B) Zoom on the ECoG signal corresponding to the stimulation (with the 10^4 gain). Cortical EPs can be observed after each stimulation artefact but are distorted after 4 stimuli. C) Mean cortical EP over 31 stimuli, with a latency of 25.92 $\pm$ 5.16 ms. The oscillations due to the amplifier have more impact on this mean artefact.

In addition, at the end of the first recording and for the second one, for the negative deflection, a double peak could be observed. This oscillation is identified as the superimposed response of the amplifier (Fig. 2.11), as further demonstrated in Chapter 3. Even though the oscillation is due to the stimulus filtering, it appeared to be more pronounced when the voltage exceeds the amplifier's linearity voltage range ($\pm$ 5 V).

2.3.3 Discussion

The effectiveness of the EPs acquisition set-up was here validated. Importantly, the differential mode improved the focality of the recording of EPs in ECoG signals with a better signal to noise ratio. Indeed, even without averaging, cortical EPs can be detected in real-time on the raw signal and quantified accurately. It may also explain why cortical EPs were measured on a single channel despite the proximity to functional sites mapped with 60 Hz DES. Besides, the oscillatory behaviour of the amplifier can be easily differentiated and thus used to avoid misidentified cortical EPs.

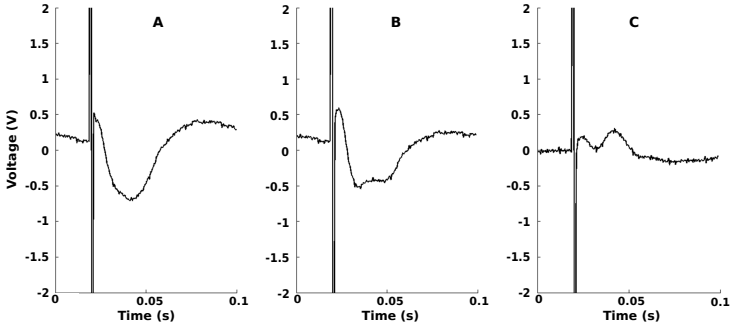

Figure 2.11: Cortical EP distortions due to the acquisition chain. A) Evoked potential when the amplifier does not saturate. B) Cortical EP with saturation of the amplifier. C) Oscillation obtained by subtracting A from B.

When methodological precautions are taken, the recording of cortical EPs is possible under 10 Hz DES. In contrast to the previous 1 Hz DES procedure, it allows averaging data on a 10 times smaller duration i.e. more stable regarding surgeon application of the electrode over the brain. Moreover, for on-line processing during the surgery, the method stabilizes 10 times quicker to get accurate data. Despite, some technical differences with others cortical EPs (DCRs or CCEPs) and ACEPs measurements (see section 1.4.4) a similar waveform was observed for the cortical EPs. The measured latencies of the first negative peak were around 20 ms in accordance with those measured for CCEPs and DCRs [MNL$^+$07, GHG94] in the literature. A 10 time higher stimulation frequency (10 Hz vs. 1 Hz) seems to induce same cortical responses of the cortical network.

The observed cortical EPs latencies corresponds to the N1 peak defined in the literature. However, due to same ranges latencies, the oscillation can be easily mixed up with the N2 peak. It is thus crucial to remains cautious before asserting that the second measured deflection is the physiological N2 peak. The characterisation of the used acquisition chain, presented in section 3.1, validated that the oscillations were not physiological but purely "artificial".

Chapter 3

Stimulation artefact withdrawal method

Contents

3.1 Characterization of the amplifier's filtering chain

The bio-signal amplifier exhibits linearity for output voltages in the range of ± 5 V; if the input signal exceeds this voltage range, the amplifier can distort the signal. The internal operating of the Gtec amplifier follows a path of filters and amplifier-stages. Thus, depending on the filters characteristics, applying them to a current template as in DES may have an impact on the signal components.

Before using this amplifier on ECoG or EEG data acquisition combined with DES, characterizing the filters is the first step to differentiate the physiological responses from the possible distortions induced by the amplifier's filtering chain. According to the given technical specifications, filters were modelled as follows: a Bessel second order filter for the low-pass, a twin-T notch filter for the 50 Hz rejection and a first order Butterworth filter for the high-pass.

3.1.1 General theory on filtering

An analog filter is a linear system which keeps only the desired frequency components of a signal. The resulting interval of allowed frequencies is called the bandwidth. Filters are characterized by their transfer function H, the relation between the input and output signals, V_{in} and V_{out} respectively. Several families of filters are defined, according to the bandwidth specificities. Among them are the high-pass, low-pass and rejecting filters. The transfer function in the Laplace space of a filter is usually expressed as a fractional polynomial function, with n the order of the filter and the constant K its static gain in the bandwidth (Eq. 3.1, H given with the Laplace notation).

$$H(p) = \frac{V_{in}}{V_{out}} = \frac{K \sum_{i=0}^{n} b_i p^i}{\sum_{i=0}^{n} a_i p^i} \tag{3.1}$$

Passive filters are commonly made of passive electrical components (resistor, capacitor and inductance). By adding an operational amplifier, an active component, to the electrical circuit, the input signal can be amplified. The template of the frequency response of a filter is given in the graphical representation of $|H(j\omega)|$ (dB) as a function of the pulsation ω (rad.s^{-1}) with (Eq. 3.2):

$$\omega = 2\pi f \tag{3.2}$$

3.1.1.1 First order high-pass filter

High-pass first order filters are defined by a cut-off frequency f_c (i.e. a cut-off pulsation $\omega_c = 2\pi f_c$). The normalized general transfer function of first order high pass filters is given in Equation 3.3.

$$H_{HP}(p) = \frac{\frac{p}{\omega_c}}{1 + \frac{p}{\omega_c}} \tag{3.3}$$

3.1.1.2 Second order filters

The transfer function of a second order system can be expressed in its canonical form (Eq. 3.4) as a function of the natural pulsation ω_0 and the damping factor m. Second order filters attenuate frequencies in the band–cut more steeply than first order filters. Thus, their Bode diagram looks the same except of a steeper slope of -40 dB/decades for second order filters. The polynomial numerator A determines the type of filter (high-pass, low-pass, etc.).

$$H_{LP}(p) = \frac{KA(p)}{1 + 2\frac{m}{\omega_0}p + \left(\frac{p}{\omega_0}\right)^2} \tag{3.4}$$

For band-stop and band-pass filters, the two cut-off pulsations at –3 dB are the two poles (roots) $\omega_{c,1}$ and $\omega_{c,2}$ of the polynomial denominator of H. Depending on the damping factor value m, the system can present oscillation and/or resonance.

- $m > 1$: the system is over-damped;
- $m = 1$: the system is critically damped;
- $\frac{\sqrt{2}}{2} \leq m < 1$: the system is under-damped;
- $0 < m < \frac{\sqrt{2}}{2}$: the system is also under-damped, but a phenomenon of resonance is added;
- $m \leq 0$: the system becomes unstable.

Bessel second order filter Bessel filters are specific second order low pass filters with a regular time delay in the bandwidth. They are optimized to obtain better transient response due to a linear phase (i.e. constant delay) in the bandpass. This means that there will be relatively poorer frequency response (less amplitude discrimination). In other words, Bessel filters lead to a minimal distortion of the signal in the time domain: the temporal shape of the filtered signal is softened but preserved. Low-pass Bessel's normalized transfer function is derived from Equation 3.4 (with $A = 1$ and $m = \frac{\sqrt{3}}{2}$ and $K = \frac{1}{3}$).

The specific case of under-damped systems In the time domain, the step response of an under-damped linear system, i.e. the response to a step, has an oscillatory behaviour ($0 < m < 1$). It is characterized by a pseudo-period of oscillation T_p (Eq. 3.5)

$$T_p = \frac{2\pi}{\omega_p} \text{ with } \omega_p = \omega_0\sqrt{1-m^2} \tag{3.5}$$

The time-delay (Fig. 3.1) after which the step response stays within ± 5 % of its final value is given by

$$t_{5\%} \simeq \frac{3}{m\omega_0} \tag{3.6}$$

Finally, the overshoot coefficient D (Eq. 3.7)defining the damping importance is

$$D_{\%} = 100 \cdot e^{-\frac{\pi m}{\sqrt{1-m^2}}} \tag{3.7}$$

For a strong damping ($m < 0.7$) the step response will be little damped, with strong oscillations and overshoot. The response will be as fast as m is low. In the contrary, a strong m value ($m > 0.7$) leads to no oscillation and a hardly visible overshoot.

Finally, when a phenomenon of resonance appears ($0 < m < \frac{\sqrt{2}}{2}$) in the frequency response of the filter, the resonant pulsation ω_r is defined in Equation 3.8:

$$\omega_r = \omega_0\sqrt{1-2m^2} \tag{3.8}$$

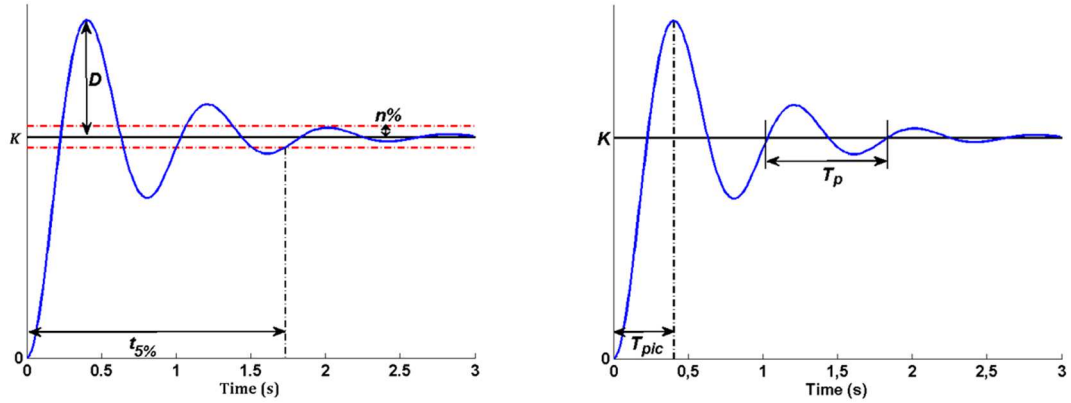

Figure 3.1: Step response of an under-damped 2^{nd} order system.

3.1.1.3 The 50 Hz–Notch filter

A twin–T filter (Fig. 3.2) is basically composed of two "T"-parts built with passive components (capacitor C and resistor R). Each "T"-part aims at filtering one band of frequencies. The values of R and C are chosen in order to have two filters with a 90° phase opposition at the center frequency, which leads to the band-rejection of the Notch filter. Thus, a 50 Hz–Notch filter passes all frequencies except those within a specific band centred on 50 Hz. Notch filters usually show an important bandstop narrowness highly attenuated over a few hertz (steep-side slopes).

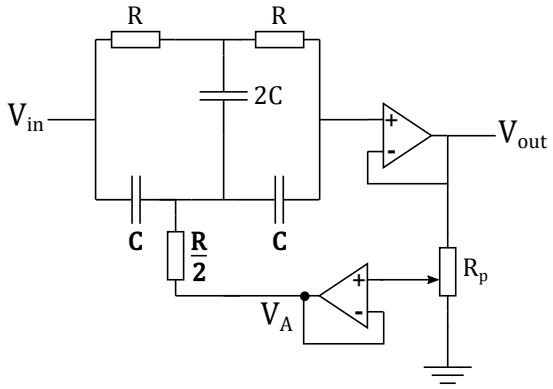

Figure 3.2: Twin–T Notch filter.

For an active 50 Hz–Notch filter, two op-amp followers (i.e. the gain is equal to 1), are added to the twin-T filter. The upper one ensures an infinite impedance input of the amplifier, to allow the determination of the filter specifications while neglecting what could come after itself (in an electrical montage). The bottom one is connected to a voltage

divider bridge, a potentiometer (R_p). Combined with the bottom op-amp follower, it feeds back in V_A a part of the output potential V_{out} to the circuit. This part enables the configuration of the damping factor m of the filter. The general transfer function is then defined as (Eq. 3.9), with α the division ratio of the potentiometer:

$$H_{Notch}(p) = \frac{1 + (RCp)^2}{(RCp)^2 + 4(1-\alpha) * RCp + 1} \tag{3.9}$$

In this way, a twin-T notch filter is a second order filter (by identification with Equation 3.4):

$$A(p) = 1 + (RCp)^2, \ \omega_0 = \frac{1}{RC}, \text{ and } m = 2(1-\alpha) \tag{3.10}$$

The bandstop is centred on the rejection pulsation ω_0 (for which $|A(j\omega_0)| = 0$) and limited by the two following cut-off frequencies at the -3 dB points:

$$\omega_{c1,2} = \pm m\omega_0 + \omega_0\sqrt{1+m^2} \tag{3.11}$$

A quality factor Q, the reciprocal of twice the damping factor, is also defined and commonly used to represent the "peaknes" of the resonance peak, i.e. the amplitude and narrowness around the natural pulsation ω_0. Here, the value of Q is determined by the potentiometer R_p value. As Notch filters are designed to give a clear attenuation in the surroundings of a single frequency, and as little attenuation as possible elsewhere, the Q value must be quite high (and thus, m must be low Fig. 3.3). Indeed, the rejected frequency band has a width Δf of (Eq. 3.12):

$$\Delta f = 2mf_0 \tag{3.12}$$

The choice of the quality factor is crucial in the design of a filter as it defines its response in the time-domain. The step response is commonly studied to estimate the temporal response of the filter. For the 50 Hz–Notch filter, it is similar to 2^{nd} order filters as described in Figure 3.1. The higher the damping factor is, the slower is the response. Moreover, having a low damping factor (necessary to a good Notch-filter) can induces undesired oscillations in the temporal response of the filter.

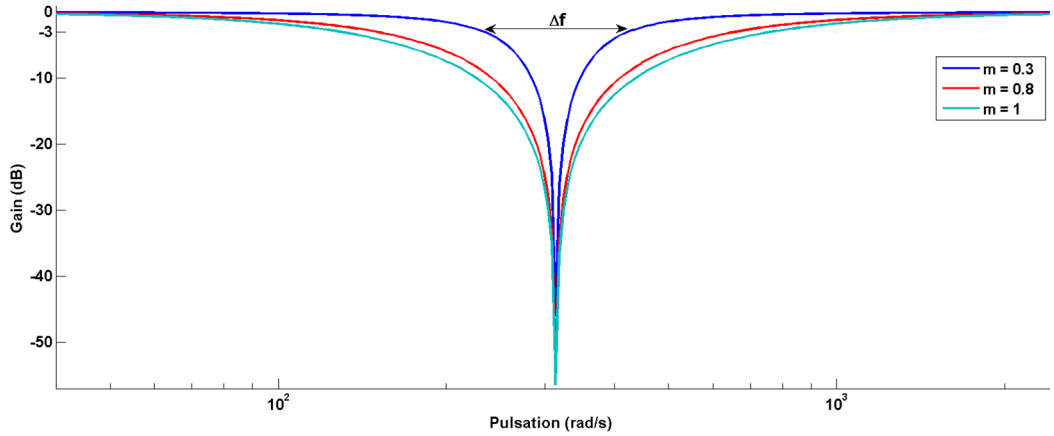

Figure 3.3: 50 Hz–Notch filter Bode diagram.

3.1.2 Mathematical model of the filtering chain

As demonstrated here above, the step response of the 50 Hz-Notch filter contains some oscillations. Given that DES consists in a square-wave biphasic stimulus, the signal resulting from the filtering process will also be distorted by these oscillations. It is thus necessary to model the impact of the all filtering chain to a DES-shaped stimulus and to understand its effects on the recorded data. This would enable sorting out physiological from electrical signals.

The model proposed in this paragraph aims at defining the final output of the filtering chain (included in the amplifier) in response to an input featuring the DES waveform (Fig. 3.4).

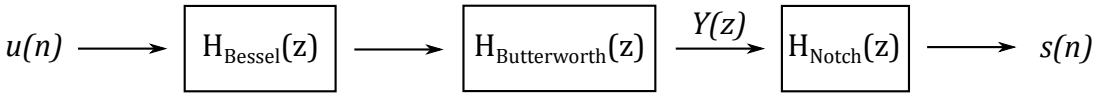

Figure 3.4: Functional diagram of the filtering system.

Model of the stimulation First of all, let's consider an input signal $u(t)$ defined as two biphasic square wave 1 ms pulses (P_w) of alterning polarity, without interpulse (Eq. 3.13). Each pulse is represented by the Heaviside function $\Gamma(t)$ (Eq. 3.14) with a normalized absolute amplitude of 1.

$$u(t) = \Gamma(t) - 2\Gamma(t-T) + \Gamma(t-2*T) \tag{3.13}$$

$$\Gamma(t) = \begin{cases} 1, & \text{for } t \geq 0 \\ 0, & \text{elsewhere} \end{cases} \tag{3.14}$$

In the discrete domain, the output is defined as a numerical suite $u(n)$ with n elements.

Recursive Notch filter Matlab software only allows the implementation of analogue Bessel filters. Thus, it is necessary to work in the z discrete plane to apply this filter to the input $u(t)$. This Z transformation can be calculated directly from the known transfer function in the Laplacian p-plane. The bilinear transformation is a standard method used to perform analog-to-digital filter conversion. The p-plane is mapped into the z-plane by (Eq. 3.15, with T_s the inverse of the sampling frequency):

$$p = \frac{2}{T_s} \cdot \frac{1 - z^{-1}}{1 + z^{-1}} \tag{3.15}$$

Using the bilinear transformation, the Notch filter transfer function (Eq. 3.9) can be expressed in the z-plane as following:

$$H_{Notch}(z) = \frac{\sum_{n=0}^{2} b_n z^{-n}}{1 + \sum_{n=0}^{2} a_n z^{-n}} \quad \text{with} \begin{cases} b_{n-2} &= 1 + (\frac{2}{\omega_0 T_s}) \\ b_{n-1} &= 2(1 - (\frac{2}{\omega_0 T_s})^2) \\ b_n &= 1 + (\frac{2}{\omega_0 T_s})^2 \\ a_{n-2} &= (\frac{2}{\omega_0 T_s})^2 - \frac{4m}{\omega_0 T_s} + 1 \\ a_{n-1} &= 2(1 - (\frac{2}{\omega_0 T_s})^2) \\ a_n &= (\frac{2}{\omega_0 T_s})^2) + \frac{4m}{\omega_0 T_s} + 1 \end{cases} \tag{3.16}$$

Filtering outcome Thanks to the convolution properties of the Z transform, the relation between the input $u(t)$ and the output $s(t)$ can be written as in Equation 3.17

$$\begin{aligned} H_{tot}(z) &= \frac{Z(s(n))}{Z(u(n))} \\ &= H_{HP}(z) \cdot H_{Bessel}(z) \cdot H_{Notch}(z) \\ &= Y(z) \cdot H_{Notch}(z) \end{aligned} \tag{3.17}$$

The output $Y(z)$ of both low-pass (H_{Bessel}) and high-pass (H_{HP}) filtering stage can be directly computed on Matlab. The Notch filter can be implemented as a recursive filter. The recurrence relation between the transitional output $y(n)$ and the final output $s(n)$ is given in Equation 3.18. The set of a_m and b_n coefficients is identical to the ones given in Equation 3.16.

$$s_n = \sum_{l=0}^{2} b_{n-l}.y_{n-l} - \sum_{l=1}^{2} a_{n-l}.s_{n-l} \tag{3.18}$$

The stimulus artefact consists in the entire transformation of the stimulus by the filtering chain $y(n)$. Two parts can be differentiated in the artefact: a *steep and fast edge* (similar to the biphasic stimulus) and a phase of stabilisation. When computing the artefact (Fig. 3.5), one can note that depending on the damping factor value, the stabilisation phase may show oscillation with extrema in the same range of latencies than the physiological evoked potentials described in the literature. Thus, knowing the value of the damping factor (m) is crucial for modelling the stimulation artefact, and thus to disentangle what is physiological from what is not in the recorded signals. As no technical data is given on the filters features, the damping factor must be empirically determined.

3.2 Characterization of the artefact

The importance of the stimulation artefact in the recorded ECoG signals rises several questions. Firstly, when looking at the signals, one can note that the artefact direction (positive or negative peak first) can be either identical or opposite for two channels for two stimulations with the same orientation of the stimulation probe. Secondly, oscillations, led by the stimulation current filtering, are of various amplitudes and superimposed to the signals of interest (brain activity). An experiment was thus performed in the lab, to determine the 50 Hz–Notch filter characteristics and the impact of the stimulation probe

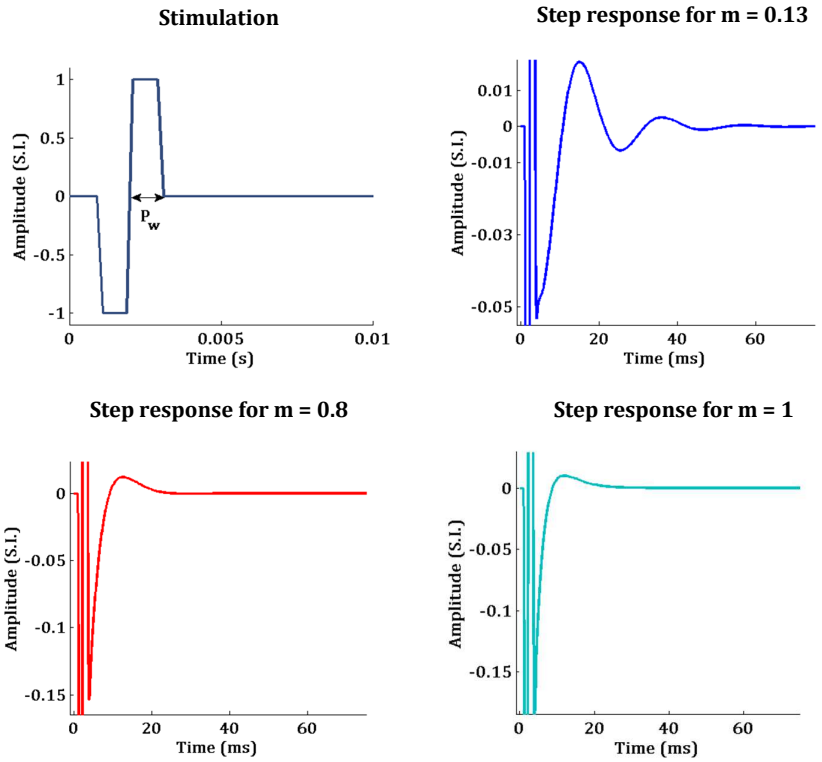

Figure 3.5: Modelled filtering of the stimulation by the acquisition chain for different m values.

orientation and distance on the recorded signal. To do so, it is necessary to record the effective signal resulting from the stimulation of an "inactive physiological" material, i.e. without any physiological response.

3.2.1 Experiment

Physiological saline (NaCl, 0.9%) is commonly used as an equivalent of the cerebrospinal fluid (CSF). Indeed, normal saline solution is often considered as isotonic to physiological fluid and is of similar conductivity (2 S/metre and 1.7 S/metre for physiological saline and CSF respectively, 37 °C and 1 kHz [GB67, SHvVB91]).

A 4-contact ECoG grid was soaked in 30 ml of this physiological saline. Three channels were recorded, in a consecutive differential way (electrodes 1-2, 2-3 3-4). The amplifier and acquisition board parameters were set to the values used in the operating theatre. The ground was connected to the saline solution by way of a 680 Ω resistor (Fig. 3.6).

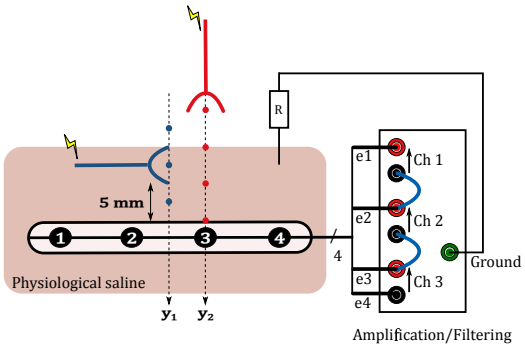

Figure 3.6: Lab experiment. Stimulations site in red and blue for parallel and perpendicular orientation of the probe respectively. Both orientation are applied to each stimulation axes.

Trains of 4 biphasic square wave stimuli (4 Hz) of 1 ms single pulse duration were delivered to the physiological saline thanks to a bipolar probe identical to the one used in the operative room. The STIMEP stimulator [GALA+17] was used to perform the stimulation. Stimulation sites were distributed along two axes: the first one (y_1) crossed two electrodes of the same bipolar measurement (electrodes 2-3), whereas the second one (y_2) was at level of a single electrode (electrode 3). Stimulations were delivered both perpendicular (4 sites) and parallel (5 sites)to the two axes. All sites of stimulation were distant of 5 mm along these axes, and stimulated 2 times – one for each 90 ° rotation of the probe (3×2 perpendicular, and 4×2 parallel, Fig. 3.6).

3.2.2 Empirical determination of the 50 Hz–Notch filter damping factor

Oscillatory pseudo-periodes T_p were measured for the three recorded channels, when they can be properly distinguished and when the signal did not exceed the amplifier linearity range. The damping factor m is estimated at 0.13 (on 90 stimuli) inducing the existence of a frequency of resonance. Table 3.1 sums up the 50 Hz–Notch filter characteristics (defined in Eq.s 3.5 to 3.7).

As demonstrated above, the stimulation artefact is followed by an oscillation induced by the filtering. This oscillatory element can affect the signal by flattening components of interest in the recorded signal. Thus, a pre-processing of the recorded data may be necessary to counterbalance the oscillations and thus, withdraw the undesired effects of the filters (50 Hz–Notch among others).

Table 3.1: 50 Hz–Notch filter technical characteristics

Parameter	Value
m	0.13
ω_0	$50 \cdot 2\pi$ rad/s
T_p	20.2 ms
D	66.24%
$t_{5\%}$	73.5 ms
f_r	49.1477 Hz
$f_{c1,2}$	43.9207 ; 56.9207 Hz

3.2.3 Impact of the distance and orientation of the probe on the recorded signal

Understanding the impact of the stimulation probe's orientation in relation to the ECoG grid can help assessing the veracity of the recorded signals, and thus of the set up.

Dipole and potentials Considering a point current source of amplitude I_0 in a uniform conducting medium of infinite extent and conductivity σ, the scalar potential field V for a concentric spherical surface of radius r, given in Equation 3.19, is constant for surfaces where r is also constant. These surfaces correspond to the equipotential lines.

$$V = \frac{I_0}{4\,\pi\,\sigma\,r} \tag{3.19}$$

In reality, a current source always consists in two sources of opposite signs, to preserve the charges. In the case of bipolar DES, the stimulation probe corresponds to a dipole. The electrode tips stand for two monopoles of opposite sign but of equal strength I_0, distant of d. Let T_1 and T_2 be the two poles, and O the center of the dipole. The field potential induced by the dipole at site distant of r (i.e. $r >> d$, dipole approximation) can be then expressed as:

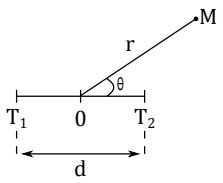

$$V_M = \frac{I_0\,d\,cos(\theta)}{4\,\pi\,\sigma\,r^2} \tag{3.20}$$

Figure 3.7: Dipole nomenclature.

The dipole potential field varies as $\frac{1}{r^2}$ whereas the monopole field varies as $\frac{1}{r}$. The equipotentials are thus not concentric spheres because of the $\cos(\theta)$ factor. The maximum dipole potential, is on the polar axis for a given r.

In Figure 3.8, equipotential lines were plotted for two stimulation axes (according to the previously described experiment) and for three stimulation probe tip orientations ($\theta = 0°$, $45°$ and $90°$). Five stimulation sites were spread each 5 mm from the ECoG grid axes (at the center of the electrode). The potentials measured by each ECoG electrode were first calculated. The current intensity I_0 was set to 2 mA, and the conductivity σ to 2 S.m^{-1}. This way, the potentials V_e (measured at the center of each ECoG electrode) was defined as sum of the potentials induced by each stimulation electrode tip (from Eq. 3.19):

$$V_e = V_{e,Tip^+} + V_{e,Tip^-} \tag{3.21}$$

The equipotential lines were then computed for all previously calculated V_e values, using the dipole approximation. The approximation is not accurate for ECoG electrodes at the vicinity of the stimulation sites (as the distance d is almost equal to r). However, for farer electrodes or stimulation sites the approximation is considered valid (accurate enough to give information on the artefact orientation).

Qualitative analysis Table 3.2 compares theoretical (Theo) and experimental (Rec) artefact polarities induced by the first stimulus position (closest to the ECoG grid) for the two stimulation axes (y_1 and y_2, configuration 1 on Fig. 3.8). Results were identical when inverting the stimulation probe tips (positive and negative). The recorded potentials for each channel were of the same order (mV) as the theoretical ones. The artefacts' polarity were consistent between the model and the acquisition for the stimulation axis y_2 but not for y_1. For the latter, variation in the artefact polarity can be observed between stimulation sites. This is probably due to a manual shift led by the manual placement of the stimulation probe. For example, artefact had the negative peak first for channels 2 and 3, for all stimulations sites along y_1 whereas it was positive first on channel 1 for the first two stimulations.

The artefact direction cannot be precisely predicted as it is highly sensitive to the orientation of the stimulation probe. Thus, even if the theory forecasts a given direction, two "identical" stimulations (same site, distance and orientation in relation to the ECoG

electrodes) can give different artefact directions. This phenomenon is due to the sensitivity of the **manual** stimulation.

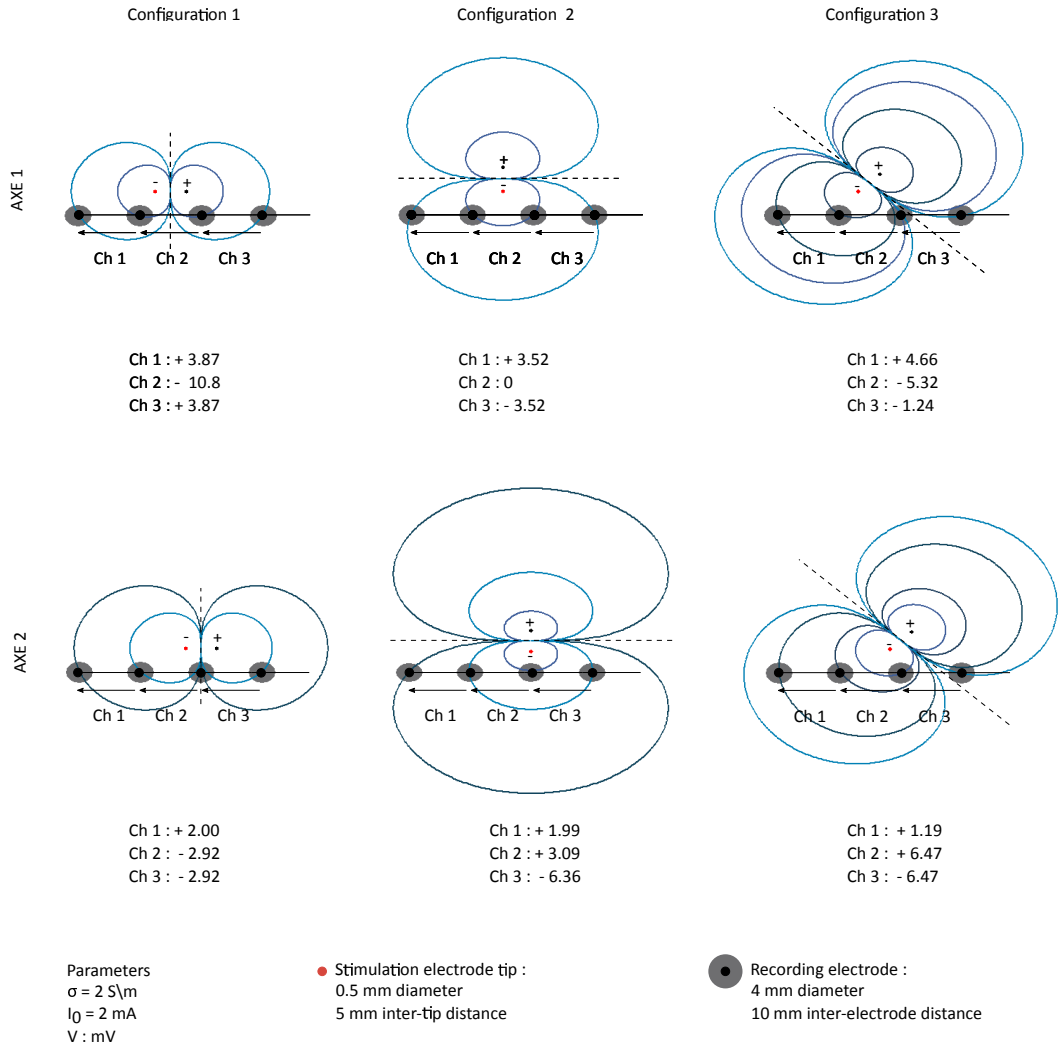

Figure 3.8: Recorded voltage vs. orientation of the stimulation probe according to the recording electrodes.

However, the experiment showed that the oscillation amplitudes slightly decreases with the artefact amplitude and the increase of the distance between the stimulation and recording sites. Looking at all the stimulation sites, axes and orientations used in the experiment (180 samples), oscillations first peaks (either positive or negative) are 110 times smaller than the artefacts ones. Most importantly, the oscillation profile (peaks positions) strictly follows the artefact orientation: negative or positive peak first in the artefact leads to negative or positive peak first in the oscillation.

Table 3.2: Comparison of theoretical and recorded artefacts orientations, for the first position of stimulation (0.5 cm away from the ECoG electrodes axis).

Stimulation probe orientation		Artefact orientaton	
		Artefact polarity 1	Artefact polarity 2
y_1 axis			
parallel	Theo	1, 3	2
	Rec	1, 2, 3	–
perpendicular	Theo	1[1]	3[1]
	Rec	1, 2, 3	–
y_2 axis			
parallel	Theo	2, 3	1
	Rec	2, 3	1
perpendicular	Theo	1, 2	3
	Rec	1, 2	3

[1] Stimulation artefact on Channel 2 is null.

This properties will be used to **(1)** disentangle physiological from non-physiological signals by performing "identical" stimulations with opposite orientations of the stimulation probe; and **(2)** to withdraw the oscillations from the ECoG signal by modelling the filtering of a stimulation of same direction as the recorded artefact.

3.3 Data processing

3.3.1 Stimulation artefact detection

All trials were visually checked for ECoG signals saturation and trending during each stimulation. All trials exceeding the ± 5 V range were discarded. Artefacts' presence was mostly detected automatically with a manual adapted threshold. Artefact detection was manually corrected if necessary.

3.3.2 Artefact correction method

To recover the early physiological signal and thus the possible evoked response, an artefact correction processing is necessary. The method detailed below aims at disentangling the stimulation artefact from the physiological brain activity.

3.3.2.1 Model of the acquisition chain

The recorded signal $r(t)$ is a combination of the "real" physiological brain activity $e(t)$ and the electrical stimulus $s(t)$, after filtering (e and s become $p(t)$ and $u(t)$ respectively, Fig. 3.9a).

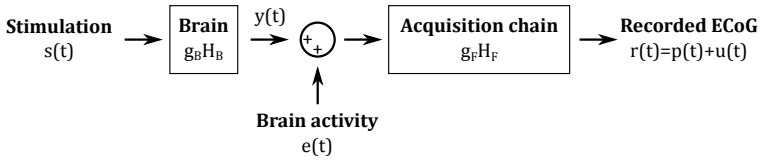

(a) ECoG acquisition diagram.

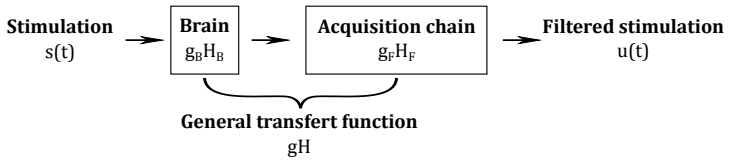

(b) Stimulus filtering diagram.

Figure 3.9: General diagram of the acquisition chain.

Both filtering systems (brain and acquisition chain) are characterized by a transfer function H_x with a specific gain g_x ($x = B$ and $x = F$ for the brain and the acquisition chain respectively). A general gain g and a transfer function H are also defined, as the combination of the gain and the transfer function of both filtering systems. The ECoG signal, brain activity after filtering, $r(t)$ can be then defined as:

$$r(t) = u(t) + p(t) \tag{3.22}$$

where $p(t)$ and $u(t)$ are expressed as follows (in the Laplace space, as defined in section 3.1.1):

$$\begin{aligned} U(p) &= gH(p).S(p) \\ \text{with} \quad g &= g_B g_F \\ \text{and} \quad P(p) &= g_F H_F(p) E(p) \end{aligned} \tag{3.23}$$

3.3.2.2 Artefact withdrawal

As the filtering (50 Hz–Notch filter in particular) induces a withdrawal of information in the range of frequencies composing the 'real' physiological signal $e(t)$, it is impossible to use direct method to reconstruct the recorded $p(t)$ (eg. filtering the oscillation). Here, an artefact correction method is proposed, based on the artefact localisation and the adaptive withdrawal of a simulated oscillation. Note that this method was developed for the perspective of on-line implementation. In the following processes described in Figures 3.10, all data given by modelling are denoted by $\hat{}$.

Artefact simulation A computation of the artefact is first performed. The stimulus $\widehat{s}(t)$ used in the model consists in a biphasic square wave, with parameters taken from the "real" recorded artefact $u(t)$ (pulse width, polarity and amplitude).

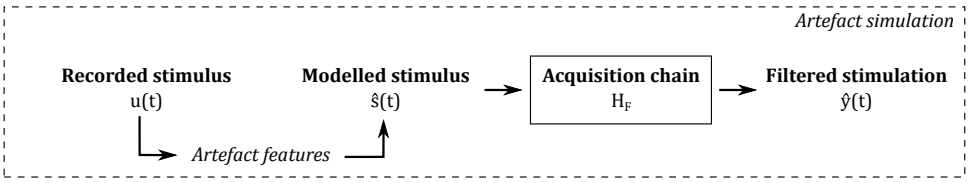

Figure 3.10: Artefact simulation diagram.

Hypothesis 1 The transfer function H_B of the brain is assumed linear and purely resistive.

Corollary 1 The artefact, stimulation current electrically transmitted by the brain, is considered to be identical to the real stimulus $s(t)$ delivered by the stimulator.

Corollary 2 The general transfer function $\widehat{H}$ is thus considered to be the transfer function of the acquisition chain $\widehat{H}_F$ alone, as defined in section 3.1.2. The brain effects (transfer function H_B) are neglected.

Hypothesis 2 The gain $\widehat{g}$ is not considered for the simulation part (as it is the unknown to determine).

The estimated stimulus artefact $\widehat{y}(t)$ can be then defined in the Laplace space as:

$$\widehat{Y}(p) = \widehat{H}_F(p).\widehat{S}(p) \tag{3.24}$$

Determination of the precise oscillation position in the signal To withdraw only the oscillatory part in the recorded signal, it is necessary to know their exact position. Since the stimulator does not provide a synchronisation output signal, the synchronisation was performed using the standard deviation of the absolute value of the recorded signal first derivative (Fig. 3.11).

The first derivative $r'(t)$ of the recorded signal contains three peaks (in most cases), representing the fast variations of the steep edge of the artefact. These peaks are defined as points were the signal exceeds a minimum height threshold $Th1$ (Fig. 3.11, step B in red). The position of the oscillation then corresponds to the first point after the artefact below a second threshold $Th2$ (Fig. 3.11, step C in magenta). The thresholds $Th1$ and $Th2$ have been empirically set to four and three times $r'(t)$ standard-deviation respectively. The determined position is then transferred on the initial raw signal $r(t)$ (step D).

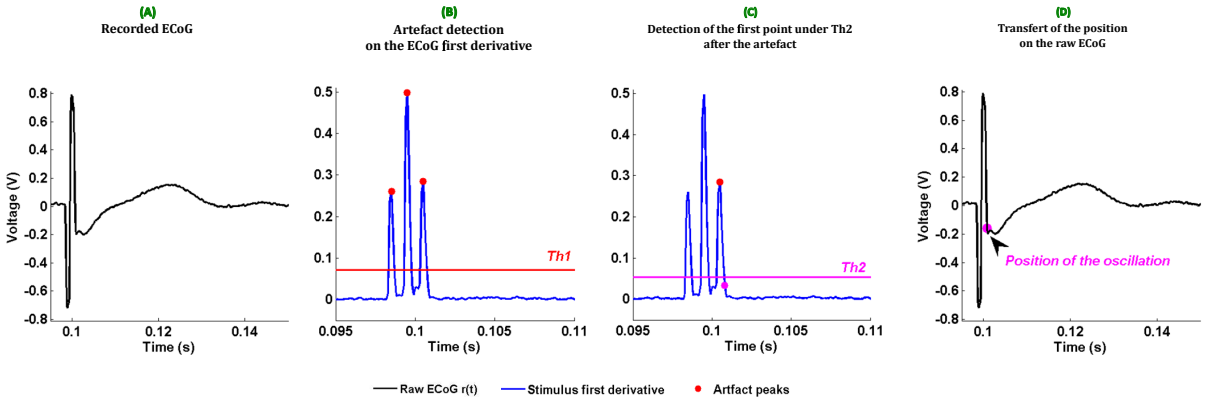

Figure 3.11: Detection of the oscillations location in one ECoG raw signal. A) Raw signal. B) Artefact detection on the raw signal's first derivative with a $Th1$ threshold. C) Detection of the oscillation position in the raw signal's first derivative: first point after the detected artefact, below $Th2$. D) Transfer of the oscillation position on the original raw signal.

Reconstruction of the physiological signal (Fig. 3.12) The physiological signal reconstruction is only performed on a section of the raw signal, starting at the previously detected oscillation position. The duration of the section to reconstruct is defined as 0.5 % of the stimulation period (inverse of the stimulation frequency). The modelled physiological signal $\widehat{p}(t)$ is divided into two following components:

A 1st order linear component, a linear trend $t_r(t)$ which is introduced to represent the unknown possible linear variation induced by both the acquisition chain and external disturbances:

$$t_r(t) = at + b \tag{3.25}$$

The slope a and the offset b represent signal variations at a wider time range than the studied signal and the milieu-electrode interface respectively.

A higher order component $c(t)$ that contains the remaining information not included in the trend.

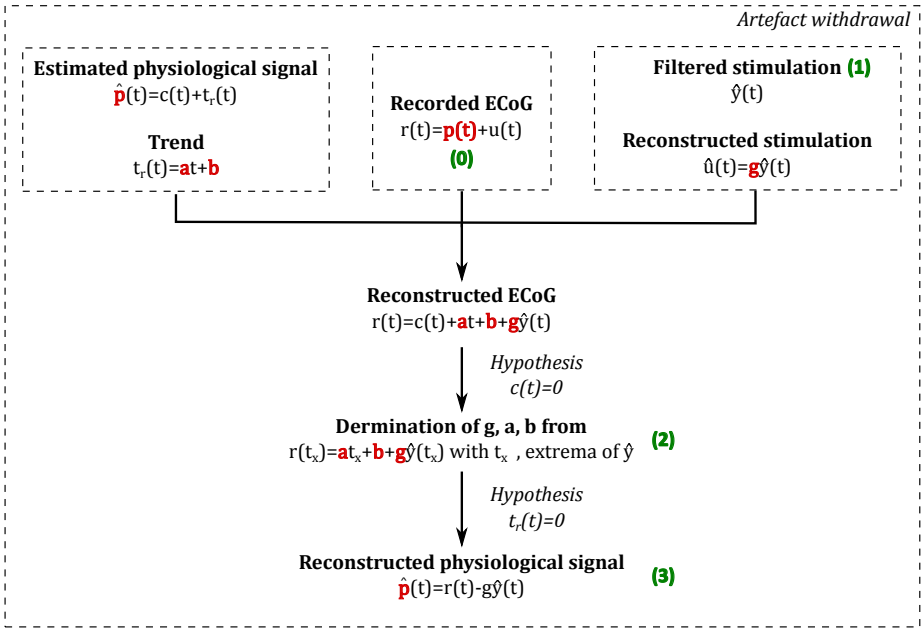

Figure 3.12: Artefact withdrawal processing.

The unknown coefficients a, b and g are computed by an algorithm that minimizes the quadratic gap between the selected points in the real signal and the simulated one: the pseudo-inverse. This transformation maximizes the approximation of $\widehat{p}(t)$ when $c(t) = 0$. This amounts to the same thing as solving the following equation (step 2 , Fig. 3.12, 3.13)):

$$r(t_x) = at_x + b + g\widehat{y}(t_x) \tag{3.26}$$

The t_x times are defined as the n-consecutive extrema of $\widehat{y}(t_x)$. A compromise is made between the signal to keep $\widehat{p}(t)$ and the number of points n to consider. Here, $\widehat{p}(t)$ is approximated at the 2^{nd} order , i.e. taking four t_x points are enough. Solving Equation 3.26 for more points is useless, as the following oscillation peaks are not significant compared to the signal baselines (step 2-3 , Fig. 3.12, 3.13).

The unknowns g, a and b are then determined (step 3) by solving the following equation:

$$r(t_x) = at_x + b + g\widehat{p}(t_x) \tag{3.27}$$

Finally, $\widehat{p}(t)$ is reconstructed by subtracting from the simulated artefact $g\widehat{y}(t)$ to the recorded ECoG $r(t)$. Figure 3.13 displays the oscillation withdrawal for the cortical stimulation presented in Figure 3.11.

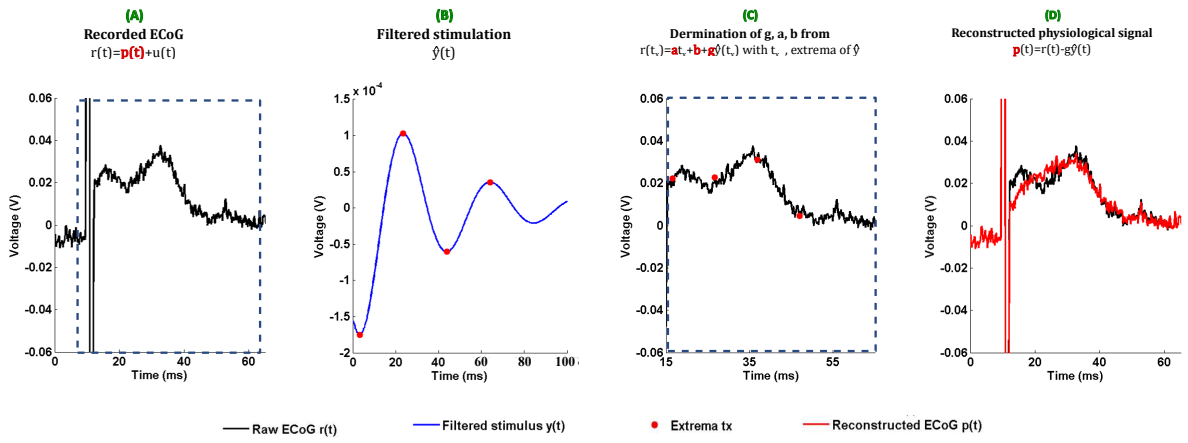

Figure 3.13: Processing of the reconstruction of the physiological signal. (0) Raw signal. (1) Detection of the four first extrema of the modelled oscillation. (2) Detection of the raw signal's amplitudes corresponding to the oscillation extrema position. (3) Reconstruction of the signal (red) by subtracting the modelled oscillation (adapted with the gain g) from the raw signal (black).

The algorithm was validated on the data obtained from the experiment conducted in the lab for the artefact characterisation. Processing of real brain ECoG signals recordings from the intra-operative experiment presented in Chapter 2 was also tested. Figure 3.14 gives three practical applications of the previously detailed algorithm on brain ECoG signals. Each single stimulus was extracted from stimulation of physiological saline (Fig. 3.14-A) and intra-operative DES (Fig. 3.14-B,C).

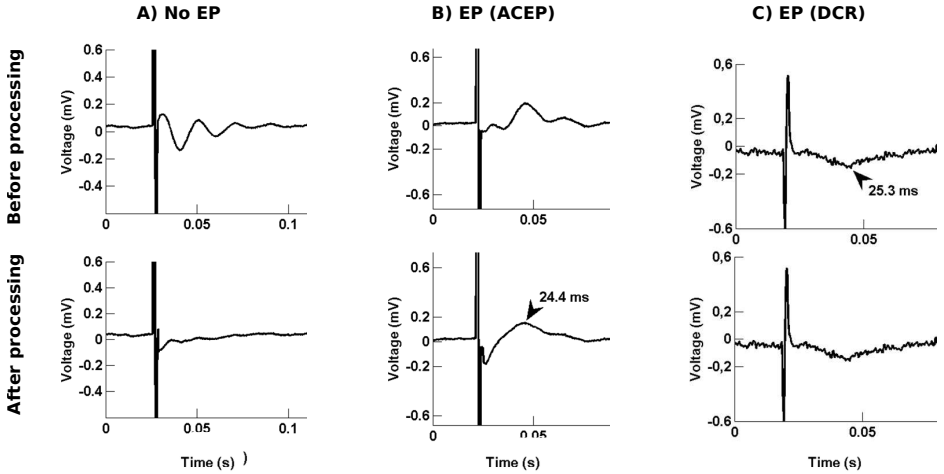

Figure 3.14: Examples of oscillation withdrawal on ECoG signals. A) The ECoG signal only contained oscillations. B) An ACEP appeared after the oscillation withdrawal. C) A raw signal with a visible EP is not altered by the oscillation withdrawal processing.

Chapter 4

Intra-operative evoked potentials induced by DES

Contents

4.1 Methods

Intra-operative ECoG recordings were performed on 6 patients undergoing left LGG awake surgery, according to the procedure detailed in section 2.2.4. All patients were right-handed. For each of the following described cases, two intra-operative pictures showing the functional mapping before (cortical mapping) and after (subcortical mapping) the tumour resection.

4.1.1 Direct electrical stimulation and functional mapping

Usual cortical and white matter mappings were completed on awake patients (constant-current biphasic square wave pulse of 1 ms duration each, 60 Hz). The current intensity was patient-specific.

Patient 1: Patient 1 refers to the case study presented in section 2.3, for the ECoG recording set-up validation. As a reminder, this patient was a 31-year old woman presenting a left pre-central gyrus (rolandic area of the left hemisphere) LGG detected after an inaugural seizure with no functional impairments.

Both cortical and subcortical DES were performed at an intensity of 2 mA. Cortical stimulations (Fig. 4.1a)) in 1 and 2 led to complete anarthria that identifies the premotor ventral cortex in the lateral part of the precentral gyrus. The subcortical mapping (Fig. 4.1b)) highlighted the different language pathways. Laterally, in 48, stimulations of the superior longitudinal fasciculus (SLF) also generates a complete anarthria. Articulatory troubles but also facial movements representative of the pyramidal tracts are induced more mesially, in 47. At the bottom of the cavity, and more anteriorly than previously, in 49, the stimulations led to semantic paraphasia suggesting the presence of the inferior fronto-occipital fasciculus.

Patient 2: This patient was a 25-year old male with a retro-central LGG, detected after an inaugural seizure with no functional impairments.

DES mapping was performed at an intensity of 2.75 mA. Cortical mapping (Fig. 4.2a)) induced an involuntary facial movement along with articulatory troubles that identify the

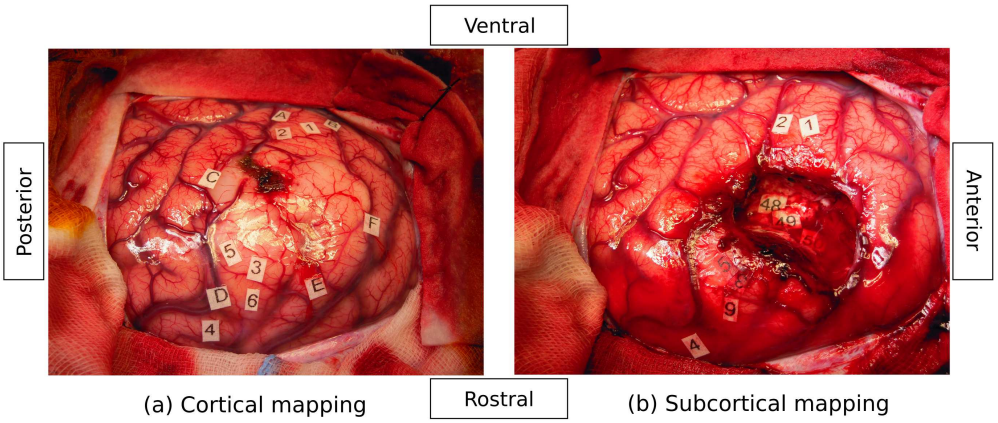

Figure 4.1: Initial 60 Hz DES mapping for Patient 1.

motor facial area (1, 2). Stimulations at the level of the retro central part of the post-central gyrus led to tongue and facial dysesthesia, in 3 and 4 respectively. Reproducible dysesthesia of the three right hand last fingers occurred when DES was applied more mesially in the retro-central gyrus 5. Subcortical mapping (Fig. 4.2b)) of the SLF led to articulatory troubles in depth (50) but also in 47. Stimulation of somato-sensory fibres of the right upper limb in 44, 45 and 48 were at the origin of both facial dysesthesia but also of articulatory troubles. Finally, involuntary movements of this same limb, representative of the pyramidal tracts, are induced in the central fold, in 46.

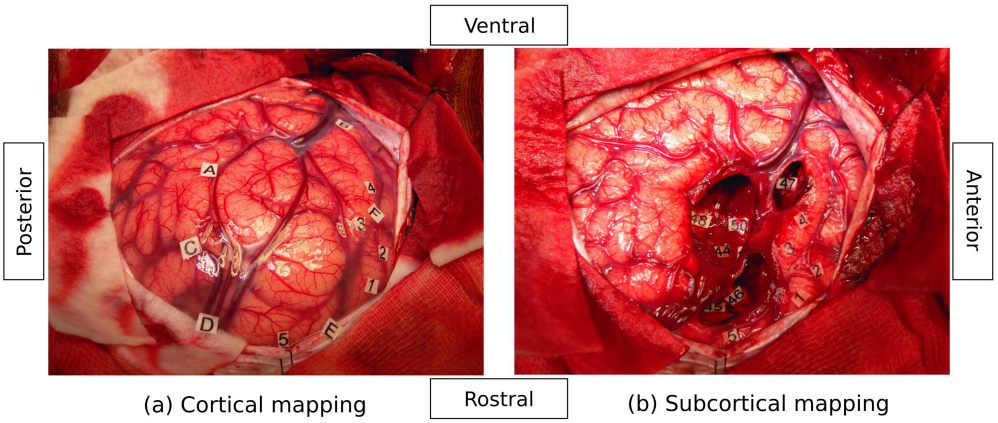

Figure 4.2: Initial 60 Hz DES mapping for Patient 2.

Patient 3: The third patient was a 34-year old woman who developed a left paralimbic LLG, with chronic drug-resistant epilepsy but a surprisingly normal pre-operative neurological assessment.

Cortical and subcortical mappings were performed at 3.5 mA. Cortical mapping (Fig. 4.3a)) in the pre-central gyrus (tag 3) induced articulatory troubles without impairing the left upper limb movement. More laterally in this gyrus, negative motor areas were identified in 1 and 2, as stimulation led not only to a complete stop of verbal fluency but also modifications of the left upper limb movements. A site of reproducible anomia was found in the front of the Labbe's vein, at the level of the superior left temporal gyrus. Regarding the subcortical mapping (Fig. 4.3b)), the dorsal articulatory and ventral semantic stream were identified in 49 and 50 respectively. Indeed, DES on site 49 induced the same disorders as cortical DES 1 and 2. Finally, the stimulation of 50 resulted in semantic disorders (paraphasia and verbal perseveration).

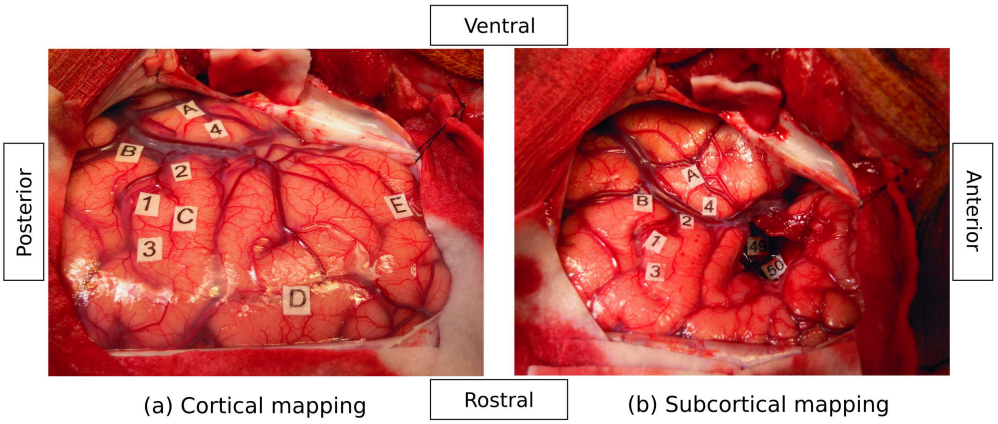

Figure 4.3: Initial 60 Hz DES mapping for Patient 3.

Patient 4: Patient 4 was a 42-year old woman, with a LGG at the level the left insular area and a normal linguistic per-operative assessment.

The cortical mapping (Fig. 4.4a)) with 3 mA DES, led to impairments in the retro-central opercularis with articulatory troubles in 1 and the ventral pre-motor cortex at the level of the lateral part of the pre-central gyrus with a verbal fluency suspension in 2. More

mesially, stimulation in 3 induced a temporary freezing of both counting and right upper limb movement, indicative of a negative motor area. The motor facial area was identified in 4 as involuntary facial movement occurred within stimulation. Lastly, anomia is generated at the level of the superior pars-opercularis segment (5). Subcortical mapping (Fig. 4.4b)) allowed the resection up to the deep white mater tracts, including the inferior fronto-occipital tracts (38), as stimulations generated significant verbal perseverance, jargon aphasia and semantic paraphasia.

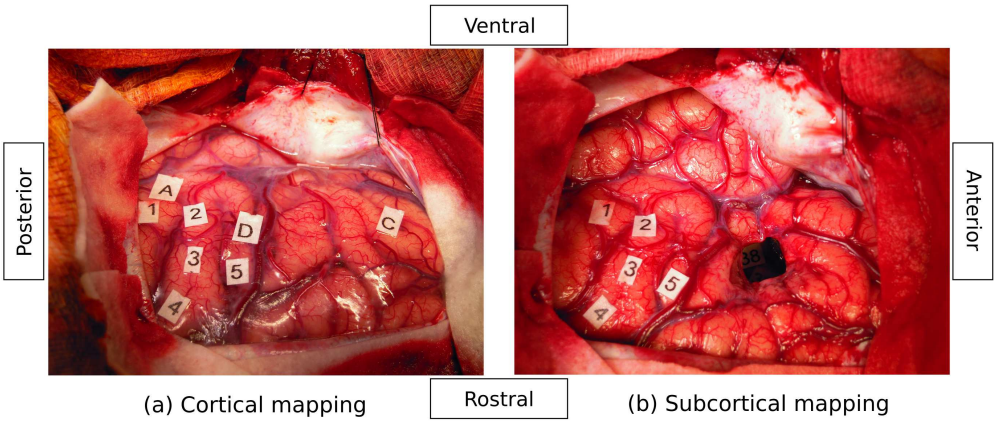

Figure 4.4: Initial 60 Hz DES mapping for Patient 4.

Patient 5: Patient 5 was a 24-year old man who developed a left-insular LGG. This patient was subject to epileptic seizures combined with linguistic disorders.

Cortical and subcortical mapping were performed at an intensity of 2.5 mA. The negative motor area in 1 and 4, was identified as cortical stimulations (Fig. 4.5) led to fluency suspension and to an arrest of right upper limb movements. More laterally, anomia was induced by DES in the lateral part of the precentral gyrus (ventral premotor cortex), but also with stimulation of the left inferior frontal gyrus of the pars opercularis (tag 2). Regarding the subcortical mapping, no functional impairments were noticed which enabled resection up to the surface of the lateral face of the lenticular nucleus.

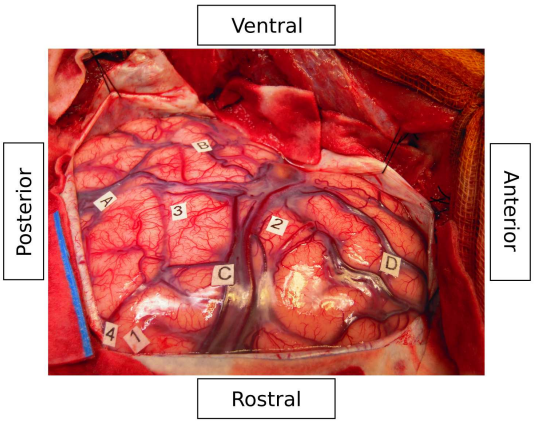

Figure 4.5: Initial 60 Hz DES mapping for Patient 5.

Patient 6: Patient 6 was a 38-year old man presenting a left fronto-callosal LGG with a starting a contra-lateral infiltration, detected after an inaugural seizure with no functional impairments.

Cortical DES (Fig. 4.6a) of 2.5 mA intensity, induced articulatory and/or vocalizations when applied to the ventral premotor cortex (tags 1 and 2). Fluency suspension and the arrest of right upper limb movements resulted from the stimulation of the negative motor area in 5. The primary motor area was identified more mesialy, in 3, as DES induced unwitting facial movements together with articulatory impairments. In the same way, stimulation of the hand area (4) was the origin of dystonic unintentional right upper limb movements. Stimulation at the junction of the ventral premotor cortex and the pars opercularis, marked 6, led to complete anomia. Subcortical mapping (Fig. 4.6b)) of the inferior fronto-occipital tract (50) induced semantic paraphasia. The negative motor network was identified in 46 as both enunciation and right upper limb movement were suspended within stimulation. More mesialy, stimulations of the SLF (48) and at the level of the head of the caudate nucleus (49) induced phonological paraphasia and frequent perseverance. Finally, "disconnection" episodes (during which the patient is not a posteriori aware of what happened during stimulation) occured when DES was applied in contact to the cingulum (47)

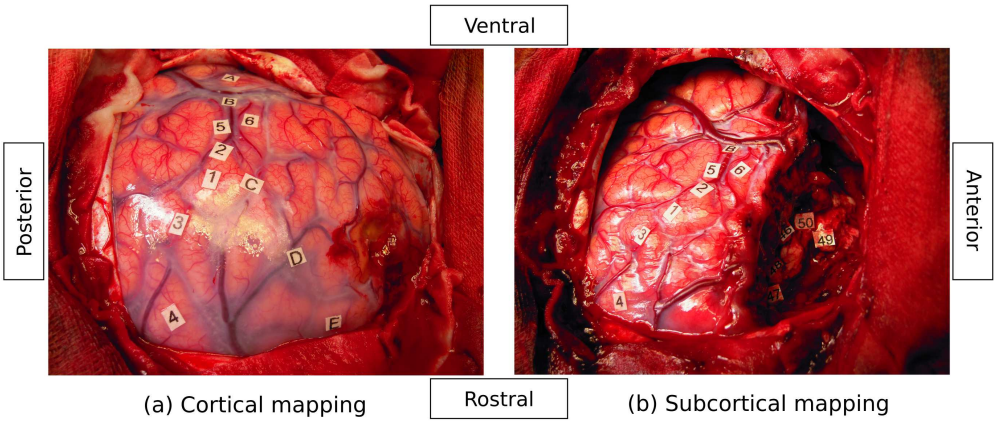

Figure 4.6: Initial 60 Hz DES mapping for Patient 6.

4.1.2 Intraoperative ECoG recordings and stimulation paradigms.

For DES-induced evoked potentials analysis, ECoG signals were acquired after tumour resection under general anaesthesia, concomitant to an adapted stimulation pattern – i.e. low frequency DES.

Two 4-contacts strips of ECoG electrodes were positioned on the surface of the brain (only one strip for Patient 5) on both sides of the tumour resection area. ECoG signals were recorded using differential (contacts 1 to 3 and 5 to 7) and referenced (contacts 4 and 8) modes (as detailed in 2.1.2). The reference electrode consisted of an Au cupule-electrode, ipsilateral to the surgery, except for Patient 3 for whom a patch electrode was used. All channels shared a common ground: a patch-electrode located on the contralateral acromion.

Low-frequency DES was performed on different cortical and subcortical sites, identified as functional during the brain mapping. On patient 1, two cortical sites were stimulated to record EPs. In depth, DES was applied once on all three identified subcortical sites (SLF, pyramidal tracts and fronto-occipital fasciculus). DES was delivered cortically on the motor facial area (tag 2) and subcortically on the SLF (47), for patient 2. Stimulations were performed alternatively on the two sites, nine times each. For patients 3 and 4, the two 4-electrodes ECoG strips were placed alongside each other, on both sides of Labbe's vein (patient 3) or of the pre-central gyrus (patient 4). This cortical area (tags

1-2) was stimulated seven and ten consecutive times for these two patients respectively. Finally, for patient 6, ECoG was first recorded on the negative motor area (1-4) while DES was applied cortically to this same site, along and on both sides of the strip (nine stimulations). The strip was then moved close to the resection cavity, with two of the electrodes placed near the pars opercularis (2), parallel or perpendicularly to the cavity. In both cases, cortical DES was performed once in 2. Finally, the ventral premotor cortex (1-2) and the hand area (4) were cortically stimulated four and five times respectively. Subcortical DES was applied at the level of the SLF (49), the caudate nucleus (49) and the cingulum (47). The corpus callosum was also stimulated four times.

Regarding the adjustable stimulation parameters (frequency and intensity), they were adapted in each case. After having validated the recording set-up on patient 1 with constant-current and constant-frequency DES, modulation in current intensity was performed for the other patients. For safety considerations, the intensity ranged from 0.1 to 2.5 mA. The effects of frequency modulation were also studied for patients 2 and 4. Table 4.1 summarises the stimulation paradigms for all six cases (S: cortical, SC: subcortical).

Table 4.1: Stimulation paradigms

Patient	Number of ECoG electrodes	DES paradigms				Indentified EPs
		Site	Number	F (Hz)	I (mA)	
1	2∗4	C, SC	3	5	2	DCR
2	2∗4	C, SC	7 2	1 – 30 5	1.25 0.5; 1	CACEP, ACEP
3	2∗4	C	7	5	0.25 – 1.25	DCR
4	2∗4	C, SC	8 4	5 1; 10	0.3 – 1.25 0.7	DCR
5	1∗4	C SC	12 2	5 5	0.995 – 1.5 0.995	DCR
6	2∗4	C SC	9 8	5 5	0.1 – 0.45 2; 2.5	ACEP

4.1.3 Trials selection and data processing

Among all ECoG recordings, all channels for which the measured voltages exceeded ± 5 V (i.e. Out of the linear behaviour of amplifiers) were rejected, with respect to the technical features of the amplifier. This resulted in keeping 351 recordings upon 568 (number of stimulations x number of channels) all patients together: 230/376 and 121/192 for cortical and subcortical DES respectively (Fig. 4.7).

Cortical EPs, i.e. EPs induced by cortical DES, were clustered into two groups according to the distance between the DES site and the recording electrode and to the literature. Here, cortical EPs are defined as DCRs for stimulation to recording sites distances smaller than 2 cm. Otherwise, they are considered as CACEPs.

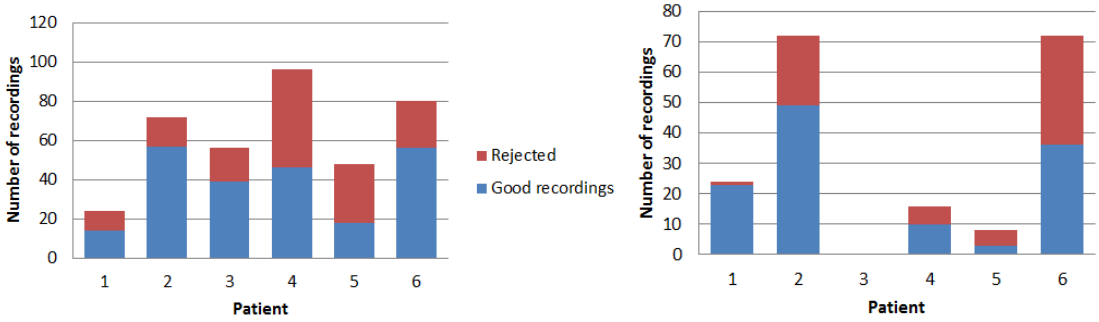

(a) Cortical DES. (b) Subcortical DES.

Figure 4.7: DES trial rejection.

For each channel displaying EPs, stimulation-recording distance were measured on intra-operative photos. The stimulation points are considered as halfway between the stimulation probe tips. For channels set up in the differential mode, the recording point was taken in the middle of the two consecutive electrodes. Regarding referenced mode channels, the distance is given in function of the center of the cortical electrode (as the referenced electrode is located on the patient's mastoid). Only estimation of the distances were given for ACEPs, as the stimulation depth cannot be estimated on the intra-operative pictures.

For a given stimulation test, i.e. position and DES settings fixed, mean EPs were obtained by averaging ECoG signal time-locked to the stimulus onset, upon a time window equal to the period of stimulation. Even if EPs are visible on an averaged stimulation,

they are not always induced by each stimulus. A significativity threshold has thus been set to accept or reject the signals. If a minimum of 50 % of the stimuli does not induce EPs, the corresponding stimulation sequence is rejected. Note that for the studied signals, EPs were almost present on an all-or-none basis. Latencies and amplitudes are measured for mean EPs, but are also averaged among all EPs measured after each artefact of the stimulation. Both amplitude and latencies are given relatively to the stimulus artefact onset. The polarity of the first phase of the stimulation artefact is considered (e.g. + for positive). Similarly, the given EPs polarity stands for the deflection peak orientation (negative or positive). Indeed, the real EP polarity is not considered as it can varies according to the differential measure.

Except for standard deviations, no statistics could be computed, due to the high non-homogeneity of patients and measurements variability. Indeed, data presented here below report case studies, with different patients, stimulation protocols and recording sites. Furthermore, a factor uncertainty is induced by (1) the measure of the distances on a video rather than an exact position, and (2) a measure of the latencies on raw noisy signals (so that the EP extrema is difficult to identify). Finally, the number of successful trials (EPs recordings) were not sufficient to draw statistical conclusions.

4.2 Oscillation withdrawal algorithm validation on intra-operative recordings

Table 4.2 summarises the averaged parameters g (gain), a and b (trend) computed for the oscillation withdrawal processing of the usable recordings.
The influence of the stimulation artefact on the signal can be identified to the gain g value. The higher g is, the more important is the presence of the oscillation on the signal. The variations of g depend on the recording-stimulation sites distance, the stimulation strength (current intensity and pressing of the probe upon the brain) and on the electrode-milieu interface (contact quality and wetness). However, the direct contribution of these factors cannot be assessed. Although intra and inter patients variations of the gain g can be observed, the range values of g are of the same order. These differences can be induced by the inter-individual variations of the brain's gain g_B, that was not taken in account in this estimation model. Even if the oscillations were modelled according to the orientation of the recorded artefact ($g > 0$ because simulated signals were smaller than

the real oscillations), g was negative in few cases (simulated and real artefacts of opposite directions). When looking at g values on a trial-by-trial basis (i.e. individually for each stimulation artecat), negative values are found on noisy signals, only, with distorted artefacts. For each g-negative, a visual checking was made to make sure that the appropriate orientation of the modelled oscillation was withdrawn.

A linear trend was added in the modelling (a and b parameters (see section 3.3.2), to improve the estimation of g. The computed values are of consistent order among patients. Moreover, a and b are of same order of magnitude as the recorded raw signals ($\mu V.s^{-1}$ and mV respectively). An accurate estimation of g is thus done at the second order.

Table 4.2: Computed parameters of the oscillation withdrawal algorithm.

Patient	g (no unit)	a ($\mu V.s^{-1}$)	b (mV)
1	22.42 ± 18.91	15.80 ± 11.70	-6.39 ± 4.90
2	7.27 ± 7.85	-3.35 ± 4.45	1.51 ± 1.81
3	5.60 ± 4.18	1.44 ± 2.01	-0.71 ± 0.84
4	11.75 ± 4.30	4.43 ± 0.88	-2.25 ± 0.43
5	21.13 ± 15.22	11.00 ± 1.33	-5.22 ± 0.43
6	19.51 ± 8.58	5.13 ± 2.39	-1.99 ± 0.91

4.3 Evoked potentials

Cortical and subcortical evoked potentials were measured for all six patients. Data presented hereinafter results from the processing of the raw recordings, by the oscillation withdrawal algorithm detailed in Chapter 3. Moreover for DCRs and ACEPs, the measure was validated by inversion of the stimulation artefact polarity, at least in one channel. Note that the voltage's signe of all peaks (positive or negative deflections) identified as EPs features is not significant as it cannot be predicted with the use of a differential mode for ECoG acquisition.

4.3.1 Direct cortical responses

DCRs were observed in four among six patients (Table 4.3). Results showed that DCR consist of one $N1$ deflection, occurring between 18.20 and 40.55 ms (mean 26.87 ms) after

the artefact onset. Repeated cortical DES (same parameters and cortical site) applied in the vicinity of the recording sites induced reproducible DCRs. Note that for Patient 1, the two stimulations, 6 and 7, were performed on a same cortical site. Yet, the second ECoG strip was moved so that channel 6 (electrode 5-6) of the first position (stimulation 6) corresponds to channel 7 (electrode 6-7) of the second position (stimulation 7). Moreover, approximative distances are given for Patient 4, as stimulations could not be identified on the surgery video (but the approximative stimulation site was known). Figure 4.8 gives an overview of the DCR's shape. Raw data and mean DCR have already been presented for Patient 1 in Chapter 2. Qualitatively, the current intensity modulation performed in Patient 3 gave no conclusive results as DCRs were measured for all DES amplitudes. No modulation of DCR responses were observed during intensity variations. Importantly, DCRs were not only recorded for DES delivered to functional cortical sites (Patient 5, almost on tag 1 and on tag 2 for Patient 4), but also for non-functional site (Patient 2 and 3). Thus, the stimulation localisation does not seem to have any influence on the DCR latencies.

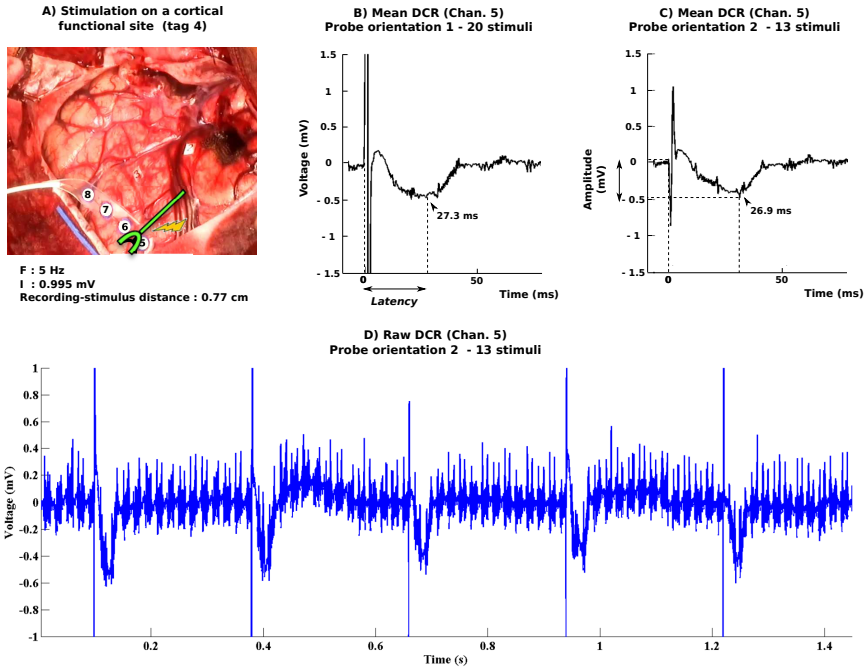

Figure 4.8: DCR, recorded on channel 5, Patient 5. A) DES was applied twice on a same functional cortical site, with a 180 ° rotation of the stimulation probe. B) Mean DCR, computed for the first stimulation probe's orientation (upon 20 stimuli). C) Mean DCR after probe's rotation (13 stimuli). The DCR is not inverted. D) Extract of the raw signal acquired for the second orientation of the stimulation probe.

Table 4.3: Direct cortical responses.

Patient	Stimulation localisation	Stimulation Parameters		Channel	Recording-stimulus distance (cm)	Stimulation artefact		Potential shape		Averaged potential			Raw potential		
		I (mA)	F (Hz)			Inversion	First peak polarity	Relative polarity	Number	Latency (ms)	Amplitude (µV)	Number of stimulus	Latency (ms)	Amplitude (µV)	Number of stimulus
1	near and parallel to elec. 5-6	2	10	4	x	no	-	-	1	16,8	-93,25	37	18,2 ± 2,46	-107,14 ± 31,3	34
				6	0,56	no	+	-	1	24	-64,43	37	23,7 ± 1,19	-890,09 ± 268,91	37
	near and parallel to elec. 6-7	2	10	7	0,51	no	+	-	1	26,3	-275,4	31	25,92 ± 5,16	-304,53 ± 265,93	31
3	parallel to the 2 grids, //at the level of electrodes 7-8	0.25	5	1	1.06	no	+	-	1	23.5	-49.93	18	21.51 ± 3.96	-60.85 ± 26.74	18
		0.5	5	1	0.9	yes	+	-	1	25.2	-105.7	15	24.6 ± 7.09	-167.36 ± 83.98	15
							-	-	1	26.5	-114.62	11	23.88 ± 3.64	-47.22 ± 28.65	11
		0.5	5	1	1.19	no	-	-	1	25.3	-52.87	26	25.43 ± 7.37	-33.69 ± 127.55	26
		1	5	7	1.05	no	+	-	1	39.3	-60.39	28	40.55 ± 8.23	-219.41 ± 195.5	28
		1.25	5	1	1.11	no	+	-	1	27.6	-71	14	29.3 ± 5.33	-127.64 ± 17.6	14
	parallel to the 2 grids, //at the level of electrodes 7-8, lefter	0.5	5	1	1.24	no	-	-	1	28.6	-70.35	31	31.01 ± 6.31	-93.81 ± 27.14	29
		0.5	5	1	1.23	no	-	-	1	18.9	13.9	31	25.44 ± 7.35	33.58 ± 34.48	28
		0.5	5	7	1.28	no	-	-	1	34.9	-49.55	31	34.86 ± 4.5	-56.49 ± 34.49	31
4	between and parallel to the 2 strips, // near elec. 3 , tag 2	1	5	2	< 1	no	+	-	1	29	-228.67	22	27.24 ± 5.54	-259.19 ± 131.02	22
		1	5				+	-	1	25.6	-148.75	25	25.85 ± 5.2	-203.53 ± 80.54	25
		1.25	5				+	-	1	25.7	-208.24	27	25.76 ± 2.54	-289 ± 94.71	37
		0.75	5				+	-	1	25	-166.85	34	26.81 ± 2.12	-286.43 ± 115.87	34
5	tag 4, close to electrode 5 (left)	0.995	5	5	0.59	no	+	-	1	29.1	-364.85	29	24.98 ± 4.64	-3577.38 ± 2513.1	29
	tag 4, close to electrode 5 (left)	0.995	5	5	0.77	yes	+	-	1	27.3	-422.54	20	25.42 ± 5.9	-940.64 ± 1279.46	20
							-	-	1	26.9	-453.63	13	30.79 ± 3.72	-638.97 ± 160.28	13
	tag 4, close to electrode 5 (left)	0.995	5	5	0.87	no	-	-	1	26.4	-443.67	29	26.1 ± 1.6	-187.95 ± 391.72	29

4.3.2 Subcortico-cortical evoked potentials (ACEPs)

Subcortical DES was performed for all patients apart from Patient 3. However, ACEPs were only recorded on Patients 2 and 6 (Table 4.4). Unlike cortical EPs (DCR and CACEP), ACEPs shapes differed between patients. Indeed, two kinds of ACEPs were identified. The first waveform (Patient 2, Fig. 4.9) consists in two consecutive deflections $N1$ and $N2$, with a 20 ms shift. The mean latencies were of 22.52 and 43.23 ms for the $N1$ and $N2$ peak respectively. The second type of ACEPs (Patient 6, Fig 4.11) only presents one $N1$ peak, 21.38 ms after stimulation.

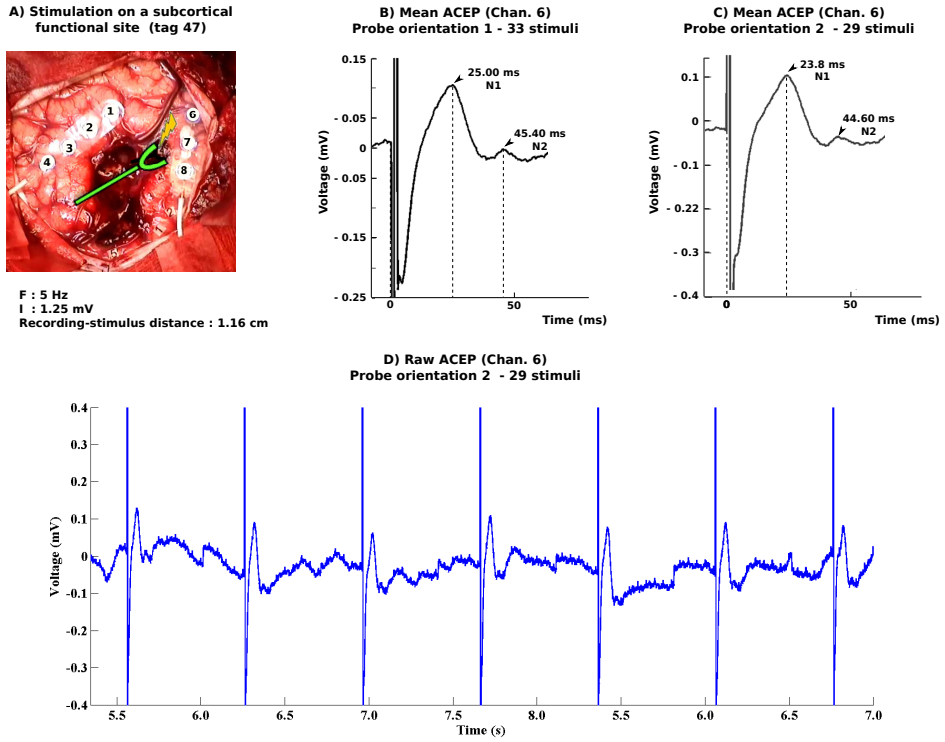

Figure 4.9: ACEP, recorded on channel 6, Patient 2. A) DES was applied twice on a same functional subcortical site, with a 180 ° rotation of the stimulation probe. B) Mean ACEP, computed for the first stimulation probe's orientation (upon 33 stimuli). C) Mean ACEP after probe's rotation (29 stimuli). D) Extract of the raw signal acquired for the second orientation of the stimulation probe.

Extract of the raw ECoG recordings are presented in Figure 4.10 for one subcortical DES applied twice on the same functional site (tag 48), but with a 180 ° rotation of the stimulation probe. Importantly, the processing of the stimulation presented in Figure 4.10-B was necessary to find out ACEP. Even though, a first deflection still preceeds the $N1$

peak which might be a physiological $N0$ peak rather than a residue of the oscillation (Fig. 4.11-C). It is thus mandatory to always compare the mean ACEP obtained from the raw signal to the processed one (without oscillations), in order to avoid wrong conclusions on ACEP characteristics (Fig. 4.11-D).

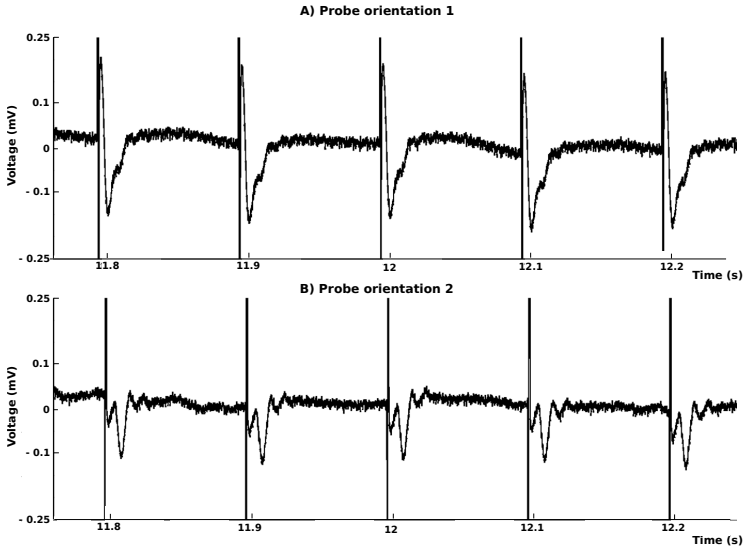

Figure 4.10: Extracts of raw signals recorded on channel 3, Patient 6. Subcortical DES was delivered to the same functional site (tag 48) twice (A and B) but with a rotation of the stimulation probe between the two trials.

For these two patients, ACEPs were recorded for subcortical DES applied closely to the SLF, on cortical sites only distant of 1.7 ± 0.7 cm (nearly above the stimulation site). A current intensity of 1.25 mA, induced ACEPs for frequencies of 1 – 10 Hz(Patient 2). However, when the current intensity was lowered to 0.5 and 1 mA (Patient 2), no ACEPs were recorded. For DES of intensities higher than 2 mA ACEPs were always induced (Patient 6).

Table 4.4: Subcortico-cortical potentials.

Patient	Stimulation localisation	Stimulation Parameters		Channel	Recording-stimulus distance (cm)	Stimulation artefact		Potential shape		Mean potential					Averaged raw potentials				
		I (mA)	F (Hz)			Inversion	First peak polarity	Relative polarity	Number	*N*1 latency (ms)	*N*1 amplitude (µV)	*N*2 latency (ms)	*N*2 amplitude (µV)	Number of stimulus	*N*1 latency (ms)	*N*1 amplitude (µV)	*N*2 latency (ms)	*N*2 amplitude (µV)	Number of stimulus
2	47, under electrode 7	1.25	1	6	1.16	yes	+	+	2	23.3	152.26	43.3	21.24	14	23.22 ± 0.85	130.62 ± 144.68	44.2 ± 1.29	-20 ± 124.1	14
							-	+	2	23.2	93.44	43.2	10.69	3	23.1 ± 0.2	109.17 ± 34.18	43.1 ± 0.1	16.67 ± 41.4	3
			5	2	3.54	no	-	+	2	14.8	6.42	35.1	0.91	62	14.88 ± 0.7	16.94 ± 13.14	35.51 ± 2.77	11.79 ± 11.65	62
				6	1.16	yes	-	+	2	25.00	94.59	45.40	-12.07	33	24.41 ± 1.34	105.69 ± 44.53	46.96 ± 9.87	-12.63 ± 33.99	33
							+	+	2	23.80	124.41	44.60	-13.63	29	24.16 ± 0.31	167.35 ± 58.85	44.88 ± 0.89	2.79 ± 37.14	29
			10	6	1.16	no	+	+	2	26.7	21.48	44.5	-12.09	62	25.3 ± 0.56	75.45 ± 41.22	44.75 ± 1.16	19.85 ± 7.3	62
6	near corpus callosum, under electrodes 3-4	2	5	3	1.61	no	+	-	1	28.3	-114.2	x	x	20	27.92 ± 4.37	-168.66 ± 116	x	x	20
	near corpus callosum, under electrodes 2-3	2	5	3	1.74	no	+	-	1	19.9	-92.57	x	x	45	20.7 ± 3.95	-164.81 ± 100.45	x	x	45
	near corpus callosum, under electrodes 2-3	2.5	5	3	1.74	yes	+	-	2	23.6	-106.08	x	x	37	23.29 ± 5.67	-248.56 ± 199.63	x	x	37
		2,5	5	3	1.74		-	-	1	22.7	-71.76	x	x	41	21.1 ± 6.93	-37.45 ± 311.52	x	x	41
	near corpus callosum, under electrodes 2-3	2.5	5	3	1.74	no	+	-	1	19.7	-81.4	x	x	34	18.81 ± 4.11	-645.41 ± 388.41	x	x	34
				4	x	no	-	-	1	15.9	-221.9	x	x	34	16.47 ± 3.33	-553.08 ± 127.19	x	x	34

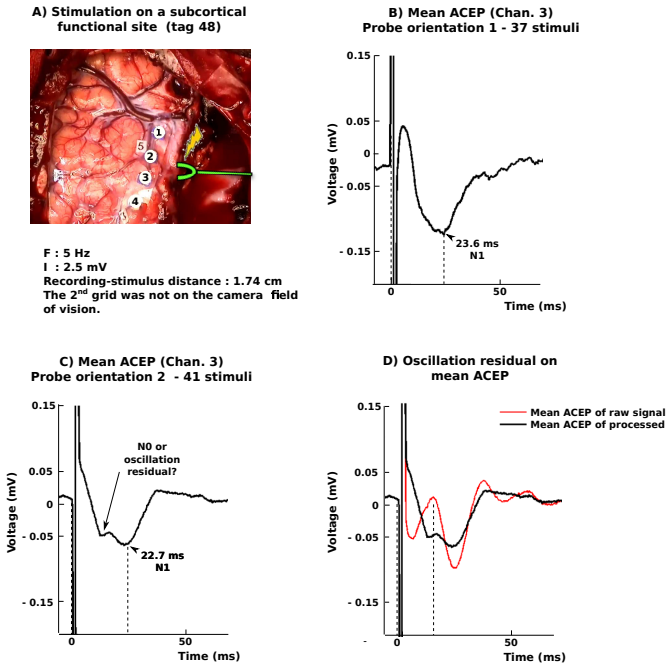

Figure 4.11: ACEP, recorded on channel 3, Patient 6. A) DES was applied twice on a same functional subcortical site, with a 180 ° rotation of the stimulation probe. B) Mean ACEP, computed for the first stimulation probe's orientation (upon 37 stimuli). C) Mean ACEP after probe's rotation (41 stimuli). Importantly, a residue of the oscillation or a physiological $N0$ peak preceeds the N1 peak. D) Comparison of the mean ACEPs obtained from the raw (red) and processed (black) signals recorded when the stimulation probe was in orientation 2 (cf. C).

4.3.3 Cortico-axono-cortical evoked potentials

Cortico-axono-cortical effects at longer distances were only recorded in Patient 2. DES of the primary motor area (1, 2) induced CACEPs in four distant cortical sites. Mean potential shapes obtained from two stimulations are shown in Figure 4.12. It consists of one deflection $N1$ with a peak latency ranging from 14.78 to 33.21 ms (mean of 26.52 ms).

Although the stimulation probe was not rotated for the two stimulation sites, a 45° rotation was made between them. This led to an inversion of the artefacts recorded on channel 6. However, the CACEP's orientation was preserved; thus validating the measure of CACEPs 3.5 cm away from the stimulation site (mean distance). CACEPs were reproducibly measured on channels 5 and 6. For both channels, the stimulation frequencies (1, 5 and 10 Hz) does not seem to affect the induced CACEPs latencies (20.22 and 31.84 ms respectively). Interestingly, CACEPs latencies for two distant recording sites

(channel 7 and 5), are significantly shorter than the closest channel 6. This phenomenon could be explained by the CACEPs propagation through subcortical pathways (channel 7, $N1$ at 14.78 ms) or through indirect cortical connections (channel 6, $N1$ at 31.84 ms).

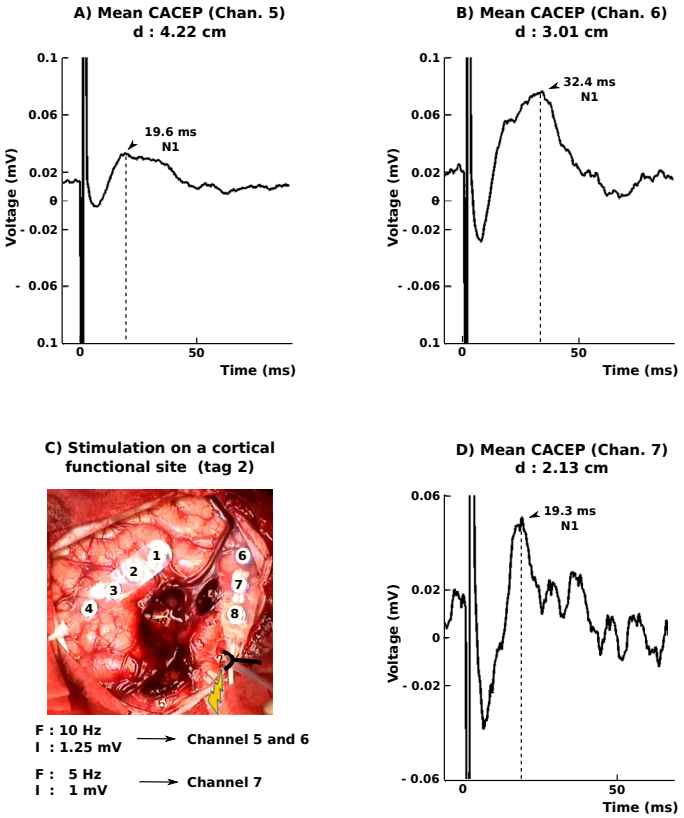

Figure 4.12: CACEPs recorded for 3 channels, Patient 2. Latencies did not vary "proportionnaly" to the stimulation to recording sites distance d. A and B) CACEPs induced by 10 Hz DES, delivered at 1.25 mA. C) Cortical DES was delivered twice to the same functional site (tag 2). D) CACEPs induced by 5 Hz DES, delivered at 1 mA.

Table 4.5: Cortico-cortical evoked potentials.

Patient	Stimulation localisation	Stimulation Parameters		Channel	Recording-stimulus distance (cm)	Stimulation artefact		Potential shape		Averaged potential			Raw potential		
		I (mA)	F (Hz)			Inversion	First peak polarity	Relative polarity	Number	*N*1 latency (ms)	*N*1 amplitude (µV)	Number of stimulus	*N*1 latency (ms)	*N*1 amplitude (µV)	Number of stimulus
2	Tag 2, parallel to strip 2	1	5	6	3.05	no	-	+	1	27.6	32.26	46	28.01 ± 7.22	51.02 ± 38.92	38
				7	2.13	no	-	+	1	19.3	38.27	46	20.93 ± 4.64	287.26 ± 521.6	46
		1.25	5	5	4.22	no	-	+	1	19.7	27.7	60	21.04 ± 3.33	39.48 ± 34.82	52
				6	3.13	no	-	+	1	31.4	76.22	60	32.13 ± 10.41	90.13 ± 47.2	60
			10	5	4.22	no	-	+	1	19.6	8.70	47	21.13 ± 4.68	30.16 ± 28.01	43
		1.25		6	3.01	no	-	+	1	32.4	55.57	47	32.66 ± 8.49	102.93 ± 157.95	18
		1.25	1	6	3.15	no	-	+	1	28.2	52.45	18	29.37 ± 8.69	82.01 ± 83.88	18
	Between tags 1 and 2 parallel to strip 2	1.25	5	5	4.49	no	+	-	1	18.8	10.22	53	20.37 ± 3.64	-11.23 ± 27.38	26[a]
				6	3.36	no	+	+	1	33.1	45.39	53	33.21 ± 3.25	45.05 ± 84.99	36

[a]Note that this stimulation is just under the 50% threshold of significativity

Chapter 5

Discussion and conclusion

Contents

Intra-operative ECoG recording aims at relating electrophysiological effects of DES to functional ones: the final goal is to probe in-vivo and in real-time the spatial and temporal connectivity. Several EPs recordings have been performed in epilepsy surgery. However, neural connectivity has to date only been poorly studied in the context of LGG awake surgery using electrophysiological recordings. Furthermore, even if consistent properties of EPs have been highlighted, their measurement validity has never been clearly questioned.

The main goal of this thesis was to understand the local and remote electrophysiological effects of DES during awake surgery of brain tumours. Eventually, it would enable to improve the stimulation procedure and the functional mapping. We aimed at investigating the neuromodulatory effects of cortical and subcortical DES. The research was guided by three main questions:

- How to assess, in real-time, the brain response to stimulation through the investigation of evoked potentials?
- How to validate the physiological relevance of the measurements?
- What is the link between the functional state of a neural area and the recorded EP?

Correctly measuring evoked potentials in the human brain induced by electrical stimulation is important in the clinical domain especially in the neurosurgical context. It remains challenging because of many pitfalls that can occur at the methodological level and few teams in the world are currently able to efficiently record these evoked potentials. Nevertheless, they can give strong real-time in-vivo insights into the functional state and connectivity of a patient's brain.

Evoked potentials described in the literature have been calculated by averaging several trials of EPs recordings, performed using the referenced mode, i.e. between a measure electrode and a reference electrode. This off-line post-processing prevents using ECoG recordings to monitor EP *in vivo* and in real-time. Therefore, we developed a novel acquisition set up based on differential ECoG recording (between two adjacent electrodes). This method improved the measure focality and thus, enabled detecting raw EPs directly in the operative room (without averaging).

5.1 Methodological conclusions

5.1.1 Methodological pitfalls when measuring evoked potentials in the brain

Measuring evoked potentials triggered by ES in the brain is somehow a difficult challenge. Some requirements are needed in order to verify and check that the putative variations in the voltage difference between the recording electrodes and their reference is not due to stimulus and filtering artefacts, which are the consequences of the electronic responses of the measuring system. Indeed, signals are composed of the ECoG - both basal activity and evoked one - the background noise and the stimulus artefacts. The issue is that these three signals may be in the same frequency range and of the same temporal shape, in particular the evoked ECoG and the recorded artefact. The challenge is then to be sure that measurements are really linked to brain response.

To achieve this goal, I characterized the artefact response as it is not only the pulse itself but its filtered output that may induce misinterpretation. As the acquisition chain is known, the response to the artefact was simulated. This model showed that oscillations, due to the 50 Hz–Notch filter may appear. To successfully record evoked EPs in the noisy environment of an operative room and to get real-time visualization, this notch filter is mandatory as the averaging of trials is not possible (to few stable measurements and real-time constraints). This response should thus be removed. Moreover, when using the notch, averaging is no more suitable as the artefact response is not discarded, except if the stimulation is performed with alternate polarity.

Indeed, one simple assessment can help in sorting ECoG vs. artefact responses: the validity of any evoked potential can be verified by reversing current polarity by switching the poles of the probe (reversing the anode and the cathode). The polarity of physiological potentials are preserved, no matter the stimulation poles orientation, whereas that of ES artefact is not. In most cases, the stimulation biphasic currents has been alternated mainly to erase the stimulation artefacts when averaging several trials together. However, averaging prevents one from determining the electronic noise induced by the system, thus precluding the measure of evoked potential on a trial-by-trial basis.

Thus, caution should be taken with respect to disturbances that can appear due to

the filter step response of the amplifier. In this case, it is important to analyse the data on a trial-by-trial basis in order to accurately identify and remove this unphysiological disturbances. Averaging several trials together without a detailed analysis of the raw signals can clearly mask those oscillations and lead to false interpretations [VRD+16].

5.1.2 Assessment on the artefact withdrawal algorithm

Removing the artefact consists in subtracting the artefact template for which only the amplitude is unknown. The algorithm first looks for the artefact position to ensure temporal alignment then estimate the amplitude through g parameter. To have a real-time algorithm, instead of using optimization routine, an explicit computation is performed based on the value of the extrema of the oscillations. These values, in the real signal, are of course including not only the artefact response but also some of the ECoG and noise signals. To limit this, the first order linear approximation of the remaining signal (trend) was also estimated and thus not included in this estimation. It means that the higher orders of the signals (in a polynomial decomposition) are neglected. The algorithm shows robust, relevant and consistent results as parameters a and b well reflect this approximation and g clearly help to remove most of the oscillation. This algorithm could be slightly improved considering the following ideas:

- Higher order can be used but could be efficient only if the noise is limited to estimate the next smaller maxima. We found that first order was enough, probably that second order could be better in clean signals and higher order useless.

- The signal could be bandpass filtered with a zero phase filter for each period to estimate the maxima more accurately. Indeed, the artefact response spectra is rather limited around the natural oscillation so that other parts of the signal frequencies may be removed. Of course subtraction remains on the raw signal.

Further tests and validations could be then performed with these enhanced algorithms and then results obtained could be compared to assess the impact on mainly two important parameters: delay and amplitude of the evoked potentials. Delay is, to my opinion, however more relevant and important as the amplitude could be influenced by many other unknown issues such as contact impedance of the ECoG grid for instance. However, our approach already greatly enhanced the raw signal and highlighted how careful we should be when processing evoked potential data in a complex surgery room environment.

5.2 Evoked potentials induced by cortical or subcortical DES

5.2.1 Electrophysiological meaning of EPs characteristics

In all reported cases, three types of EPs induced by cortical and subcortical DES have been successfully recorded. Even though some discrepancies can be noticed, there are similarities with the EPs described in the literature (see section 1.4.4).

Whatever the stimulation frequencies and intensities used, cortical DES applied in the vicinity (< 2 mm) of recording sites evoked DCR, 26 ms after stimulation. The DCR latencies recorded in the here-above reported cases are slightly longer than the 20 ms recorded by Goldring et al. [GJH$^+$61]. Similarly, recordings were performed at slightly more distant sites from the stimulation (0.5 to 2 cm) than Goldring's (up to 1 cm). On the contrary, for any DES intensity inducing EPs, neither the second negative deflection nor the early spikes described in the literature were measured (probably because of a too low DES intensity)

For ACEPs, two shapes were observed. First, one-peak ACEPs were recorded. Since its averaged latency was of 22 ms, the first peak likely corresponds to the N1 peak described by Yamao et al. [YMK$^+$14] and Mandonnet et al. [MDP$^+$16]. Unlike what have already been mentioned in the literature, two-peaks ACEPs were also recorded, with a second peak occurring 20 ms after $N1$.

Cortical DES evoked a 26 ms one-peak deflection at cortical sites distant of 2 cm or more. This deflection corresponds to the $N1$-peak of CACEPs defined by Matsumoto and colleagues [MNL$^+$04]. The $N2$ deflection mentioned in their studies (latency around a hundred of milliseconds) was however never recorded.

Thereby, the $N1$ peak appears to be a common feature to all three types of recorded EPs. Moreover, regardless the stimulation site, recorded EPs (DCR, ACEP and CACEPs) always have the same latencies (Fig. 5.1). This property suggests that the $N1$ peak response latency is mostly limited and determined by the cortical output (i.e. the latter cortical elements and in particular, the pluri-synaptic responses, as detailed below).

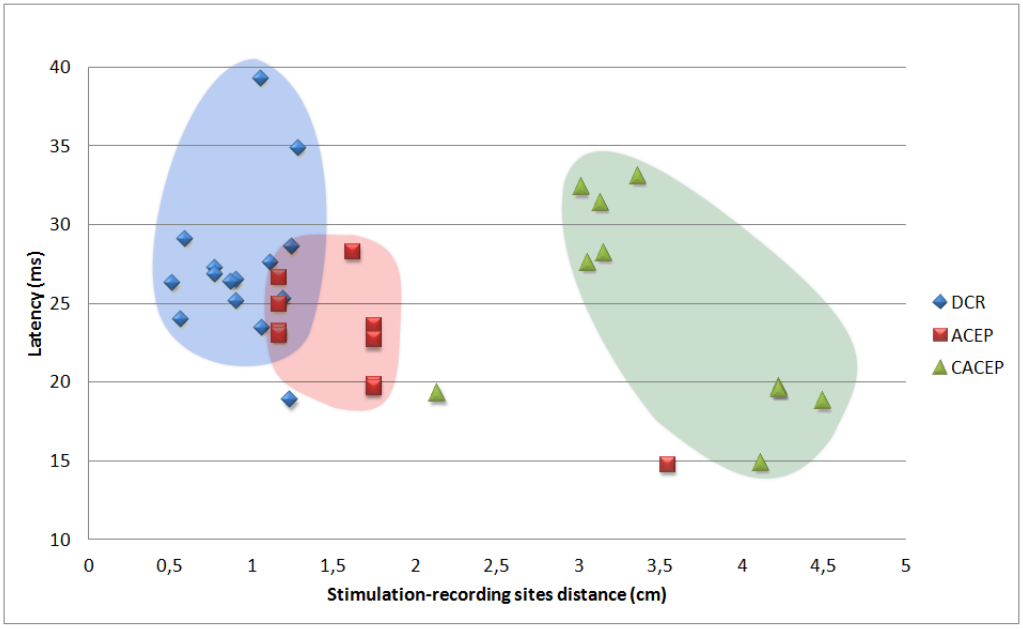

Figure 5.1: EPs latencies in function of the distance from the stimulation site.

Therefore, we are not able to determine if the spread of the stimulation inducing DCR is over short U-fibres, as it may be purely cortico-cortical. In the case of ACEPs, the conduction velocity of the stimulated axon do not have any influence on the negative response since its shape and latencies are similar to DCRs and CACEPs ones. Finally, for CACEPs, if action potentials spread over the very cortical thickness, longer latencies and wider shape would be expected. As in our intra-operative cases, those resemble ACEPs, it suggests that they propagates through subcortical white matter pathways.

Furthermore, according to Goldring et al. [GHG94], this $N1$ peak corresponds to the "primary negative potential" (Fig. 1.10). The shape of this first negative wave (large EP with long latency) suggests that no myelinated axons were involved in this response. It was ascribed to represent the excitatory post-synaptic potentials of apical dendrites [LC62, SGO64]. Interestingly, by using surface recordings on the somatosenrory cortex and direct intracellular recordings in cats, Li and Chou [LC62] have demonstrated that for low stimulations, spike discharges were following the primary negative peak that was recorded on the cortical surface (Fig. 5.2, left panel), whereas a further increase in the stimulus strength shortened the latency of the depolarization potentials and spike discharges, and also increased the amplitude of the former one (Fig. 5.2, right panel).

Indeed, they demonstrated that a stimulus, not strong enough to evoke cortical surface response, still induced a synaptic (or depolarisation) potential (first two lines in Fig. 5.2, right panel). This depolarisation rises with the increase of the stimulation strength, until a threshold of spiking discharges. With strong stimulus, the synaptic potential latency is shorten, as to coincide to the start of the surface response. In the same way, spiking discharges latencies was also significantly shorten with the stimulus strength increase.

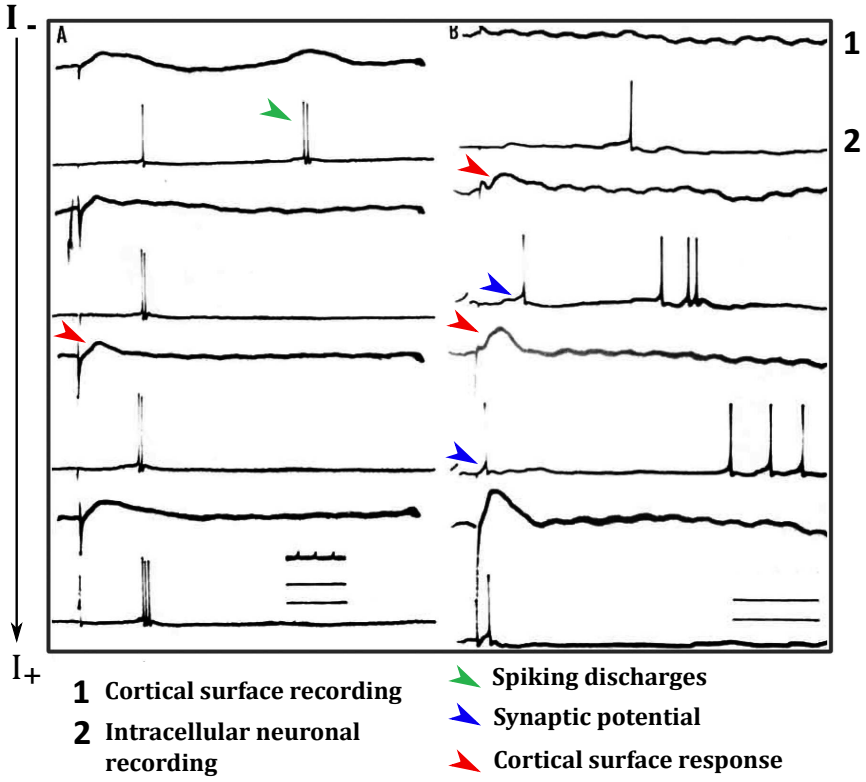

Figure 5.2: Responses to single shocks of gradually increasing strength. Simultaneous recordings from cortical surface and a neuron in two experiments. Time marks 10 msec.; voltage calibration, 20 mV. In this and subsequent illustrations, upward deflection recorded with surface electrodes represents negativity; upward deflection recorded with microelectrodes, positivity. From [LC62]

Finally, they showed that the amplitude of the synaptic potentials changed proportionately with initial surface-negative potentials simultaneously recorded from the surface (Fig. 5.3). Altogether, it thus strongly suggests that excitatory post-synaptic potentials (EPSP) determined the primary negative potential $N1$ in response to DES.

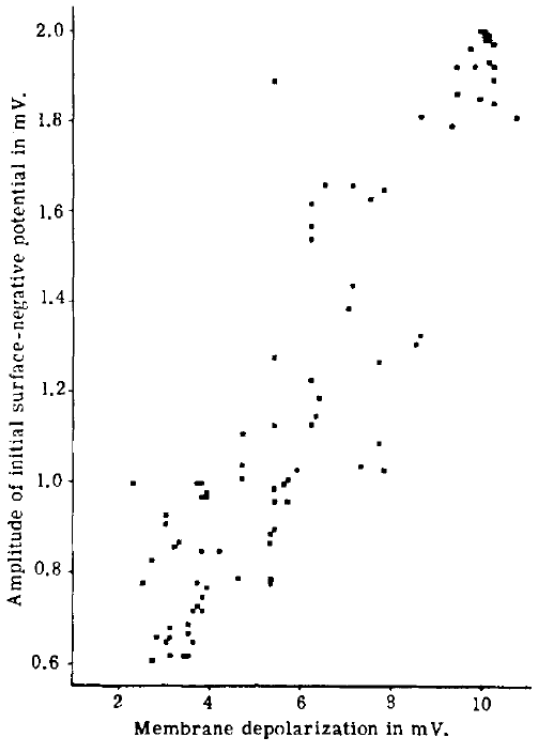

Figure 5.3: Amplitude of surface-negative waves recorded from surface and synaptic potentials recorded from a neuron. From [LC62]

They further demonstrated that 95% of the cells under study responded within 22 ms after stimulation. They concluded that synaptic bombardments were more effective than stimulation presumably applied directly to the neuron in producing excitation.

With even more increasing stimulus, Li and Chou (Figure 5.4) observed that the shape of the surface EP depends on the stimulation strength. A stimulation close to the activation threshold induced a surface-negative potential. When stimulation exceed this threshold (supra-maximum stimulation), either a surface-negative-positive potential ($N1$) or a first surface-negative potential followed by a surface-negative wave ($N2$) are generated. The second negative wave was induced for strong stimulation in particular. Note that only voltage-stimulation was used in their study. More generally and importantly, in most of these studies, the methodology used for the stimulation and the recordings was very poorly described.

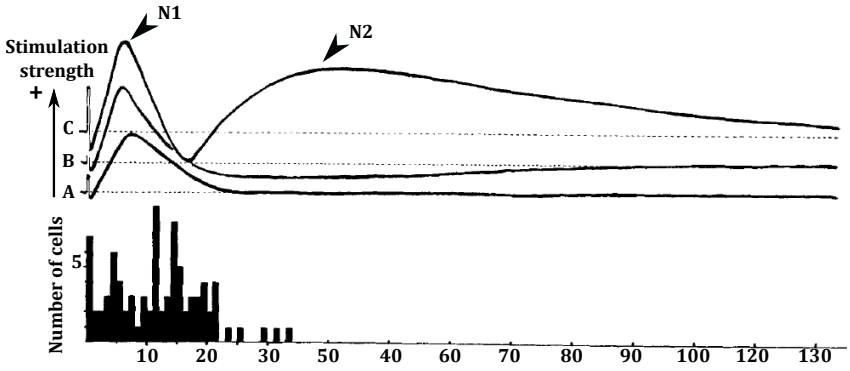

Figure 5.4: Spike response latencies in ms of 48 intra-cellularly and 40 extracellularly recorded units. Tracings according to the same time scale represent typical surface responses $N1$ for threshold stimulation (A), and supra-maximum stimulation inducing a surface-negative-positive potential $N1$ (B) followed by a by a surface-negative wave $N2$ (C). From [LC62]

In our intra-operative recordings, the second negative potential was most certainly obliterated by anaesthetics, as ECoG recordings were performed under general anaesthesia. In the same way, the low current intensities (< 2 mA used for DES were probably not sufficient enough to trigger the positives spikes defined as the "all or none" discharges in the soma of cortical neurons [GHG94].

5.2.2 Stimulation's intensity modulation and the conditions to obtain CACEP

Performing an amplitude modulation for low-frequency DES aimed at identifying the neurons activation threshold and the all-or-none principle of neuronal firing. At a fixed frequency of 5 Hz, a threshold effect was observed for CACEPs, as they were only evoked for intensities higher than 1 mA. In the same way, ACEPs were only induced for intensities exceeding 1.25 mA. Conversely, no intensity threshold was detected for DCRs.

However, previous DCR recordings done by Goldring et al. [GHG94] showed that the stimulation intensity had a direct effect on the DCRs shape (Fig 1.10). Furthermore, the stimulation strength (current intensity in particular) seems to be a crucial parameter in inducing CACEPs. Indeed, as mentioned previously, CACEPs have only been measured in the context of epilepsy [MNL$^+$04, KHM$^+$14], when ES was applied thanks to subdural grids and two contacts were used as a cathode and an anode for bipolar stimulations and with higher current strengths (10 – 15 mA).

It has also been demonstrated experimentally and theoretically through modelling, that the generation of action potentials in an axon is obtained with less charge injections when the pulse width (P_w) is shorter than the chronaxie [MBJ05, MAYB90]. The relationship between the charges injected to reach the threshold and the P_w is not flat but roughly an affine function with a positive slope (see Fig. 1.8). The more the P_w decreases the more the required charges to inject to reach the threshold decrease. So hypothetically, reducing the P_w could also facilitate the generation of CACEPs. Interestingly, in the literature presenting CACEPs measured with grids of 1 cm-spaced electrode, P_w are inferior to that used commonly during intra-operative mapping with 5 mm–spaced bipolar Ojemann's stimulation.

In addition, such CACEPs had not been yet reported when stimulating with a classical 5 mm spaced bipolar probe. The comparison between these two modes of ES is important and yields a main hypothesis to explain why it could be more difficult to observe CACEPs with a classical 5 mm spaced bipolar probe rather than with grid electrodes. In the former situation, ES may not reach the deeper layers of the cortical columns due to insufficient intensity. To overcome this issue, the biophysics of ES suggest (i) increasing the inter-electrode distance and (ii) increasing stimulus intensity. Indeed, for bipolar ES applied on the cortical surface, the depth of the electrical field is determined by the inter-electrode distance. The longer the inter-electrode distance is, the deeper in the cortex the electrical field is. In this vein, it has been demonstrated that large-diameter axons in the subcortex are the most excitable neural elements, when electrical fields are generated and extend from the cortical surface to the subcortical white matter [LBC65]. In addition, when the delivered current intensity is increased, as the medium is almost linear, the deeper electrical field is also increased. This interpretation is illustrated in Figure 5.5. Further studies should disambiguate the effect of the P_w and the inter-electrodes spacing.

Finally, another important aspects should also be taken into account to better understand the generation of CACEPs. With a monopolar probe, electrical charges spread over longer distance from the source, so it may also be possible that this mode of ES could generate CACEPs with a lower charge injection but with a lower focalisation.

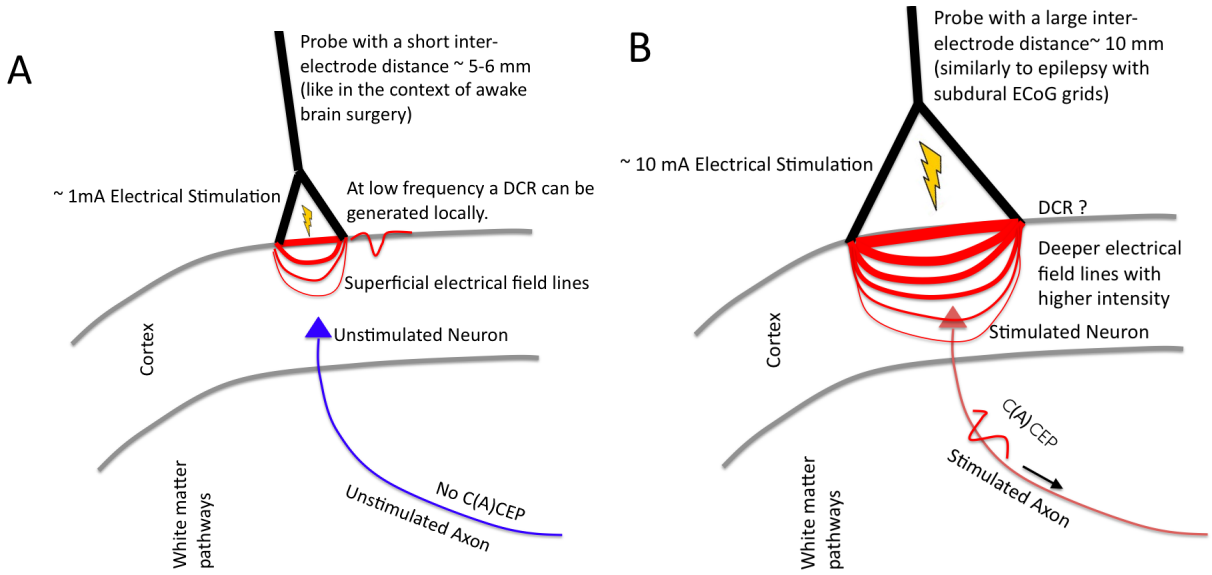

(a) Superficial cortical effects of the ES

(b) Deeper cortical effects

Figure 5.5: **a**. Superficial cortical effects of the ES when the space between the two poles of the bipolar electrode is not sufficient (~ 0.5 cm) to excite deeper neurons and axons to induce a CACEP. Only local effects can be triggered (DCR) at low frequency. When the ES frequency is increased (up to 20 Hz) the basal electrophysiological level may be hyperpolarized progressively and the DCR may be attenuated thereby perturbing the functional connectivity of the whole network. **b**. Deeper cortical effects of the ES when the space between the two poles is sufficiently large (~ 1 cm) and current is increased ($\sim [10; 20]$ mA) like when using two electrodes of a subdural ECoG grid in epilepsy. The electrical field lines vehicle a sufficient charge in the deeper cortical layer to excite neurons or axons with long range projections to more distant cortical areas, and thereby induce a CACEP.

5.2.3 Frequency impact on EPs: why are 50 – 60 Hz DES commonly used?

Regarding the stimulation frequency, its modulation (1 to 15 Hz) aimed at seeing if the measured EPs corresponds to integrated responses of the brain or only to synchronous responses of a small pool of neurons. Nevertheless, the frequency modulation does not appear to induce changes in the recorded intra-operative EPs (latency, shape).

Interestingly, it has however been demonstrated that with 20 Hz ES slow negativities of the separated DCR of a series fuse to produce a negative shift of the cortical electro-

physiological baseline level. As such a shift develops, the sequentially DCRs are reduced in amplitude [GJH$^+$61]. It is thus tempting to suggest that when the frequency of stimulation is increased, a progressive hyperpolarisation is locally induced around the site of stimulation that may perturb the functioning of this area. Indeed, this slow negative shift of the baseline with attenuation of the DCRs may be representative of a global hyperpolarisation (and not a depolarisation) because no output response is generated (unless the intensity is much increased to trigger more directly an all or none somatic response, see Figure 1.10 (Fig. 2 from [GHG94] and its interpretation).

More precisely, it may illustrate the fact that the membranes of certain neural elements which are under the ES do not have an all or none property but saturate and did not recover their resting state due to the cumulating DCRs. In this vein and importantly, the duration of the DCR is 15 – 20 ms, which corresponds to the period of the 50 – 60 Hz ES. Thus, when successive ES are applied too frequently, the cortex may not respond due to the saturation of the membranes occurring during the cumulating cortical responses.

To date, the remote effects of DES are not well known. Indeed, it is not very clear whether a local application of DES affects foreign cortical areas. Li and Chou [LC62] have demonstrated that trans-callosal stimulation produced hyperpolarisation of various latencies and duration, most likely due to the presence of varying numbers of inter-neurons on the synaptic pathways.

Recently, recordings of intra-operative EEG (iEEG) were used to study whether cortical or subcortical 60 Hz- DES have neuromodulatory effects on electrophysiological signals [VRPC$^+$16]. The evolution of the ECoG signal frequency content between pre-, intra-, and post-stimulation periods was studied, according to the common frequency band division of EEG (Fig. 2.3a and section 2.1.1). Significant changes in the frequency content distribution (variations of the median frequencies) were highlighted in EEG signals recorded from different ipsi- and contra-lateral sites to the surgery (Fig. 5.6). Most of these neuromodulation were induced directly after stimulation. Finally, it was observed more recording sites were affected by subcortical DES than cortical DES.

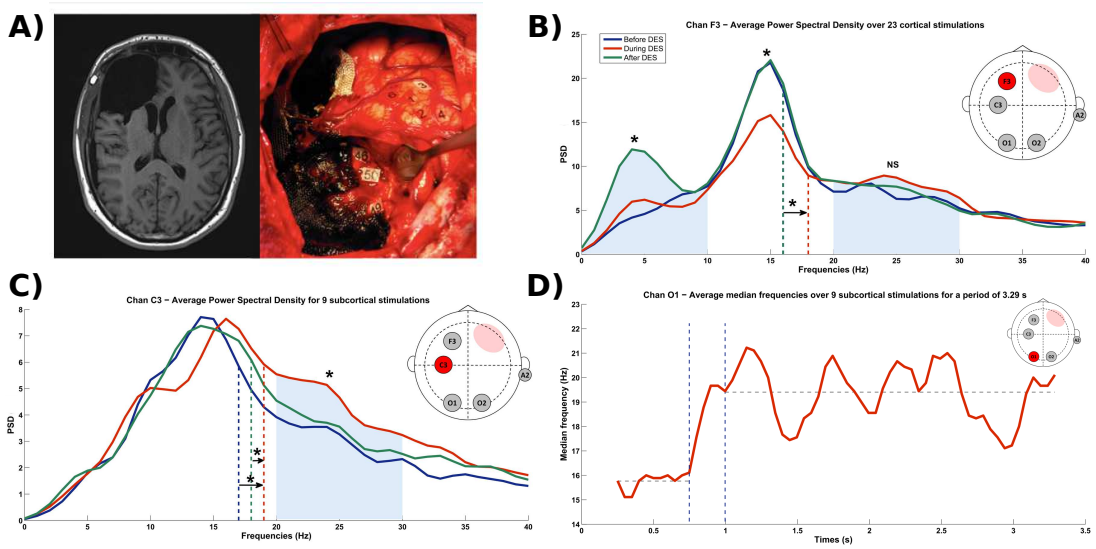

Figure 5.6: **A)** Post-operative MRI of the patient's brain, showing the right frontal cavity and an intraoperative view of the brain with the main anatomical landmarks. Cortical mapping: the premotor cortex with speech impediments in 6, 5 and 3; more medially, the motor cortex of the face with facial movements in 1, 2 and 4; no functional sites detected in the frontal area. Subcortical mapping with movement interruption induced by the DES: the anterior arm of the internal capsule in 46; periventricular structures in 49, just in front of the pyramidal tract from the motor cortex; and the junction between the corona radiata and the posterior arm of the capsule in 50, with complete anarthria when DES was applied (suggesting that fibres from the motor cortex of the face are stimulated). **B)** The mean PSD of the iEEG signal before (blue), during (red) and after (green) each period of cortical DES (computed for durations of 2.3 s, [1.3, 10.2] s and 2.3 s, respectively), as measured at F3. The red ellipse on the top view of the head corresponds roughly to the tumour site and the resection. The median frequency increased with time when DES was applied. Interestingly, the power of the [0, 10] Hz frequency band increased (although after DES was applied), inducing after-effects in the theta band. **C)** The mean PSD of the iEEG signal before (blue), during (red) and after (green) each period of subcortical DES (computed for durations of 5.2 s, [3.3, 11.6] s and 5.2 s, respectively), as measured at C3. The median frequency and power of the [20, 30] Hz band increased with DES. **D)** The moving window median frequency (500 ms, with an overlap of 90%) averaged over nine subcortical DESs period for PSD measured at O1. The median frequency was quite stable during the first 750 ms (at around ∼16 Hz) and then increased after 1 s (to around ∼19 Hz). These measurements were made for the first 3 s of DES (∼ the shortest period of subcortical DES). NS: non-significant.

5.3 Towards novel ways of electrically stimulating the brain: insights from FES of peripheral nerves

The biophysics of the generation and propagation of APs in peripheral nerves is probably better understood than that of the cortical tissue [GM95, MBJ05, Teh96]. This may be mostly due to the inhomogeneity of cortical tissue. Research on FES suggests that there are many ways of modifying ES modalities functional brain mapping. In theory, some important parameters can be modified to improve and optimise ES in general and the spatial selectivity of the stimulated neural tissue in particular. Waveforms (most of which are currently biphasic square waves) and electrode design (geometry, monopolar vs. multipolar configurations, etc.) could be modified so as to induce different types of current within peripheral nerves [MBJ05] and within the brain. For instance, the membrane excitability and the selectivity of peripheral nerve (related to the fibre diameter) can be manipulated by varying the biphasic pulse parameters during bipolar stimulation. According to the strength-duration curve, increasing the duration of the second pulse increases the selectivity (as long as the pulse intensity is decreased in order to balance the charge injected by the first activating pulse) [GM95]. This simple variation in the pulse waveform needs to be tested at the cortical level, in order to investigate the differences between cortical stimulations and nerve stimulation and to better understand the effect of ES on the whole-brain level. To the best of our knowledge, this type of simple manipulation has never been performed. In theory, many other parameters could be modulated to probe the effect of ES on the whole-brain level. It would be also possible (for instance) to try to improve spatial selectivity by using multipolar electrodes (or bipolar and concentric electrodes). With this configuration, adjacent neural elements could be inhibited with a long duration pulse (to inactivate sodium channels) [GM83, MBJ05] and then the central electrode could be stimulated to increase its independence with regard to the surrounding neural elements. Similarly, paired stimulation protocols could also be used to probe the electrophysiological states of the neural networks, and the stimulation frequency could be manipulated to make it resemble natural discharge patterns [KM07]. All these approaches are technically feasible and can be underpinned by electrophysiological theory and modelling of the electrode-tissue interface. This very active area provides the rationale for further development of DES. These new approaches may be of great value in better understanding the effect of ES on the brain and optimising the effects of ES during functional mapping *in vivo*.

5.4 Perspectives

DES combined with intra-operative electrophysiological recordings can be used to probe *in vivo* and in real-time the spatiotemporal connectivity and dynamics of both short- and long-range networks. Only averaged EPs have been presented in the reviewed literature, which prevent a real-time analysis of the electrophysiological responses. We developed a new recording set-up, based on a differential acquisition mode, allowing identification of the EPs directly on the raw data. Moreover, to ensure the validity of the measurement, i.e. to ensure the physiological aspect of the recorded signal methodological pitfalls have been defined. A post-processing algorithm has been implemented to reduce signal distortions induced by the acquisition hardware.

Today, the reliability and the reproducibility of the measurement protocol and the data acquisition system have been validated. It is now necessary to go further on the EP analysis, to study the immediate and persistent effects of DES on the connectivity between different sites. The next step of EP analysis would be the investigation of the relationship between the recorded EPs and the functional disturbances in awake patients. This relationship between electrophysiology (EP) and behaviour (function) is crucial in LGG surgery, as it can help defining which cortical areas must be preserved and kept connected to the underlying functional network. It is an important constraint in LGG surgery. To study this relationship, it would be interesting to apply DES and record EP at precise functional and non-functional cortical sites determined during the 60 Hz brain mapping.

The resection could be validated by a real-time identification of the functional networks thanks to the analysis of the electrophysiological changes. It would help to improve the DES technique that remains archaic despite many technological innovations are theoretically possible (reducing the amount of injected charges, improvement of the spatial selectivity, etc.). Moreover, evoked potentials could be used to establish in real-time and in vivo the electrophysiological state of a particular area as for instance the level of excitability [VRD$^+$16].

Finally, the long-range connectivity of DES and its neuromodulatory effects could be assessed by recording EP at remote distances from the DES site. In this case, the recorded response would not be the direct EPs but rather an integrated response, involving a wider

population of neurons. To do so, non-invasive EEG recordings can be performed during the entire surgery. This would also help following the evolution of the frequency content of brain activity throughout the all surgery [VRPC$^+$16].

A better understanding of the mechanisms underlying DES, in particular through the measurement of electrophysiological responses, should help designing more perfected protocols. This should make the approach even more robust to variations related to the patient and surgery, and thus further diminish the potential sequelae. All this in order to improve the surgical planning and the quality of life of the patients.

Publications

International Journals

1. Marion Vincent, David Guiraud, Hugues Duffau, Emmanuel Mandonnet, and François Bonnetblanc. Electrophysiological brain mapping: Basics of recording evoked potentials induced by electrical stimulation and its physiological spreading in the human brain. *Clinical Neurophysiology*, 128(10):1886–1890, 2017

2. Marion Vincent, Olivier Rossel, Mitsuhiro Hayashibe, Guillaume Herbet, Hugues Duffau, David Guiraud, and François Bonnetblanc. The difference between electrical microstimulation and direct electrical stimulation–towards new opportunities for innovative functional brain mapping? *Reviews in the Neurosciences*, 27(3):231–258, 2016

3. Marion Vincent, Olivier Rossel, Bénédicte Poulin-Charronnat, Guillaume Herbet, Mitsuhiro Hayashibe, Hugues Duffau, David Guiraud, and François Bonnetblanc. Case report: Remote neuromodulation with direct electrical stimulation of the brain, as evidenced by intra-operative eeg recordings during wide-awake neurosurgery. *Clinical Neurophysiology*, 127(2):1752–1754, 2016

Reviewed Conference proceedings

1. Marion Vincent, Olivier Rossel, Hugues Duffau, Francois Bonnetblanc, and David Guiraud. A measure of cortico-cortical potentials evoked by 10hz direct electrical stimulation of the brain and by means of a differential recording mode of electrocorticographic signals. In *Engineering in Medicine and Biology Society (EMBC), 2016 IEEE 38th Annual International Conference of the*, pages 4543–4546. IEEE, 2016

Bibliography

[Adr36] Edgar D Adrian. The spread of activity in the cerebral cortex. *The Journal of physiology*, 88(2):127, 1936.

[AM87] William F Agnew and Douglas B McCreery. Considerations for safety in the use of extracranial stimulation for motor evoked potentials. *Neurosurgery*, 20(1):143–147, 1987.

[BAK12] György Buzsáki, Costas A Anastassiou, and Christof Koch. The origin of extracellular fields and currents—eeg, ecog, lfp and spikes. *Nature reviews neuroscience*, 13(6):407–420, 2012.

[BDD06] François Bonnetblanc, Michel Desmurget, and Hugues Duffau. Low grade gliomas and cerebral plasticity: fundamental and clinical implications. *Medecine sciences: M/S*, 22(4):389–394, 2006.

[BHLK12] Svenja Borchers, Marc Himmelbach, Nikos Logothetis, and Hans-Otto Karnath. Direct electrical stimulation of human cortex—the gold standard for mapping brain functions? *Nature Reviews Neuroscience*, 13(1):63–70, 2012.

[BR97] Mitchel S Berger and Robert C Rostomily. Low grade gliomas: functional mapping resection strategies, extent of resection, and outcome. *Journal of neuro-oncology*, 34(1):85–101, 1997.

[CED+11] Christopher R Conner, Timothy M Ellmore, Michael A DiSano, Thomas A Pieters, Andrew W Potter, and Nitin Tandon. Anatomic and electrophysiologic connectivity of the language system: a combined dti-ccep study. *Computers in biology and medicine*, 41(12):1100–1109, 2011.

[Cus09] Harvey Cushing. A note upon the faradic stimulation of the postcentral gyrus in conscious patients. 1. *Brain*, 32(1):44–53, 1909.

[DBD07] Michel Desmurget, François Bonnetblanc, and Hugues Duffau. Contrasting acute and slow-growing lesions: a new door to brain plasticity. *Brain*, 130(4):898–914, 2007.

[DCS+02] Hugues Duffau, Laurent Capelle, Nicole Sichez, Dominique Denvil, Manuel Lopes, Jean-Pierre Sichez, Ahmad Bitar, and Denis Fohanno. Intraoperative mapping of the subcortical language pathways using direct stimulations. *Brain*, 125(1):199–214, 2002.

[DeA01] Lisa M DeAngelis. Brain tumors. *New England Journal of Medicine*, 344(2):114–123, 2001.

[DGM+08] Hugues Duffau, Peggy Gatignol, Emmanuel Mandonnet, Laurent Capelle, and Luc Taillandier. Intraoperative subcortical stimulation mapping of language pathways in a consecutive series of 115 patients with grade ii glioma in the left dominant hemisphere. 2008.

[DMGM14] Hugues Duffau, Sylvie Moritz-Gasser, and Emmanuel Mandonnet. A re-examination of neural basis of language processing: proposal of a dynamic hodotopical model from data provided by brain stimulation mapping during picture naming. *Brain and language*, 131:1–10, 2014.

[DSL00] Hugues Duffau, Jean-Pierre Sichez, and Stéphane Lehéricy. Intraoperative unmasking of brain redundant motor sites during resection of a precentral angioma: evidence using direct cortical stimulation. *Annals of neurology*, 47(1):132–135, 2000.

[dSUD+05] Michel Thiebaut de Schotten, Marika Urbanski, Hugues Duffau, Emmanuelle Volle, Richard Lévy, Bruno Dubois, and Paolo Bartolomeo. Direct evidence for a parietal-frontal pathway subserving spatial awareness in humans. *Science*, 309(5744):2226–2228, 2005.

[Duf04] Hugues Duffau. Cartographie fonctionnelle per-opératoire par stimulations électriques directes: Aspects méthodologiques. *Neurochirurgie*, 50(4):474–483, 2004.

[Duf05] Hugues Duffau. Lessons from brain mapping in surgery for low-grade glioma: insights into associations between tumour and brain plasticity. *The Lancet Neurology*, 4(8):476–486, 2005.

[Duf14] Hugues Duffau. The huge plastic potential of adult brain and the role of connectomics: new insights provided by serial mappings in glioma surgery. *Cortex*, 58:325–337, 2014.

[Duf15] Hugues Duffau. Stimulation mapping of white matter tracts to study brain functional connectivity. *Nature Reviews Neurology*, 11(5):255–265, 2015.

[Dur99] Dominique M Durand. Electric stimulation of excitable tissue. In *The Biomedical Engineering Handbook, Second Edition. 2 Volume Set*. CRC press, 1999.

[DWHRZ+12] Philip C De Witt Hamer, Santiago Gil Robles, Aeilko H Zwinderman, Hugues Duffau, and Mitchel S Berger. Impact of intraoperative stimulation brain mapping on glioma surgery outcome: a meta-analysis. *Journal of Clinical Oncology*, 30(20):2559–2565, 2012.

[EKO+16] Rei Enatsu, Aya Kanno, Shunya Ohtaki, Yukinori Akiyama, Satoko Ochi, and Nobuhiro Mikuni. Intraoperative subcortical fiber mapping with subcortico-cortical evoked potentials. *World neurosurgery*, 86:478–483, 2016.

[EMP+13] Rei Enatsu, Riki Matsumoto, Zhe Piao, Timothy O'Connor, Karl Horning, Richard C Burgess, Juan Bulacio, William Bingaman, and Dileep R Nair. Cortical negative motor network in comparison with sensorimotor network: a cortico-cortical evoked potential study. *Cortex*, 49(8):2080–2096, 2013.

[FA35] Otfrid Foerster and Hans Altenburger. Elektrobiologische vorgänge an der menschlichen hirnrinde. *Journal of Neurology*, 135(5):277–288, 1935.

[Fer74] David Ferrier. Experiments on the brain of monkeys.–no. i. *Proceedings of the Royal Society of London*, 23(156-163):409–430, 1874.

[FH09] Gustav Fritsch and Eduard Hitzig. Electric excitability of the cerebrum (über die elektrische erregbarkeit des grosshirns). *Epilepsy & Behavior*, 15(2):123–130, 2009.

[GALA+17] Thomas Guiho, David Andreu, Victor Manuel López-Alvarez, Paul Cvancara, Arthur Hiairrassary, G Granata, L Wauters, Winnie Jensen, Jean-Louis Divoux, Silvestro Micera, et al. Advanced 56 channels stimulation system to drive intrafascicular electrodes. In *Converging Clinical and Engineering Research on Neurorehabilitation II*, pages 743–747. Springer, 2017.

[GB67] Leslie A Geddes and LE Baker. The specific resistance of biological material—a compendium of data for the biomedical engineer and physiologist. *Medical and Biological Engineering and Computing*, 5(3):271–293, 1967.

[GHG94] Sidney Goldring, Gary W Harding, and Erik M Gregorie. Distinctive electrophysiological characteristics of functionally discrete brain areas: a tenable approach to functional localization. *Journal of neurosurgery*, 80(4):701–709, 1994.

[GJH+61] Sidney Goldring, Michael J Jerva, Thomas G Holmes, James L O'Leary, and John R Shields. Direct response of human cerebral cortex. *Archives of neurology*, 4(6):590–598, 1961.

[GLR+90] Barry Gordon, Ronald P Lesser, Naomi E Rance, John Hart, Robert Webber, Sumio Uematsu, and Robert S Fisher. Parameters for direct cortical electrical stimulation in the human: histopathologic confirmation. *Electroencephalography and clinical neurophysiology*, 75(5):371–377, 1990.

[GM83] Peter H Gorman and J Thomas Mortimer. The effect of stimulus parameters on the recruitment characteristics of direct nerve stimulation. *IEEE Transactions on Biomedical Engineering*, (7):407–414, 1983.

[GM95] Warren M Grill and J Thomas Mortimer. Stimulus waveforms for selective neural stimulation. *IEEE Engineering in Medicine and Biology Magazine*, 14(4):375–385, 1995.

[HH52] Alan L Hodgkin and Andrew F Huxley. A quantitative description of membrane current and its application to conduction and excitation in nerve. *The Journal of physiology*, 117(4):500–544, 1952.

[KHM+14] Corey J Keller, Christopher J Honey, Pierre Mégevand, Laszlo Entz, Istvan Ulbert, and Ashesh D Mehta. Mapping human brain networks with cortico-

cortical evoked potentials. *Phil. Trans. R. Soc. B*, 369(1653):20130528, 2014.

[KLL+04] G Evren Keles, David A Lundin, Kathleen R Lamborn, Edward F Chang, George Ojemann, and Mitchel S Berger. Intraoperative subcortical stimulation mapping for hemispheric perirolandic gliomas located within or adjacent to the descending motor pathways: evaluation of morbidity and assessment of functional outcome in 294 patients. *Journal of neurosurgery*, 100(3):369–375, 2004.

[KLS+12] Mohamad Z Koubeissi, Ronald P Lesser, Alon Sinai, William D Gaillard, Piotr J Franaszczuk, and Nathan E Crone. Connectivity between perisylvian and bilateral basal temporal cortices. *Cerebral Cortex*, 22(4):918–925, 2012.

[KM07] Daniel L Kimmel and Tirin Moore. Temporal patterning of saccadic eye movement signals. *Journal of Neuroscience*, 27(29):7619–7630, 2007.

[KMM+12] Takayuki Kikuchi, Riki Matsumoto, Nobuhiro Mikuni, Yohei Yokoyama, Atsuhito Matsumoto, Akio Ikeda, Hidenao Fukuyama, Susumu Miyamoto, and Nobuo Hashimoto. Asymmetric bilateral effect of the supplementary motor area proper in the human motor system. *Clinical Neurophysiology*, 123(2):324–334, 2012.

[Kra09] Fedor Krause. Die operative behandlung der epilepsie. *Med. Klin*, 5:1418–1422, 1909.

[KYKM15] Takeharu Kunieda, Yukihiro Yamao, Takayuki Kikuchi, and Riki Matsumoto. New approach for exploring cerebral functional connectivity: review of cortico-cortical evoked potential. *Neurologia medico-chirurgica*, 55(5):374–382, 2015.

[Lap07] Louis Lapicque. Recherches quantitatives sur l'excitation electrique des nerfs traitee comme une polarisation. *J. Physiol. Pathol. Gen*, 9(1):620–635, 1907.

[LBC65] WM Landau, GH Bishop, and MH Clare. Site of excitation in stimulation of the motor cortex. *Journal of neurophysiology*, 28(6):1206–1222, 1965.

[LBT09] Steven Laureys, Melanie Boly, and Giulio Tononi. Functional neuroimaging. *The Neurology of Consciousness: cognitive neuroscience and neuropathology*, (s 1), 2009.

[LC62] Choh-Luh Li and Shelley N Chou. Cortical intracellular synaptic potentials and direct cortical stimulation. *Journal of Cellular Physiology*, 60(1):1–16, 1962.

[Lem08] Roger N Lemon. Descending pathways in motor control. *Annu. Rev. Neurosci.*, 31:195–218, 2008.

[LS17] Alexander SF Leyton and Charles S Sherrington. Observations on the excitable cortex of the chimpanzee, orang-utan, and gorilla. *Experimental Physiology*, 11(2):135–222, 1917.

[Lüd08] Hans O Lüders. *Textbook of epilepsy surgery*. CRC Press, 2008.

[MAYB90] Douglas B McCreery, William F Agnew, Ted GH Yuen, and Leo Bullara. Charge density and charge per phase as cofactors in neural injury induced by electrical stimulation. *IEEE Transactions on Biomedical Engineering*, 37(10):996–1001, 1990.

[MBJ05] Daniel R Merrill, Marom Bikson, and John GR Jefferys. Electrical stimulation of excitable tissue: design of efficacious and safe protocols. *Journal of neuroscience methods*, 141(2):171–198, 2005.

[MDP+16] Emmanuel Mandonnet, Yoël Dadoun, Isabelle Poisson, Catherine Madadaki, Sebastien Froelich, and P Lozeron. Axono-cortical evoked potentials: A proof-of-concept study. *Neurochirurgie*, 62(2):67–71, 2016.

[MJA13] Naoyuki Matsuzaki, Csaba Juhász, and Eishi Asano. Cortico-cortical evoked potentials and stimulation-elicited gamma activity preferentially propagate from lower-to higher-order visual areas. *Clinical Neurophysiology*, 124(7):1290–1296, 2013.

[MNI+12] Riki Matsumoto, Dileep R Nair, Akio Ikeda, Tomoyuki Fumuro, Eric LaPresto, Nobuhiro Mikuni, William Bingaman, Susumu Miyamoto, Hidenao Fukuyama, Ryosuke Takahashi, et al. Parieto-frontal network in

humans studied by cortico-cortical evoked potential. *Human brain mapping*, 33(12):2856–2872, 2012.

[MNL+04] Riki Matsumoto, Dileep R Nair, Eric LaPresto, Imad Najm, William Bingaman, Hiroshi Shibasaki, and Hans O Lüders. Functional connectivity in the human language system: a cortico-cortical evoked potential study. *Brain*, 127(10):2316–2330, 2004.

[MNL+07] Riki Matsumoto, Dileep R Nair, Eric LaPresto, William Bingaman, Hiroshi Shibasaki, and Hans O Lüders. Functional connectivity in human cortical motor system: a cortico-cortical evoked potential study. *Brain*, 130(1):181–197, 2007.

[MP11] Emmanuel Mandonnet and Olivier Pantz. The role of electrode direction during axonal bipolar electrical stimulation: a bidomain computational model study. *Acta neurochirurgica*, 153(12):2351–2355, 2011.

[MWD10] Emmanuel Mandonnet, Peter A Winkler, and Hugues Duffau. Direct electrical stimulation as an input gate into brain functional networks: principles, advantages and limitations. *Acta neurochirurgica*, 152(2):185–193, 2010.

[NAGG12] Luis F Nicolas-Alonso and Jaime Gomez-Gil. Brain computer interfaces, a review. *Sensors*, 12(2):1211–1279, 2012.

[OOLB89] George Ojemann, Jeff Ojemann, EREEGT Lettich, and M Berger. Cortical language localization in left, dominant hemisphere: an electrical stimulation mapping investigation in 117 patients. *Journal of neurosurgery*, 71(3):316–326, 1989.

[PAF01] Dale Purves, George J Augustine, and David Fitzpatrick. et al., editors. neuroscience. sunderland (ma), 2001.

[PB37] Wilder Penfield and Edwin Boldrey. Somatic motor and sensory representation in the cerebral cortex of man as studied by electrical stimulation. *Brain: A journal of neurology*, 1937.

[Pen47] Wilder Penfield. Ferrier lecture: some observations on the cerebral cortex of man. *Proceedings of the Royal Society of London. Series B, Biological Sciences*, pages 329–347, 1947.

[PPF+57] Dominick P Purpura, JL Pool, MJ Frumin, EM Housepian, et al. Observations on evoked dendritic potentials of human cortex. *Electroencephalography and clinical neurophysiology*, 9(3):453–459, 1957.

[Ran75] James B Ranck. Which elements are excited in electrical stimulation of mammalian central nervous system: a review. *Brain research*, 98(3):417–440, 1975.

[Rat99] Frank Rattay. The basic mechanism for the electrical stimulation of the nervous system. *Neuroscience*, 89(2):335–346, 1999.

[RHMGD14] Fabien Rech, Guillaume Herbet, Sylvie Moritz-Gasser, and Hugues Duffau. Disruption of bimanual movement by unilateral subcortical electrostimulation. *Human brain mapping*, 35(7):3439–3445, 2014.

[RHN+15] Gratianne Rabiller, Ji-Wei He, Yasuo Nishijima, Aaron Wong, and Jialing Liu. Perturbation of brain oscillations after ischemic stroke: A potential biomarker for post-stroke function and therapy. *International journal of molecular sciences*, 16(10):25605–25640, 2015.

[SB08a] Nader Sanai and Mitchel S Berger. Glioma extent of resection and its impact on patient outcome. *Neurosurgery*, 62(4):753–766, 2008.

[SB08b] Nader Sanai and Mitchel S Berger. Glioma extent of resection and its impact on patient outcome. *Neurosurgery*, 62(4):753–766, 2008.

[SCC+12] Nicole C Swann, Weidong Cai, Christopher R Conner, Thomas A Pieters, Michael P Claffey, Jobi S George, Adam R Aron, and Nitin Tandon. Roles for the pre-supplementary motor area and the right inferior frontal gyrus in stopping action: electrophysiological responses and functional and structural connectivity. *Neuroimage*, 59(3):2860–2870, 2012.

[SCL+08] Justin S Smith, Edward F Chang, Kathleen R Lamborn, Susan M Chang, Michael D Prados, Soonmee Cha, Tarik Tihan, Scott VandenBerg, Michael W McDermott, and Mitchel S Berger. Role of extent of resection in the long-term outcome of low-grade hemispheric gliomas. *Journal of Clinical Oncology*, 26(8):1338–1345, 2008.

[SG01] Charles S Sherrington and ASF Grünbaum. An address on localisation in the" motor" cerebral cortex. *The British Medical Journal*, pages 1857–1859, 1901.

[SGO64] Eiichi Sugaya, Sidney Goldring, and James L O'Leary. Intracellular potentials associated with direct cortical response and seizure discharge in cat. *Electroencephalography and clinical neurophysiology*, 17(6):661–669, 1964.

[SHvVB91] Johannes J Struijk, Jan Holsheimer, Benno K van Veen, and Herman BK Boom. Epidural spinal cord stimulation: calculation of field potentials with special reference to dorsal column nerve fibers. *IEEE transactions on biomedical engineering*, 38(1):104–110, 1991.

[SMM+15] Taiichi SaiTo, Yoshihiro Muragaki, Takashi Maruyama, Manabu Tamura, Masayuki Nitta, and Yoshikazu Okada. Intraoperative functional mapping and monitoring during glioma surgery. *Neurologia medico-chirurgica*, 55(1):1–13, 2015.

[Teh96] Edward J Tehovnik. Electrical stimulation of neural tissue to evoke behavioral responses. *Journal of neuroscience methods*, 65(1):1–17, 1996.

[THMG+14] Matthew C Tate, Guillaume Herbet, Sylvie Moritz-Gasser, Joseph E Tate, and Hugues Duffau. Probabilistic map of critical functional regions of the human cerebral cortex: Broca's area revisited. *Brain*, 137(10):2773–2782, 2014.

[TK04] Martin JB Taphoorn and Martin Klein. Cognitive deficits in adult patients with brain tumours. *The Lancet Neurology*, 3(3):159–168, 2004.

[TOK+16] Yukie Tamura, Hiroshi Ogawa, Christoph Kapeller, Robert Prueckl, Fumiya Takeuchi, Ryogo Anei, Anthony Ritaccio, Christoph Guger, and Kyousuke Kamada. Passive language mapping combining real-time oscillation analysis with cortico-cortical evoked potentials for awake craniotomy. *Journal of neurosurgery*, 125(6):1580–1588, 2016.

[UG86] Adrian RM Upton and John P Girvin. Cerebral (cortical) biostimulation. *Pacing and Clinical Electrophysiology*, 9(5):764–771, 1986.

[VGD+17] Marion Vincent, David Guiraud, Hugues Duffau, Emmanuel Mandonnet, and François Bonnetblanc. Electrophysiological brain mapping: Basics of recording evoked potentials induced by electrical stimulation and its physiological spreading in the human brain. *Clinical Neurophysiology*, 128(10):1886–1890, 2017.

[VRD+16] Marion Vincent, Olivier Rossel, Hugues Duffau, Francois Bonnetblanc, and David Guiraud. A measure of cortico-cortical potentials evoked by 10hz direct electrical stimulation of the brain and by means of a differential recording mode of electrocorticographic signals. In *Engineering in Medicine and Biology Society (EMBC), 2016 IEEE 38th Annual International Conference of the*, pages 4543–4546. IEEE, 2016.

[VRH+16] Marion Vincent, Olivier Rossel, Mitsuhiro Hayashibe, Guillaume Herbet, Hugues Duffau, David Guiraud, and François Bonnetblanc. The difference between electrical microstimulation and direct electrical stimulation–towards new opportunities for innovative functional brain mapping? *Reviews in the Neurosciences*, 27(3):231–258, 2016.

[VRPC+16] Marion Vincent, Olivier Rossel, Bénédicte Poulin-Charronnat, Guillaume Herbet, Mitsuhiro Hayashibe, Hugues Duffau, David Guiraud, and François Bonnetblanc. Case report: Remote neuromodulation with direct electrical stimulation of the brain, as evidenced by intra-operative eeg recordings during wide-awake neurosurgery. *Clinical Neurophysiology*, 127(2):1752–1754, 2016.

[VV19] Cécile Vogt and Oskar Vogt. *Allgemeine ergebnisse unserer hirnforschung*, volume 21. JA Barth, 1919.

[Wei90] Georges Weiss. Sur la possibilite de rendre comparables entre eux les appareils servant a l'excitation electrique. *Archives Italiennes de Biologie*, 35(1):413–445, 1990.

[WGD92] Eduardo N Warman, Warren M Grill, and Dominique Durand. Modeling the effects of electric fields on nerve fibers: determination of excitation thresholds. *IEEE Transactions on Biomedical Engineering*, 39(12):1244–1254, 1992.

[WK03] David G Walker and Andrew H Kaye. Low grade glial neoplasms. *Journal of clinical neuroscience*, 10(1):1–13, 2003.

[YMGD11] Yordanka N Yordanova, Sylvie Moritz-Gasser, and Hugues Duffau. Awake surgery for who grade ii gliomas within "noneloquent" areas in the left dominant hemisphere: toward a "supratotal" resection: clinical article. *Journal of neurosurgery*, 115(2):232–239, 2011.

[YMK+14] Yukihiro Yamao, Riki Matsumoto, Takeharu Kunieda, Yoshiki Arakawa, Katsuya Kobayashi, Kiyohide Usami, Sumiya Shibata, Takayuki Kikuchi, Nobukatsu Sawamoto, Nobuhiro Mikuni, et al. Intraoperative dorsal language network mapping by using single-pulse electrical stimulation. *Human brain mapping*, 35(9):4345–4361, 2014.

Titre
Mesure des effets électrophysiologiques de la stimulation électrique directe du cerveau lors de chirurgies éveillées des gliomes de bas grade.

Résumé
La "chirurgie éveillée du cerveau" consiste à retirer des tumeurs cérébrales infiltrantes (gliomes de bas grade, GIBG) à progression lente chez un patient éveillé. Une cartographie anatomo-fonctionnelle du cerveau est réalisée par stimulation électrique directe (SED) des zones proches de la tumeur afin de discriminer les aires cérébrales fonctionnelles de celles qui ne le sont plus. Les effets inhibiteurs de la stimulation sont mis en évidence par les tests neuropsychologiques réalisés par le patient lors de la chirurgie. Cependant, la SED est paramétrée de manière totalement empirique bien qu'utilisée de façon standardisée. De plus, si ses effets comportementaux sont mis en avant, ses effets électrophysiologiques restent plus méconnus. La conservation de la relation entre électrophysiologie (potentiel évoqué, PE) et comportement (fonction) est cruciale lors de chirurgies des GIBG : l'analyse des PE en temps réel permettrait une identification de ces relations au cours même de la chirurgie. Pour cela, nous avons réalisé des enregistrements peropératoires de l'activité électro-corticographique (ECoG) du cortex (CPP, n° ID-RCB : 2015-A00056-43). L'étude de ces enregistrements a permis de mesurer les effets electrophysiologiques de la SED corticale et sous-corticale, en évaluant la réponse du cerveau à la stimulation au travers des PE. Une chaine d'acquisition spécifique à la mesure de l'ECoG a été développée afin de pouvoir à terme mesurer et visualiser les PE en temps réel. De plus, un algorithme de post-traitement a été implémenté afin de réduire la contamination du signal par l'artefact de stimulation. Mieux comprendre les mécanismes sous-jacents à la SED, notamment au travers de la mesure des réponses électrophysiologiques, doit permettre de proposer des protocoles peropératoires plus objectifs afin d'améliorer la planification chirurgicale et la qualité de vie des patients.

Mots clés : Stimulation électrique directe (SED), Mesures electrophysiologiques, Potentiels évoqués (PE), Cartographie fonctionnelle peropératoire, Chirurgie éveillée, Tumeur cérébrale.

Title
Measuring the Electrophysiological Effects of Direct Electrical Brain Stimulation during Awake Surgery of Low-Grade Glioma.

Abstract
The 'Awake brain surgery' consists in removing some slow-growing infiltrative brain tumor (low grade glioma, LGG) in a patient, to delay its development while preserving the functions. An anatomo-functional mapping of the brain is performed by electrically stimulating brain areas near the tumor to discriminate functional versus nonfunctional areas. The inhibitory effects of this direct electrical stimulation (DES) are evidenced by the neuropsychological tests undergone by the patient during the tumor resection. However, the DES parameters are empirically set even though its use is standardised. Moreover, even if its behavioural effects are well known, its electrophysiological effects have been partially depicted. Preserving the relationship between electrophysiology (evoked potential, EP) and behaviour (function) is crucial in LGG surgery. Intra-operative electrocorticographic recordings (ECoG) of the brain activity were thus performed (CPP, n° ID-RCB : 2015-A00056-43). The electrophysiological effects of cortical and subcortical DES on brain activity have been highlighted, by assessing the response of the brain to the stimulation through EP recordings analysis. A new acquisition set-up has also been specifically developed for ECoG recordings in order to measure and eventually visualise the EP in real-time. Furthermore, a post-processing algorithm has been implemented to reduce the signal disturbances induced by the stimulation artefact. A better understanding of the underlying DES mechanisms, in particular through the measurement of electrophysiological responses, should enable designing more perfected protocols in order to improve the surgical planning, and quality of life of the patients.

Keywords : Direct electrical stimulation (DES), Electrophysiological recordings, Evoked potentials (EP), Intra-operative functional mapping, Awake surgery, Brain tumours.

Discipline : Génie Informatique, Automatique et Traitement du signal

Intitulé et adresse du laboratoire :
Institut national de recherche en informatique et en automatique (INRIA)
Université Montpellier Bâtiment 5 - CC05 017
860 rue de St Priest 34095 Montpellier Cedex 5, France